

## **Copyright Warning & Restrictions**

The copyright law of the United States (Title 17, United States Code) governs the making of photocopies or other reproductions of copyrighted material.

Under certain conditions specified in the law, libraries and archives are authorized to furnish a photocopy or other reproduction. One of these specified conditions is that the photocopy or reproduction is not to be “used for any purpose other than private study, scholarship, or research.” If a user makes a request for, or later uses, a photocopy or reproduction for purposes in excess of “fair use” that user may be liable for copyright infringement,

This institution reserves the right to refuse to accept a copying order if, in its judgment, fulfillment of the order would involve violation of copyright law.

**Please Note: The author retains the copyright while the New Jersey Institute of Technology reserves the right to distribute this thesis or dissertation**

Printing note: If you do not wish to print this page, then select “Pages from: first page # to: last page #” on the print dialog screen

The Van Houten library has removed some of the personal information and all signatures from the approval page and biographical sketches of theses and dissertations in order to protect the identity of NJIT graduates and faculty.

## INFORMATION TO USERS

This was produced from a copy of a document sent to us for microfilming. While the most advanced technological means to photograph and reproduce this document have been used, the quality is heavily dependent upon the quality of the material submitted.

The following explanation of techniques is provided to help you understand markings or notations which may appear on this reproduction.

1. The sign or "target" for pages apparently lacking from the document photographed is "Missing Page(s)". If it was possible to obtain the missing page(s) or section, they are spliced into the film along with adjacent pages. This may have necessitated cutting through an image and duplicating adjacent pages to assure you of complete continuity.
2. When an image on the film is obliterated with a round black mark it is an indication that the film inspector noticed either blurred copy because of movement during exposure, or duplicate copy. Unless we meant to delete copyrighted materials that should not have been filmed, you will find a good image of the page in the adjacent frame.
3. When a map, drawing or chart, etc., is part of the material being photographed the photographer has followed a definite method in "sectioning" the material. It is customary to begin filming at the upper left hand corner of a large sheet and to continue from left to right in equal sections with small overlaps. If necessary, sectioning is continued again—beginning below the first row and continuing on until complete.
4. For any illustrations that cannot be reproduced satisfactorily by xerography, photographic prints can be purchased at additional cost and tipped into your xerographic copy. Requests can be made to our Dissertations Customer Services Department.
5. Some pages in any document may have indistinct print. In all cases we have filmed the best available copy.

University  
Microfilms  
International

300 N ZEEB ROAD, ANN ARBOR, MI 48106  
18 BEDFORD ROW, LONDON WC1R 4EJ, ENGLAND

7902978

FALSAFI-HAGHIGHI, RAHIM  
INTERACTION BETWEEN STRUCTURES AND FLUIDS.

NEW JERSEY INSTITUTE OF TECHNOLOGY,  
D.ENG.SC., 1978

University  
Microfilms  
International 300 N ZEEB ROAD, ANN ARBOR, MI 48106

© 1978

RAHIM FALSAFI-HAGHIGHI

ALL RIGHTS RESERVED

PLEASE NOTE:

In all cases this material has been filmed in the best possible way from the available copy. Problems encountered with this document have been identified here with a check mark .

1. Glossy photographs \_\_\_\_\_
2. Colored illustrations \_\_\_\_\_
3. Photographs with dark background \_\_\_\_\_
4. Illustrations are poor copy \_\_\_\_\_
5. Print shows through as there is text on both sides of page \_\_\_\_\_
6. Indistinct, broken or small print on several pages \_\_\_\_\_ throughout  
\_\_\_\_\_
7. Tightly bound copy with print lost in spine \_\_\_\_\_
8. Computer printout pages with indistinct print
9. Page(s) \_\_\_\_\_ lacking when material received, and not available  
from school or author \_\_\_\_\_
10. Page(s) \_\_\_\_\_ seem to be missing in numbering only as text  
follows \_\_\_\_\_
11. Poor carbon copy \_\_\_\_\_
12. Not original copy, several pages with blurred type \_\_\_\_\_
13. Appendix pages are poor copy \_\_\_\_\_
14. Original copy with light type \_\_\_\_\_
15. Curling and wrinkled pages \_\_\_\_\_
16. Other \_\_\_\_\_

INTERACTION BETWEEN STRUCTURES AND FLUIDS

BY

RAHIM FALSAFI-HAGHIGHI

A DISSERTATION

PRESENTED IN PARTIAL FULFILLMENT OF

THE REQUIREMENTS FOR THE DEGREE

OF

DOCTOR OF ENGINEERING SCIENCE

IN MECHANICAL ENGINEERING

AT

NEW JERSEY INSTITUTE OF TECHNOLOGY

This dissertation is to be used only with due regard to the rights of the author. Bibliographical references may be noted, but passages must not be copied without permission of the Institute and without credit being given in subsequent written or published work.

Newark, New Jersey  
1978

## ABSTRACT

A finite element model for the study of solid-fluid interaction, with applications in flow-induced vibration analysis of reactor vessel and heat exchanger internals, is presented. The model is based on the discretization of the solid equation of motion and the fluid continuity and momentum equations and employs the solid displacements together with the fluid pressure and velocity components as the nodal degrees of freedom. This permits a realistic and accurate implementation of boundary conditions, in contrast with methods using solid displacements and fluid pressure as the only field variables. The numerical solution of the resulting matrix equation, involving non-symmetric matrices, is achieved by a combination of matrix decomposition, iterative scheme and analytic integration which allows the application of the elemental matrices, rather than the system global matrices, at considerable economy in computer storage and running time. Plane triangular finite elements for fluid, solid and solid-fluid continua and equivalent mass, damping and stiffness matrices and interaction load array have been developed for the study of wave propagation phenomena in a two-dimensional flow field. This is verified by solving a wave propagation flow problem consisting of water, between two elastic parallel plates, initially at rest and accelerated suddenly by applying a step pressure at one end. The results obtained are in good agreement with a previous study based on the finite element discretization of the two-dimensional wave equation. Furthermore, the results are also compared with those obtained for flow between two rigid parallel plates. These results indicate the development of water hammer phenomenon and pressure surge in the transverse direction, for the elastic wall case, which may have important implications in the design of fluid systems.

APPROVAL OF DISSERTATION

INTERACTION BETWEEN STRUCTURES AND FLUIDS

BY

RAHIM FALSAFI-HAGHIGHI

FOR

DEPARTMENT OF MECHANICAL ENGINEERING

NEW JERSEY INSTITUTE OF TECHNOLOGY

BY

FACULTY COMMITTEE

APPROVED: \_\_\_\_\_, Advisor

\_\_\_\_\_

\_\_\_\_\_

\_\_\_\_\_

\_\_\_\_\_

September, 1978



ACKNOWLEDGEMENT

The author wishes to express his deep and sincere appreciation to his advisor, Dr. Amir N. Nahavandi, whose continued guidance, insight, patience and persistence made this study possible. These traits, and his willingness to assist the student has encouraged the author in the successful completion of this dissertation.

The author also wishes to express his special appreciation to Dr. Benedict C. Sun, the Doctoral Committee Chairman, who helped in bringing this dissertation to completion.

TABLE OF CONTENTS

	<u>Page</u>
ABSTRACT	i
APPROVAL OF DISSERTATION	ii
ACKNOWLEDGEMENTS	iii
TABLE OF CONTENTS	iv
LIST OF FIGURES	vi
LIST OF TABLES	viii
INTRODUCTION	1
PART ONE-- DEVELOPMENT AND RESULTS OF FINITE ELEMENT MODEL FOR THE RIGID WALL CASE	8
1. INTRODUCTION	9
2. MATHEMATICAL FORMULATION	12
3. NUMERICAL SOLUTION	16
4. PRESENTATION OF RESULTS	19
5. CONCLUSIONS	34
PART TWO-- DEVELOPMENT AND RESULTS OF FINITE ELEMENT MODEL FOR THE ELASTIC WALL CASE	35
1. INTRODUCTION	36
2. MATHEMATICAL FORMULATION	39
3. NUMERICAL SOLUTION	45
4. PRESENTATION OF RESULTS	50
5. CONCLUSIONS	67
NOMENCLATURE	69
APPENDIX 1 - DERIVATION OF THE FLUID FINITE ELEMENT EQUATIONS	74
APPENDIX 2 - DEVELOPMENT OF FLUID SHAPE FUNCTION AND MATRICES	80
APPENDIX 3 - DERIVATION OF SOLID FINITE ELEMENT EQUATIONS	85

	<u>Page</u>
APPENDIX 4 - DERIVATION OF THE SOLID-FLUID SUPERELEMENT EQUATIONS	89
REFERENCES	95
PART THREE--USER'S MANUAL	97
1. DESCRIPTION OF FASINT PROGRAM	98
1.1 MAIN PROGRAM	103
1.2 CLEAR SUBROUTINE	103
1.3 GDATA SUBROUTINE	103
1.4 LOAD SUBROUTINE	104
1.5 FORMK SUBROUTINE	104
1.6 STIFT 1 (N) SUBROUTINE	104
1.7 STIFT 2 (N) SUBROUTINE	105
1.8 STIFT 3 (N) SUBROUTINE	105
1.9 SF FUNCTION SUBROUTINE	105
1.10 FORCE SUBROUTINE	106
1.11 AINTEG SUBROUTINE	106
2. DESCRIPTION OF INPUT DATA	107
3. DESCRIPTION OF OUTPUT DATA	119
3.1 Output Data Not Under Debug Option Control	119
3.2 Output Data Under the Control of the Debug Option	119
3.3 Error Printouts	121
3.4 Output Data Defining The Problem Solution	121
4. OPERATING PROCEDURE	122
5. FASINT NOMENCLATURE	126
5.1 Subscripted Variable	126
5.2 Non-Subscripted Variable	131
PROGRAM LISTING AND SAMPLE RUN	133
VITA	173

LIST OF FIGURES

<u>Figure No.</u>	<u>Caption</u>	<u>Page</u>
1a	Rigorous approach to the solution of interaction between structures and fluids	3
1b	The approach used in this study for the solution of interaction between structures and fluids	3
1c	Simplified approach to the solution of interaction between structures and fluids	3
Part one	Fluid finite element model for the rigid wall case	
2	Plane triangular fluid finite element for pressure-velocity formulation	14
3	Two-dimensional flow configuration with rigid wall	20
4	48 triangular finite element fluid model for pressure-velocity formulation	21
5	A comparison of multi-variable and single-variable pressure time histories for inviscid case at $x = 6.9$ inches	24
6	A comparison of multi-variable and single-variable pressure time histories for inviscid case at $x = 23.7$ inches	25
7	A comparison of multi-variable and single-variable velocity time histories for inviscid case for element 13	27
8	A comparison of multi-variable and single-variable velocity time histories for inviscid case for element 37	28
9	A comparison of multi-variable and single-variable pressure time histories for slightly viscous case at $x = 6.9$ and $x = 23.7$ inches	30
10	A comparison of multi-variable and single-variable velocity time histories for slightly viscous case for element 13	31
11	A comparison of multi-variable and single-variable pressure time histories for highly viscous case at $x = 6.9$ and $x = 23.7$ inches	32
12	A comparison of multi-variable and single-variable velocity time histories for highly viscous case for element 13	33
Part two	Solid-fluid finite element model for the elastic wall case	
13	Plane triangular solid finite element	41
14	Plane quadrilateral solid-fluid superelement	43
15	Flow configuration	51

<u>Figure No.</u>	<u>Caption</u>	<u>Page</u>
16	72 Element solid-fluid model	52
17	A comparison of multi- and single-variable pressure and displacement time histories for elastic wall case with inviscid flow at (x=6.9 in.)	54
18	A comparison of multi- and single-variable fluid velocity time histories for elastic wall case with inviscid flow (at x = 6.9 in.)	55
19	A comparison of pressure and displacement time histories for elastic and rigid wall cases with inviscid flow ( at x = 6.9 in.)	59
20	A comparison of fluid velocity time histories for elastic and rigid wall cases with inviscid flow ( at x = 6.9 in. near the wall )	60
21	A comparison of fluid velocity time histories for elastic and rigid wall cases with inviscid flow ( at x = 6.9 in. near the channel centerline )	62
22	A comparison of pressure and displacement time histories for elastic and rigid wall cases with inviscid flow( at x = 23.7 in.)	63
23	A comparison of fluid velocity time histories for elastic and rigid wall cases with inviscid flow ( at x = 23.7 in. near the channel centerline )	64
24	A comparison of pressure and displacement time histories for elastic and rigid wall cases with highly viscous flow( at x = 6.9 in.)	65
25	A comparison of fluid velocity time histories for elastic and rigid wall cases with highly viscous flow( at x = 6.9 in.)	66
Part three	User's manual	
26	Simplified flowchart of FASINT program	100

LIST OF TABLES

<u>Table No.</u>	<u>Title</u>	<u>Page</u>
1	Upstream and downstream positions for which time histories are plotted for the rigid wall case	22
2	Physical data for the rigid wall case	29
3	Physical data for the elastic wall case	56

## INTRODUCTION

During the recent years, dynamicists have been confronted with complex, new problems involving the motion of structures subjected to an external and/or internal flowing fluid. These problems belong to the branch of engineering known as "flow-induced vibration." Flow-induced vibration problems have become significant as structures have become lighter and more slender due to the use of high-strength materials, and as advanced nuclear power reactors have been developed [ 1,2,13,14 ]<sup>1</sup>. Flow-induced vibration is frequently encountered in the operation of many reactor systems and components. Vibratory stresses and dynamic instabilities of nuclear fuel bundle and heat-exchanger tubes are a few examples of flow-induced vibration phenomena often observed.

The most important potential excitations are: vortex shedding, fluidelastic mechanisms, turbulent excitation and acoustic noises. Depending on conditions, any of several excitation sources can be the dominant excitation mechanism. When fluidelastic mechanism is dominant, fluid flowing through the system is a source of energy that can induce structural vibration and instability characterized by transversal motions. At small flow velocities, the structure vibrates at small amplitude which is called subcritical vibration. As the flow velocity increases, a certain value is reached at which the structure loses stability by buckling; this behavior is called instability. The forces causing this instability are affected by the deflection of the structure from its undeformed state. The essential parameters associated with fluid

---

<sup>1</sup>

Number in brackets designate references given at the end of part two

elastic instability are system damping and fluidelastic forces. When flow velocity increases to certain value, the work done on the structure by fluidelastic forces exceeds the energy dissipated by damping. As a result, large amplitude oscillations occur. A study of fluidelastic excitation requires the consideration of both solid and fluid motions including their interactive forces and constraints and, mathematically, it poses a more difficult problem than the other flow-induced vibration sources stated earlier(i.e. vortex shedding, turbulent excitation and acoustic noises). The importance of fluidelastic excitation in such systems as nuclear reactor fuel bundles, thermal shields, and core barrels has created a need for detailed investigations of the interaction between structures and fluids. Experimental and analytical studies have been performed that confirm the importance of the interaction between structures and fluids[ 5,8,19,11 ].

The solution of interaction problems between structures and fluids for components involving realistic geometries is extremely complicated. This is due to the fact that when a structural element vibrates, the fluid surrounding and/or contained within the structure must be displaced to accomodate the motions. Rigorously speaking, motions should be studied by coupling between a structure represented by matrix equations of motion and a flow field simulated by continuity and Navier-Stokes equations including the interactive forces and constraints, as shown schematically in Fig. 1a. This approach has not yet been attempted.

A simplified approach to the solution of interaction between struc-



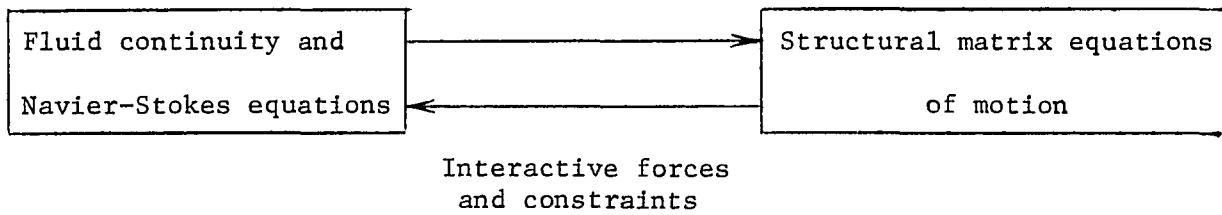


FIG. 1a RIGOROUS APPROACH TO THE SOLUTION OF INTERACTION BETWEEN STRUCTURES AND FLUIDS

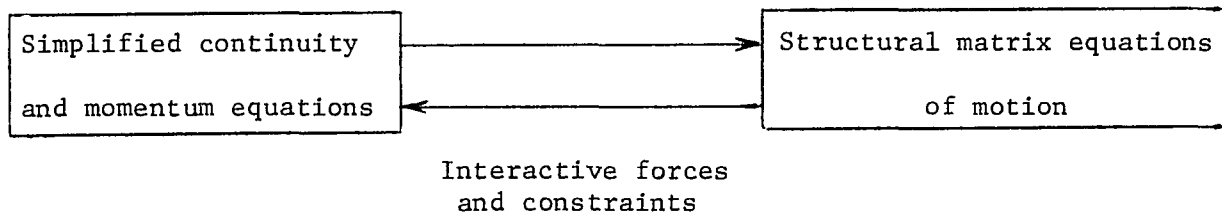


FIG. 1b THE APPROACH USED IN THIS STUDY FOR THE SOLUTION OF INTERACTION BETWEEN STRUCTURES AND FLUIDS

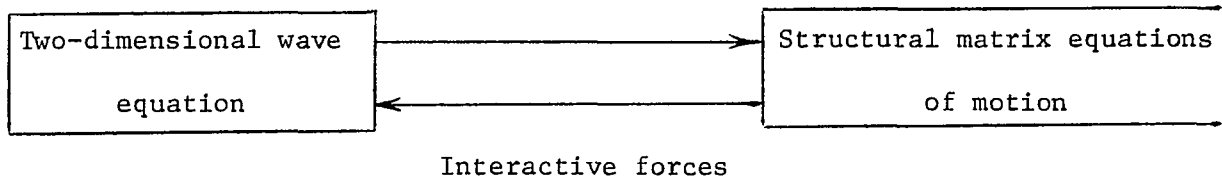


FIG. 1c SIMPLIFIED APPROACH TO THE SOLUTION OF INTERACTION BETWEEN STRUCTURES AND FLUIDS

tures and fluids shown schematically in Fig. 1c has been developed in Ref. [11]. In this approach a generalized solid-fluid interaction package has been presented which develops a fluid finite element compatible with existing structural elements and at the same time establishes the interaction between the solid and fluid elements. This study has employed the solid displacements and the fluid pressure as the only nodal degrees of freedom. The finite element models have been based on the discretization of solid matrix equations of motion and the two-dimensional wave equation including the interactive forces. The main objective of the above acousto-structural interaction is the determination of acoustic fields produced by the interaction between solid structures and the fluid contained within the structure. The mathematical formulation of acousto-structural analysis, although useful in the study of acoustic fields, cannot be readily employed in the analysis of practical solid-fluid interaction involving specified boundary conditions on the fluid velocity components. This type of problems arises in the hydraulic analysis of nuclear reactor systems in which the boundary conditions are often specified in terms of the fluid velocity components as well as pressure. Furthermore, the extension of the approach used in Fig. 1c to that of Fig. 1a is not straightforward. Therefore, to bridge the gap between the two approaches, an intermediate technique as shown schematically in Fig. 1b should be developed which uses the simplified continuity and momentum equations as a compromise between the simplified wave equation and the Navier-Stokes equations. This approach constitutes the basis for this study and uses the pressure and velocity as field variables thus avoiding the difficulty with the implementation of the boundary conditions. Expanding

the number of main dependent variables in the fluid to include the fluid velocity components among the main dependent variables, boundary conditions on the velocity components as well as pressure may be easily accommodated while this is not the case for the acousto-structural analysis which can treat boundary conditions expressed in terms of pressure only.

Specifically, the purpose of the present study is to examine the problem of fluid elastic excitation by developing a mathematical model for the interaction between an elastic solid and a fluid medium using finite element approach. The objective is to employ the solid displacements and the fluid pressure and velocity components as the nodal degrees of freedom. The finite element models is based on the discretization of solid matrix equations of motion and two-dimensional continuity and simplified momentum equations including the interactive forces and constraints as shown in Fig. 1b. These simplified momentum equations permit the verification of the results with the previously mentioned solid-fluid studies based on the solid matrix equations of motion and the two-dimensional wave equation including the interactive forces shown in Fig. 1c [11], since the elimination of velocity components among the continuity and the simplified momentum equations used results in the two-dimensional wave equation.

The contributions of this study are as follows:

- 1) The mathematical formulation used in this study employs the solid displacements together with the fluid pressure and velocity components as the nodal degrees of freedom. This facilitates the implementation of realistic boundary conditions in terms of pressure and velocity components, in contrast with formulations using stream function, vorticity and pressure as the only fluid field variables.
- 2) The mathematical formulation used in this study lays the foundation for the ultimate coupling between a structure represented by the matrix equations of motion and a flow field simulated by the continuity and Navier-Stokes equations including the interactive forces and constraints as shown in Fig. 1a.
- 3) Nodal velocity components time histories are the distinctive features of the present formulation since the formulation using pressure as the only fluid field variable can provide only an elemental velocity calculated from the nodal pressures.
- 4) The elemental matrices are used in the numerical solution. This feature results in a considerable saving in computer storage and running time, in contrast with most schemes that the assembly and storage of system global matrices are essential to numerical solution.
- 5) In contrast with the approach used in Fig. 1c, the approaches described in Figs. 1a and 1b involve non-symmetric fluid matrices which precludes modal superposition method. Efficient numerical solution technique for the integration of these non-symmetric matrices are developed.

The approach used in this study is tested for a flow configuration consisting of water, between two elastic parallel plates, subjected to a step pressure at one end. Verification of the model is achieved by comparing the results with previous fluid elastic studies [11] based on the finite element discretization of solid matrix equation of motion and the two-dimensional wave equation including the interactive forces.

This dissertation is conveniently divided into three parts:

- Part (1): This part presents the finite element model for the rigid wall case.
- Part (2): This part presents the finite element model for the elastic wall case.
- Part (3): Part three, user's manual of this study is provided to aid the user in understanding the computer program and to use it effectively.

PART ONE

DEVELOPMENT AND RESULTS OF FINITE ELEMENT MODEL FOR THE

RIGID WALL CASE

## 1. INTRODUCTION

During the recent years, the finite element technique has been recognized as an effective analysis tool for the solution of a wide range of incompressible and compressible, inviscid and viscous flow problems including wave propagation phenomena [6]. Wave propagation problems are of particular interest in the loss-of-coolant accident analysis of pressurized water reactors.

Most investigators employ a stream function formulation for two-dimensional problems and a vorticity approach for three-dimensional flow fields which offer the advantage that one governing equation need be considered in the finite element discretization in a manner similar to structural analysis. The major disadvantage of stream function and vorticity approaches is the difficulty associated with the implementation of pressure, velocity, velocity gradient and stress boundary conditions. Several researchers have favored a formulation using the pressure and velocity as field variables thus avoiding the difficulty with the implementation of the boundary conditions [10]. However, this pressure-velocity formulation leads to non-symmetric matrices which precludes the application of the modal superposition to the finite element analysis [11]. The numerical solution would then require a direct numerical integration which is often hampered by excessive computer memory requirement and running time for the storage and algebraic manipulation of global matrices.

The main objective of this part is to develop an efficient technique for the finite element analysis of wave propagation problems in fluids employing the pressure-velocity formulation. This formulation reduces both the computer storage and running time requirements significantly by essentially working with the elemental matrices rather than the global matrices. Furthermore, each elemental matrix is broken into two submatrices—one diagonal matrix consisting of the terms along the diagonal and one matrix consisting of the off-diagonal coupling terms. The elemental diagonal matrices are assembled for the entire flow field, conveniently stored in a global array and kept in the left hand side of the matrix differential equations. The elemental off-diagonal matrices are stored individually and carried to the right hand side, multiplied by the respective freedom arrays and treated as time-dependent forcing functions. These elemental forcing functions are also stored in a global array. In this manner, boundary conditions on pressure and velocity as well as external forcing functions are easily introduced and the matrix equation reduces to a set of uncoupled ordinary differential equations which is readily solved by analytic integration.

The distinctive features of this efficient technique are small memory requirement, simple logic and reduced running time and computational cost. Problems requiring large high speed computers can be solved on minicomputers with limited storage and computational speed.

Specifically, this part presents a plane triangular finite element fluid model for wave propagation phenomena in a two-dimensional flow field employing the pressure-velocity formulation. This fluid element is verified numerically by solving a wave propagation flow problem consisting of water, between two flat plates, initially at rest and



accelerated suddenly by applying a step pressure at one end. The results obtained are compared with a previous study[11,12] based on the finite element discretization of the two-dimensional wave equation with a single-variable formulation in which pressure is considered as the only dependent variable ( referred to as the single-variable pressure formulation ).

## 2. MATHEMATICAL FORMULATION

The simplifying assumptions employed in the development of this fluid finite element model with pressure-velocity formulation are:

- 1) The fluid flow is assumed to be compressible, two-dimensional and isothermal.
- 2) The main dependent variables for the fluid are the pressure and the two components of velocity in x and y directions.
- 3) The conservation laws for the fluid flow are simplified by the weak wave approximation by assuming that the density oscillations are of small magnitude.
- 4) The components of fluid shear stress are assumed to be proportional to their respective velocity components.
- 5) The momentum flux terms in the equation of motion are neglected.

The above assumptions permit the verification of the results with a finite element model based on the two-dimensional wave equation.

The differential equations governing the motion of the fluid are given by:

Continuity equation:

$$\frac{\partial \rho}{\partial t} + \rho_f \left( \frac{\partial v_x}{\partial x} + \frac{\partial v_y}{\partial y} \right) = 0 \quad (1)$$

Momentum equations:

$$\frac{\partial v_x}{\partial t} = - \frac{1}{\rho_f} \frac{\partial p}{\partial x} - k_f v_x \quad (2)$$

$$\frac{\partial v_y}{\partial t} = - \frac{1}{\rho_f} \frac{\partial p}{\partial y} - k_f v_y \quad (3)$$

Equation of state:

$$\left(\frac{\partial p}{\partial \rho}\right)_s = c^2 = \text{Constant} \quad (4)$$

in which  $\rho$ ,  $p$ ,  $v_x$ ,  $v_y$  are fluid density, pressure and velocity components along  $x$  and  $y$  axis at time  $t$ ,  $c$  is velocity of the acoustic waves in the fluid,  $\rho_f$  is the mean fluid density, and  $k_f$  is the viscous damping coefficient. Eliminating  $\rho_f$  between equations (1) and (4), the governing equations of motion reduces to

$$\frac{1}{c^2} \frac{\partial p}{\partial t} + \rho_f \left( \frac{\partial v_x}{\partial x} + \frac{\partial v_y}{\partial y} \right) = 0 \quad (5)$$

$$\frac{\partial v_x}{\partial t} + \frac{1}{\rho_f} \frac{\partial p}{\partial x} + k_f v_x = 0 \quad (6)$$

$$\frac{\partial v_y}{\partial t} + \frac{1}{\rho_f} \frac{\partial p}{\partial y} + k_f v_y = 0 \quad (7)$$

As shown in Appendix 1, the discretization of the above equations on finite element subdivisions of the fluid region, shown in Fig.2, leads to

$$[D_e] \{\dot{Z}_e\} + [E_e] \{Z_e\} = 0 \quad (8)$$

where  $[D_e]$  and  $[E_e]$  are the unsymmetric fluid inertia and fluidity matrices for the element,  $\{Z_e\}$  is the elemental array involving nodal degrees of freedom--pressure,  $x$ -component of velocity, and  $y$ -component of velocity as defined in Appendix 1, and  $\{\dot{Z}_e\}$  is the time derivative of  $\{Z_e\}$ .

The pressure-velocity formulation permits the introduction of specified nodal pressure and/or velocity components into  $\{Z_e\}$  and  $\{\dot{Z}_e\}$

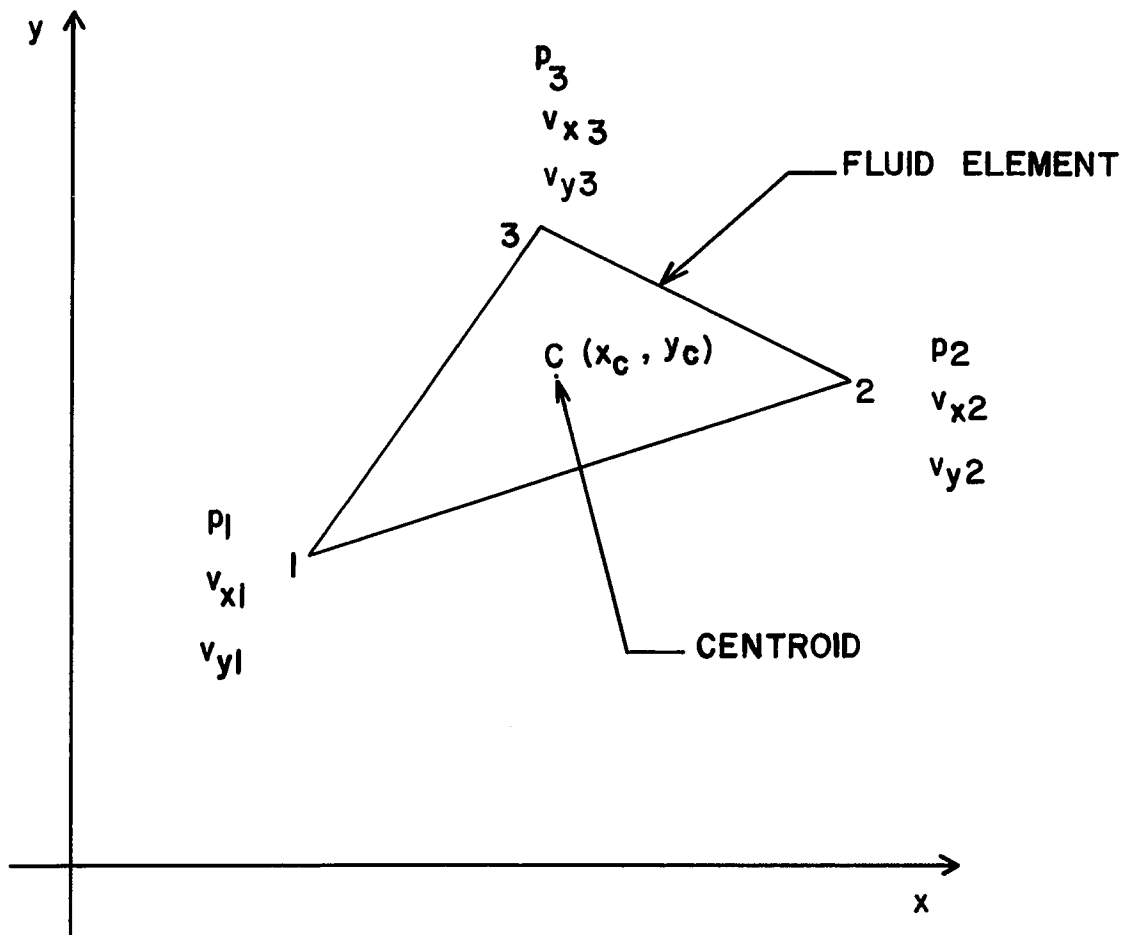


FIG. 2 PLANE TRIANGULAR FLUID FINITE ELEMENT FOR PRESSURE-VELOCITY FORMULATION

arrays. This is in contrast with the pressure formulation which is derived by the elimination of the velocity components  $v_x$  and  $v_y$  in equations (5), (6) and (7) leading to the two dimensional wave equation

$$\frac{\partial^2 p}{\partial x^2} + \frac{\partial^2 p}{\partial y^2} = \frac{1}{c^2} \left( \frac{\partial^2 p}{\partial t^2} + k_f \frac{\partial p}{\partial t} \right) \quad (9)$$

The discretization of the above equation on finite element subdivisions of the fluid region will then give the matrix differential equation based on the pressure formulation as follows [12]:

$$[G_e] \{\ddot{p}_e\} + [L_e] \{\dot{p}_e\} + [H_e] \{p_e\} = \{F_e\} \quad (10)$$

where  $[G_e]$ ,  $[L_e]$  and  $[H_e]$  are the elemental inertia, viscous damping and fluidity matrices,  $\{p_e\}$ ,  $\{\dot{p}_e\}$  and  $\{\ddot{p}_e\}$  are the elemental nodal pressure arrays, its first and second time derivatives, and  $\{F_e\}$  is the contribution due to the boundary integrals corresponding to the prescribed motion. The pressure formulation permits the introduction of specified pressures into  $\{p_e\}$ ,  $\{\dot{p}_e\}$  and  $\{\ddot{p}_e\}$  arrays. The specified boundary conditions on velocity components can be only implemented indirectly if these conditions can be expressed in terms of nodal pressures. The derivation of the elemental matrices and the boundary integral array for equation (10), the assembly of the global matrix equation and the numerical method of solution for the pressure formulation are presented elsewhere [12].

### 3. NUMERICAL SOLUTION

The numerical solution for the pressure-velocity formulation is achieved by first breaking each of the fluid matrices  $[D_e]$  and  $[E_e]$  in equation (8) into two submatrices -- one diagonal and one off-diagonal matrix. Upon substitution, equation (8) becomes

$$\overline{D}'_{e_j} \dot{\{Z_e\}} + \overline{E}'_{e_j} \{Z_e\} = - [D''_e] \dot{\{Z_e\}} - [E''_e] \{Z_e\} \quad (11)$$

where

$$[D_e] = \overline{D}'_{e_j} + [D''_e] \quad (12)$$

$$[E_e] = \overline{E}'_{e_j} + [E''_e] \quad (13)$$

in which  $\overline{D}'_{e_j}$  and  $\overline{E}'_{e_j}$  are two diagonal matrices whose terms are the diagonal terms of  $[D_e]$  and  $[E_e]$  respectively while  $[D''_e]$  and  $[E''_e]$  are off-diagonal matrices with zeros along their diagonals and off-diagonal terms equal to those of  $[D_e]$  and  $[E_e]$  respectively. Employing temporarily the past values of  $\dot{\{Z_e\}}$  and  $\{Z_e\}$  for the right hand side of equations (11), these equations become completely uncoupled and the elemental matrix equation becomes

$$\overline{D}'_{e_j} \dot{\{Z_e\}} + \overline{E}'_{e_j} \{Z_e\} = \{F'_e\} \quad (14)$$

where

$$\{F'_e\} = - [D''_e] \dot{\{Z_e\}}_o - [E''_e] \{Z_e\}_o \quad (15)$$

in which the diagonal matrices  $\overline{D}'_{e_j}$  and  $\overline{E}'_{e_j}$  as well as the forcing function  $\{F'_e\}$  can be conveniently stored in three separate arrays at significant savings in computational storage and time requirements. Assembling the above elemental equations for all n system elements, the

final differential equations for the flow field are

$$\overline{D}'_j \dot{\{Z\}} + \overline{E}'_j \{Z\} = \{F'\} \quad (16)$$

where

$$\overline{D}'_j = \sum_{e=1}^{e=n} \overline{D}'_{e_j} \quad \overline{E}'_j = \sum_{e=1}^{e=n} \overline{D}'_{e_j} \quad \{F'\} = \sum_{e=1}^{e=n} \{F'_e\} \quad (17)$$

Equation (16) constitutes a set of  $3n$  uncoupled first order differential equations with time-varying forcing function each having the following form

$$\sigma \dot{z} + \mu z = f(t) \quad (18)$$

in which  $\sigma$  and  $\mu$  are constants representing the diagonal terms of  $\overline{D}'_j$  and  $\overline{E}'_j$  respectively. Equation (18) can be readily integrated analytically within each small time increment  $\Delta t$  as follows:

1) If  $\sigma$  and  $\mu$  are nonzero,

$$z_j = z_{j-1} e^{-k\Delta t} + e^{-k\Delta t} \int_t^{t+\Delta t} e^{k\tau} f(\tau) d\tau \quad (19)$$

where

$$k = \frac{\mu}{\sigma}$$

and  $z_{j-1}$  and  $z_j$  are the present and the updated values of the integrated variables respectively. Since  $\Delta t$  is small, it would be possible to interpolate  $f(\tau)$  linearly in the interval  $t \leq \tau \leq t+\Delta t$  from present and updated values of "f" by

$$f(\tau) = f_{j-1} + (f_j - f_{j-1}) \frac{\tau}{\Delta t} \quad (20)$$

and perform the integration indicated by equation (19), assuming an

an average value for  $f = \frac{1}{2}(f_j + f_{j-1})$  within the time interval. Performing this operation one obtains

$$z_j = z_{j-1} e^{-k\Delta t} + \frac{1}{2\mu} (f_{j-1} + f_j) (1 - e^{-k\Delta t}) \quad (21)$$

and

$$\dot{z}_j = -k [z_{j-1} - \frac{1}{2\mu} (f_{j-1} + f_j) e^{-k\Delta t}] \quad (22)$$

2) If  $\sigma$  is nonzero but  $\mu$  is equal to zero

$$z_j = z_{j-1} + \frac{\Delta t}{2\sigma} (f_{j-1} + f_j) \quad (23)$$

and

$$\dot{z}_j = \frac{1}{2\sigma} (f_{j-1} + f_j) \quad (24)$$

It should be noted that since the updated values of  $f_j$  in the above equations are not yet known, an iterative procedure would be necessary. First, the value of  $f_j$  are set equal to  $f_{j-1}$  and the first trial values  $z_j^1$  and  $\dot{z}_j^1$  are calculated from equation (21) through (24). Substituting these values into equation (15), the first updated values are computed and used in equations (21) through (24) to calculate the second trial values  $z_j^2$  and  $\dot{z}_j^2$ . This iterative procedure is continued until the values of  $z_j$  converge within a prescribed error.

The combined analytical and iterative solution is repeated for successive time increments (with the origin of time at the beginning of each interval conveniently set equal to zero) until the entire problem time is covered.



#### 4. PRESENTATION OF RESULTS

The finite element model with pressure-velocity formulation, developed in this study, is verified by comparing the results with a previous study based on a finite element model with pressure considered as the only dependent variable, obtained from the two-dimensional wave equation [11,12]. A two-dimensional channel flow, 29.4" long and 24" wide with rigid wall, shown in Figure 3, is analyzed. Water initially at rest is accelerated suddenly by applying a step pressure  $p_0$  at the channel entrance while maintaining a zero pressure at the channel exit.

The flow region is divided into 48 triangular element as shown in Figure 4. Three values of viscous damping are studied: (1) inviscid case,  $k_f = 0$ ; (2) slightly viscous case,  $k_f = 1406.666 \text{ sec}^{-1}$ ; (3) highly viscous case,  $k_f = 3062.426 \text{ sec}^{-1}$ .

The FASINT digital program, described in part 3, is employed to solve the problem. Response time histories are obtained numerically for all three cases indicated above. Typical nodal pressure and axial velocity component for one position upstream and one position downstream are plotted for the present study employing the multi-variable pressure-velocity formulation, a previous study using single-variable pressure formulation based on two-dimensional wave equation [11,12], and a simplified one-dimensional analytical solution. The positions and variables selected for plotting are shown in Table 1 together with the corresponding figure numbers.

To establish the convergence of the numerical solution, the minimum

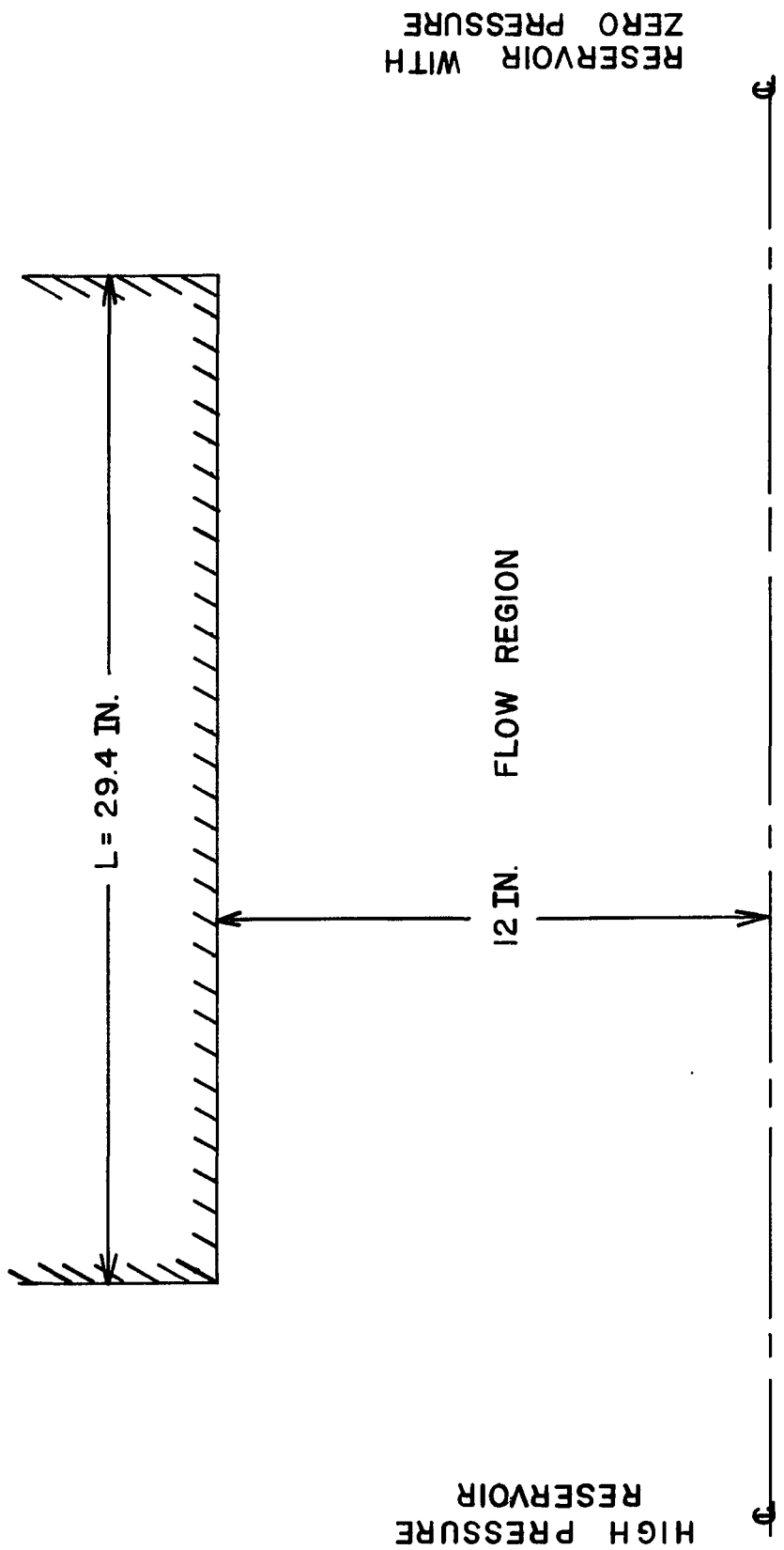
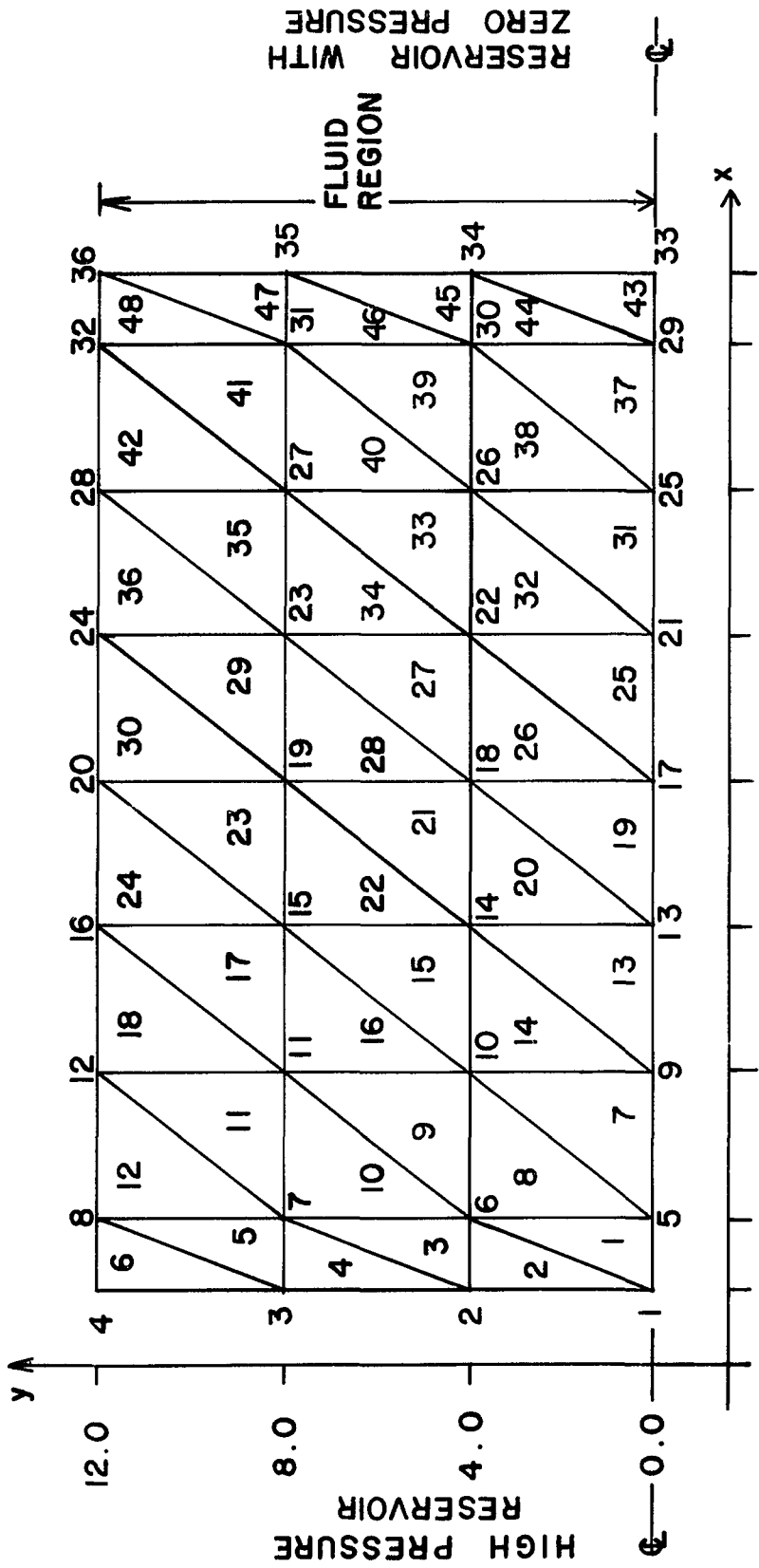


FIG. 3 TWO-DIMENSIONAL FLOW CONFIGURATION WITH RIGID WALL



0.0 6.9 11.1 15.3 19.5 23.7 27.9 30.0

FIG. 4 48 TRIANGULAR FINITE ELEMENT FLUID MODEL FOR PRESSURE-VELOCITY FORMULATION

Table 1.

Upstream and Downstream Positions

for which Time Histories are Plotted

Upstream Node i	Position $(x_i - x_1)/L$	Variable	Figs. No.	Downstream Node i	Position $(x_i - x_1)/L$	Variable	Figs. No.
9	0.214	p	4, 8, 10	25	0.786	p	5, 8, 10
10	0.214	p	4	26	0.786	p	5
11	0.214	p	4	27	0.786	p	5
12	0.214	p	4, 8, 10	28	0.786	p	5, 8, 10
9	0.214	$v_x$	6, 9, 11	25	0.786	$v_x$	7
13	0.357	$v_x$	6, 9, 11	29	0.929	$v_x$	7
14	0.357	$v_x$	6, 9, 11	30	0.929	$v_x$	7

period associated with the smallest length increment is calculated from the following relation

$$T_{\min} = 2\pi \frac{\ell_{\min}}{c}$$

Since  $\ell_{\min} = 2.1$  inches and  $c = 60,000$  in/sec,  $T_{\min}$  become equal to 0.00022. Examination of computer results shows that this period is indeed present in the nodal time histories on the element close to the element with the smallest length. To ascertain the convergence of the solution, the integration time step was set less than  $\frac{1}{50}$  th of this minimum period at  $\Delta t = 0.0000025$  sec. This time increment led to a convergent solution for all cases studied. The convergence of the solution was established when doubling the time interval produced no significant change in the pressure and velocity time histories.

The inviscid flow pressure and velocity time histories are typically shown in Figs. 5 to 8. The pressure time responses at upstream and downstream nodes, shown in Figs. 5 and 6, for both the multi-variable pressure-velocity formulation and the single-variable pressure formulation (based on the two-dimensional wave equation) oscillate about the simplified one-dimensional analytically-calculated rectangular wave form and are all in reasonable agreement. However, the simplified one-dimensional analytical solution allows only axial motion or pressure variation and, therefore, cannot be expected to be accurate for a two-dimensional flow field under consideration. The single-variable approach allows a two-dimensional pressure variation and for this reason the pressure response is oscillatory. This oscillatory behavior has also been observed by many investigators such as: 1) Conway and Jakubowski [ 3 ] who investigated wave propagation in axially impacted bars of short length

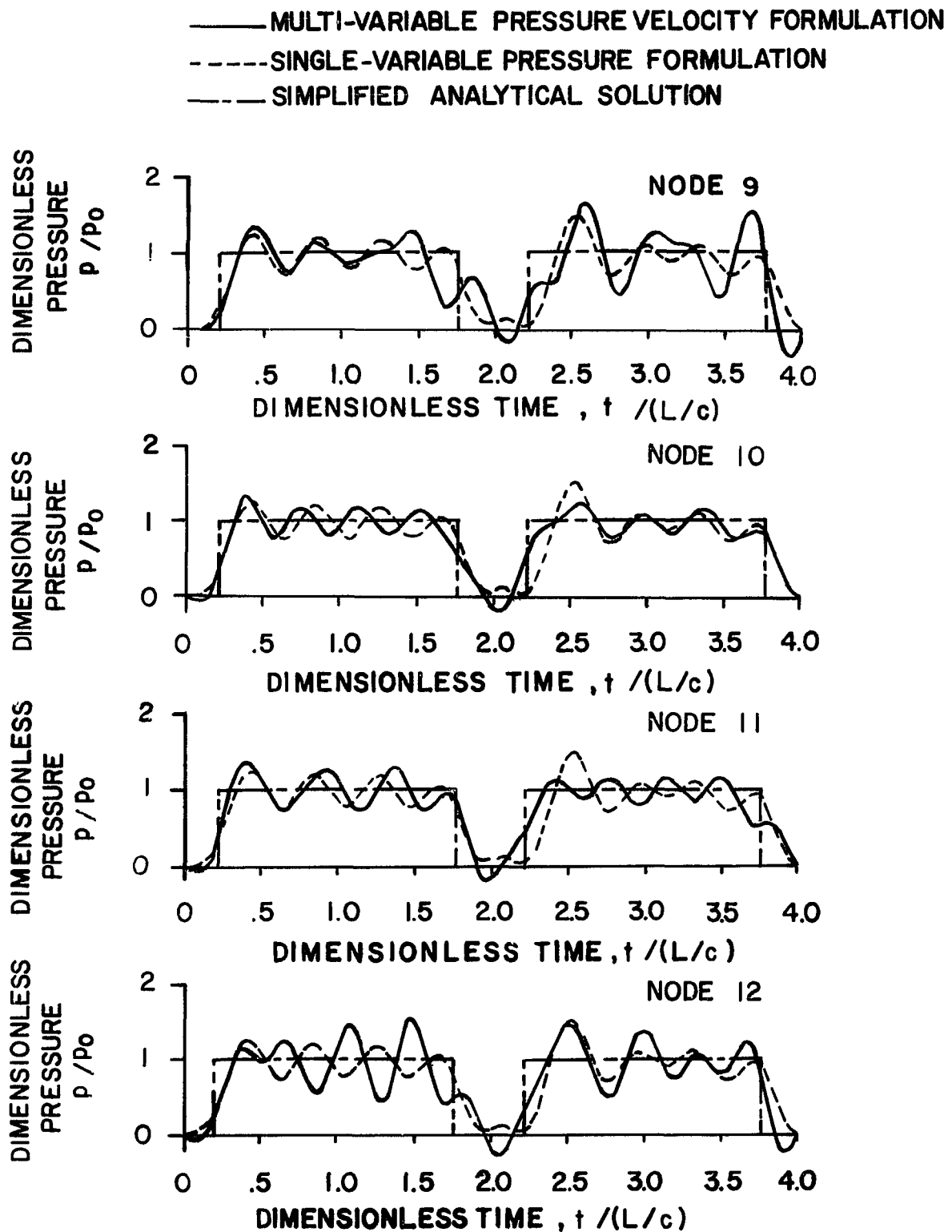


FIG. 5 A COMPARISON OF MULTI-VARIABLE AND SINGLE-VARIABLE PRESSURE TIME HISTORIES FOR INVISCID CASE AT  $x = 6.9$  INCHES

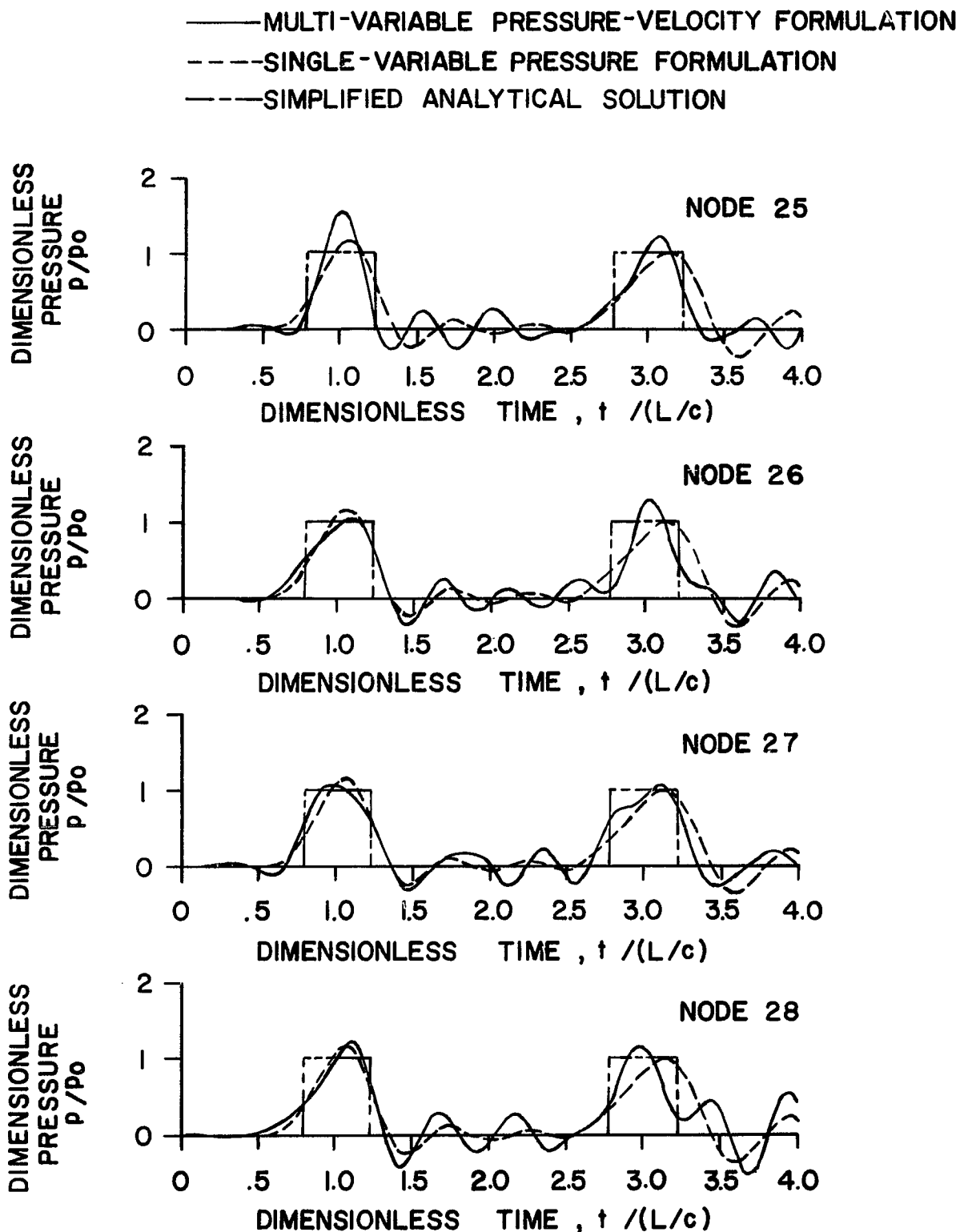


FIG. 6 A COMPARISON OF MULTI-VARIABLE AND SINGLE-VARIABLE PRESSURE TIME HISTORIES FOR INVISCID CASE AT  $x = 23.7$  INCHES

experimentally and analytically; and 2) Zielké[22] , Holmboe and Rouleau [ 9 ], and Tarantine and Rouleau [20] who conducted experiments on the propagation of pressure pulse and flow surge in liquid transmission lines and compared the results with theory.

However, since the velocity components are not among the system degrees of freedom in the single-variable pressure formulation, the time response is not fully realistic. The multi-variable approach allows for a complete two-dimensional pressure and velocity variation and for this reason the pressure response is somewhat more oscillatory and, therefore, more realistic as compared with the single-variable pressure formulation. To demonstrate the feedback effect between the nodal pressure and the velocity components, the y velocity component for node 10 is typically plotted in Fig. 7. The y-component of velocity at node 10 oscillates about zero because of the fluid compressibility and transversal boundary constraints. These oscillations affect the x-component of velocity at node 10 and make it more oscillatory which in turn increases the pressure-velocity vibratory response amplitudes in the entire flow field.

The velocity time response at upstream and downstream nodes, shown in Figs. 7 and 8, are the distinctive features of the pressure-velocity formulation presented herein since the single-variable pressure formulation can provide only an elemental velocity calculated from the nodal pressures. A comparison between the multi-variable and single-variable velocity time histories has been made possible by averaging the nodal velocities from the multi-variable study and comparing the result with the elemental velocity from the single-variable approach which show a good agreement.

The pressure and velocity time histories for slightly viscous case



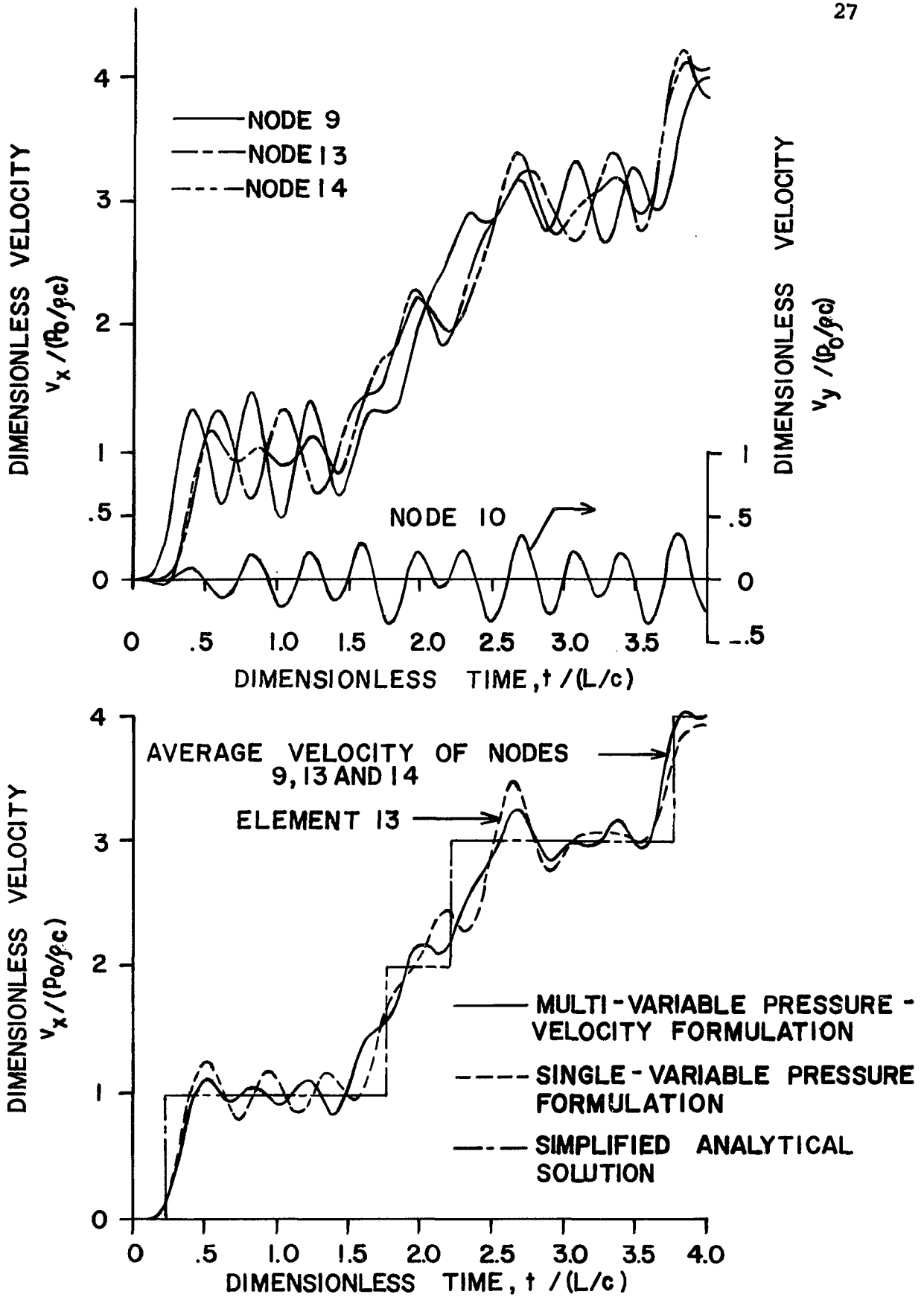


FIG. 7 A COMPARISON OF MULTI-VARIABLE AND SINGLE-VARIABLE VELOCITY TIME HISTORIES FOR INVISCID CASE FOR ELEMENT 13

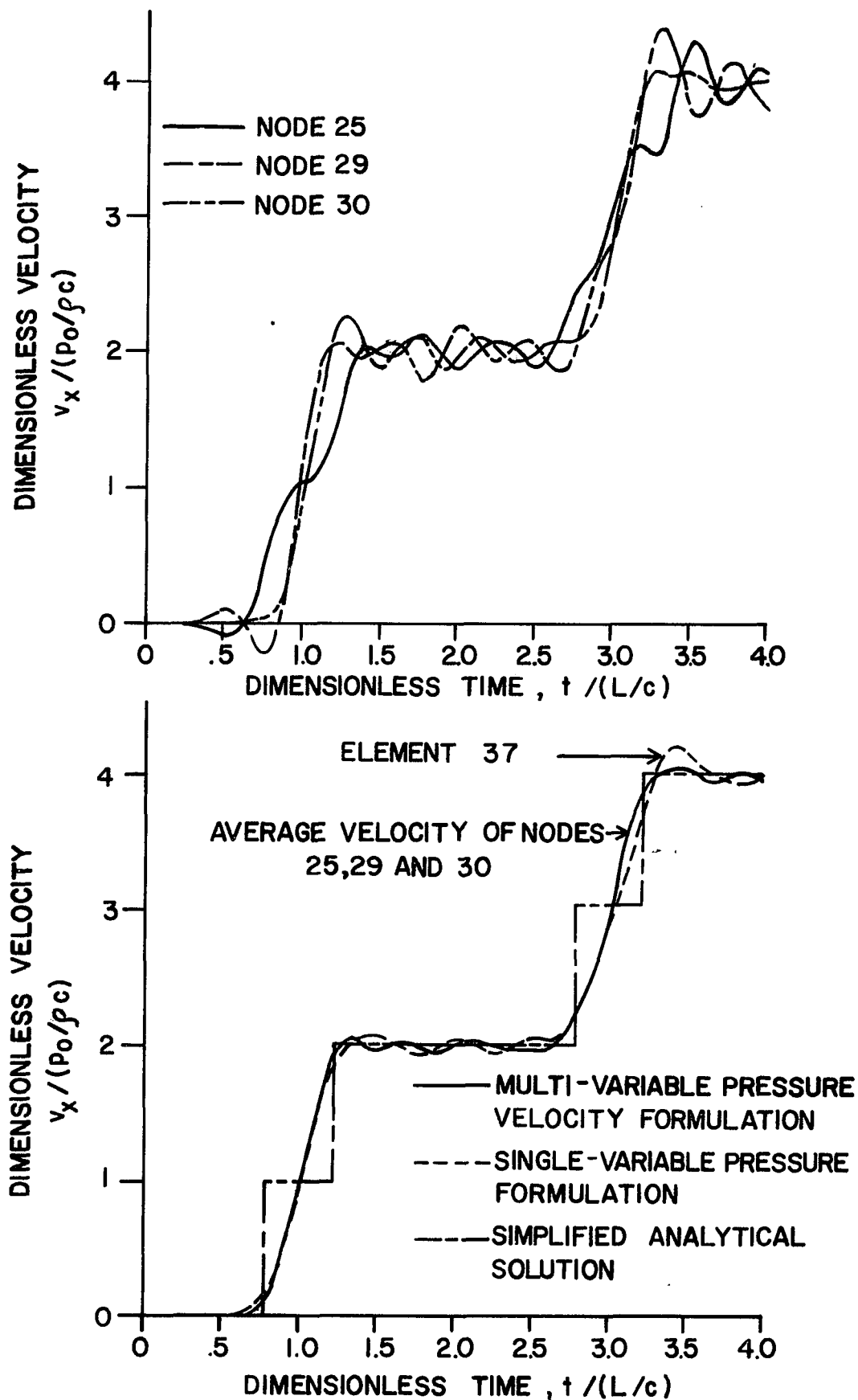


FIG. 8 A COMPARISON OF MULTI-VARIABLE AND SINGLE-VARIABLE VELOCITY TIME HISTORIES FOR INVISCID CASE FOR ELEMENT 37

typically shown in Figs.9 and 10, exhibit a pattern similar to inviscid flow case except for the fact that all responses clearly show the viscous damping effect and indicate that ultimately a steady state pressure and velocity distribution will be reached.

The pressure and velocity time histories for highly viscous case typically shown in Figs. 11 and 12, exhibit a highly damped behavior and closely follow the single-variable and simplified analytical solutions. This is to be expected since the highly viscous condition tends to damp out the transverse pressure gradients and velocities and reduce their feedback on the longitudinal pressure and velocity distribution. All pressure and velocity responses approach their final steady state values. All physical data for the cases studied are presented in Table 2.

Table 2. Physical Data for the Rigid Wall Case

<u>Parameter</u>	<u>SI Unit</u>	<u>British Unit</u>
Density	999.78 N sec <sup>2</sup> /m <sup>4</sup>	9.3552 x 10 <sup>-5</sup> lbf-sec <sup>2</sup> /in <sup>4</sup>
Speed of sound	1524. m/sec	6 x 10 <sup>4</sup> in/sec
Pressure at channel inlet	68948. Pa	10 psia
Channel length	0.747 m	29.4 in
Channel width	0.61 m	24.0 in
Viscous damping:		
Inviscid case	0. sec <sup>-1</sup>	0. sec <sup>-1</sup>
Slightly viscous case	1046.666 sec <sup>-1</sup>	1046.666 sec <sup>-1</sup>
Highly viscous case	3062.467 sec <sup>-1</sup>	3062.467 sec <sup>-1</sup>

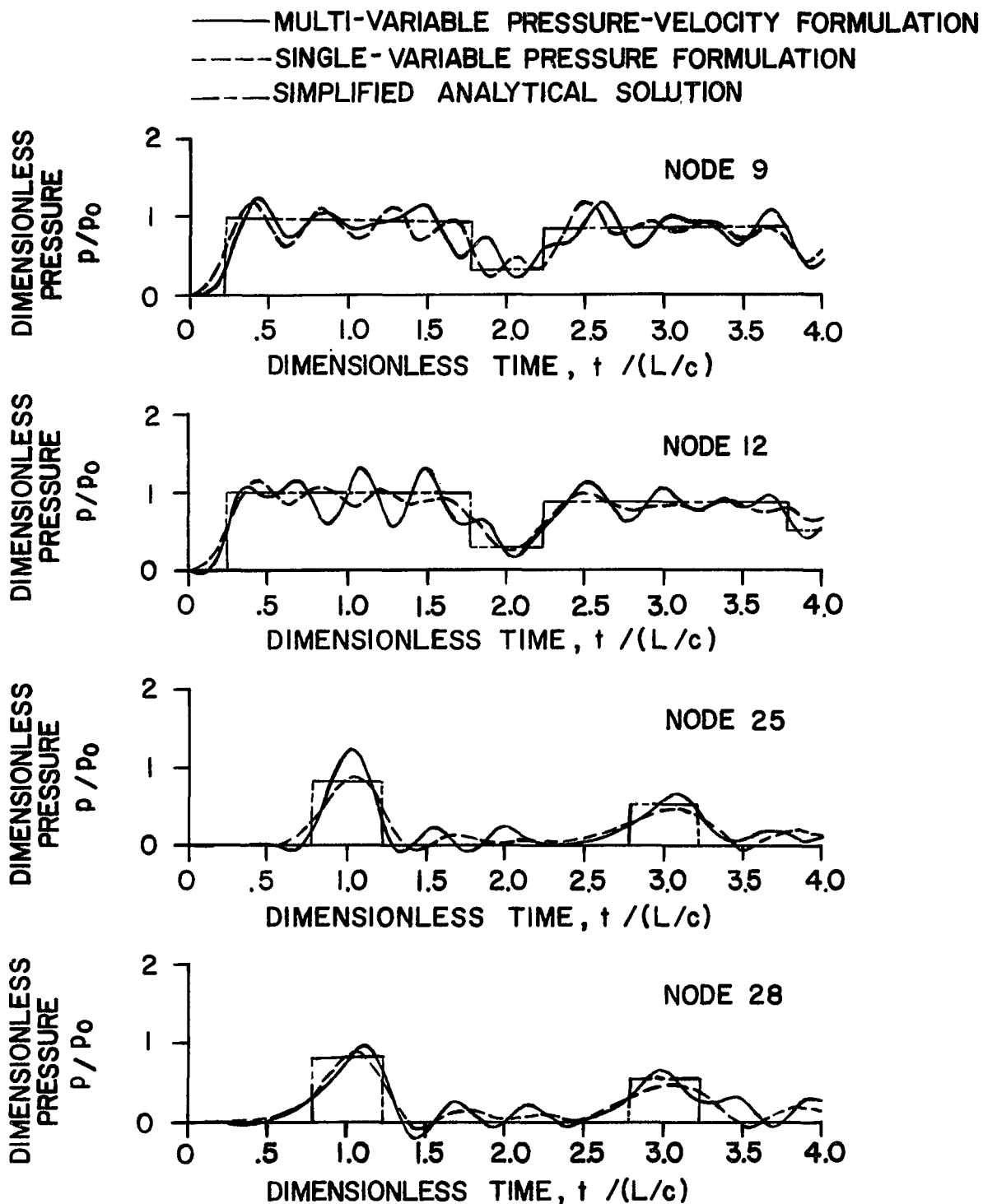


FIG. 9 A COMPARISON OF MULTI-VARIABLE AND SINGLE-VARIABLE PRESSURE TIME HISTORIES FOR SLIGHTLY VISCOUS CASE AT  $x = 6.9$  AND  $x = 23.7$  INCHES

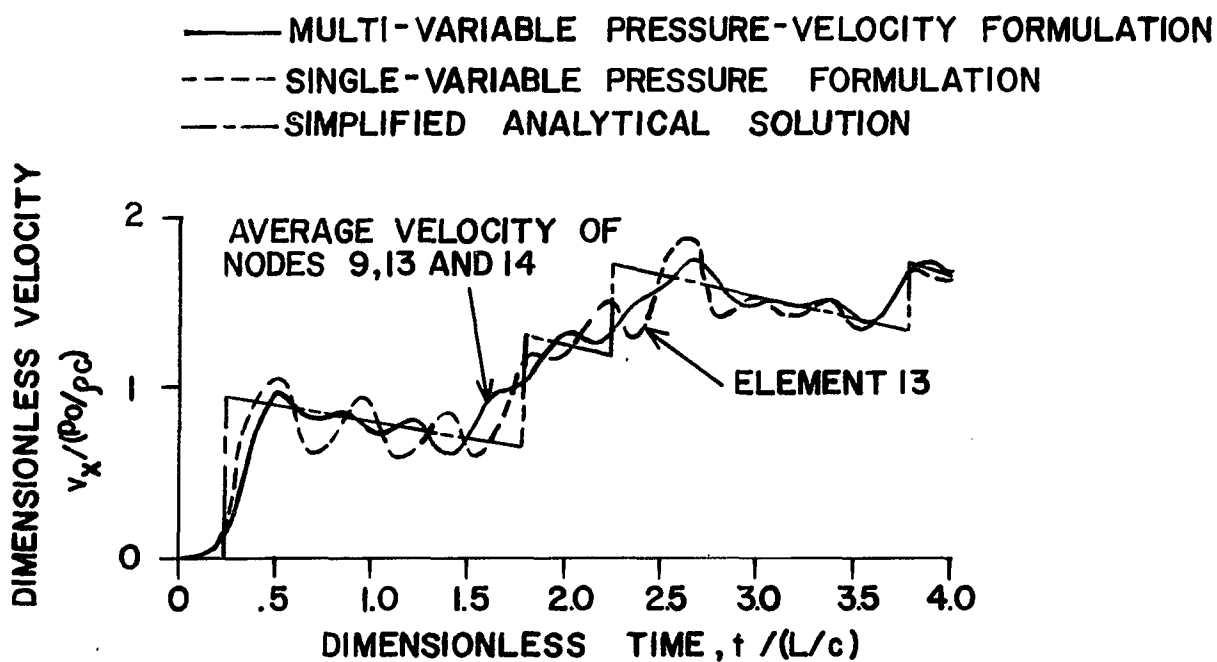
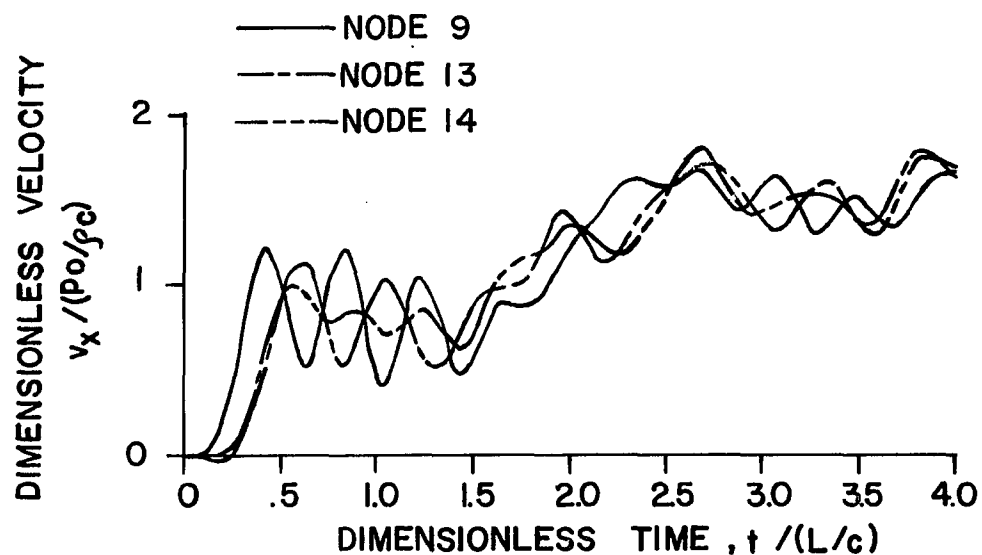


FIG. 10 A COMPARISON OF MULTI-VARIABLE AND SINGLE-VARIABLE VELOCITY TIME HISTORIES FOR SLIGHTLY VISCOUS CASE FOR ELEMENT 13

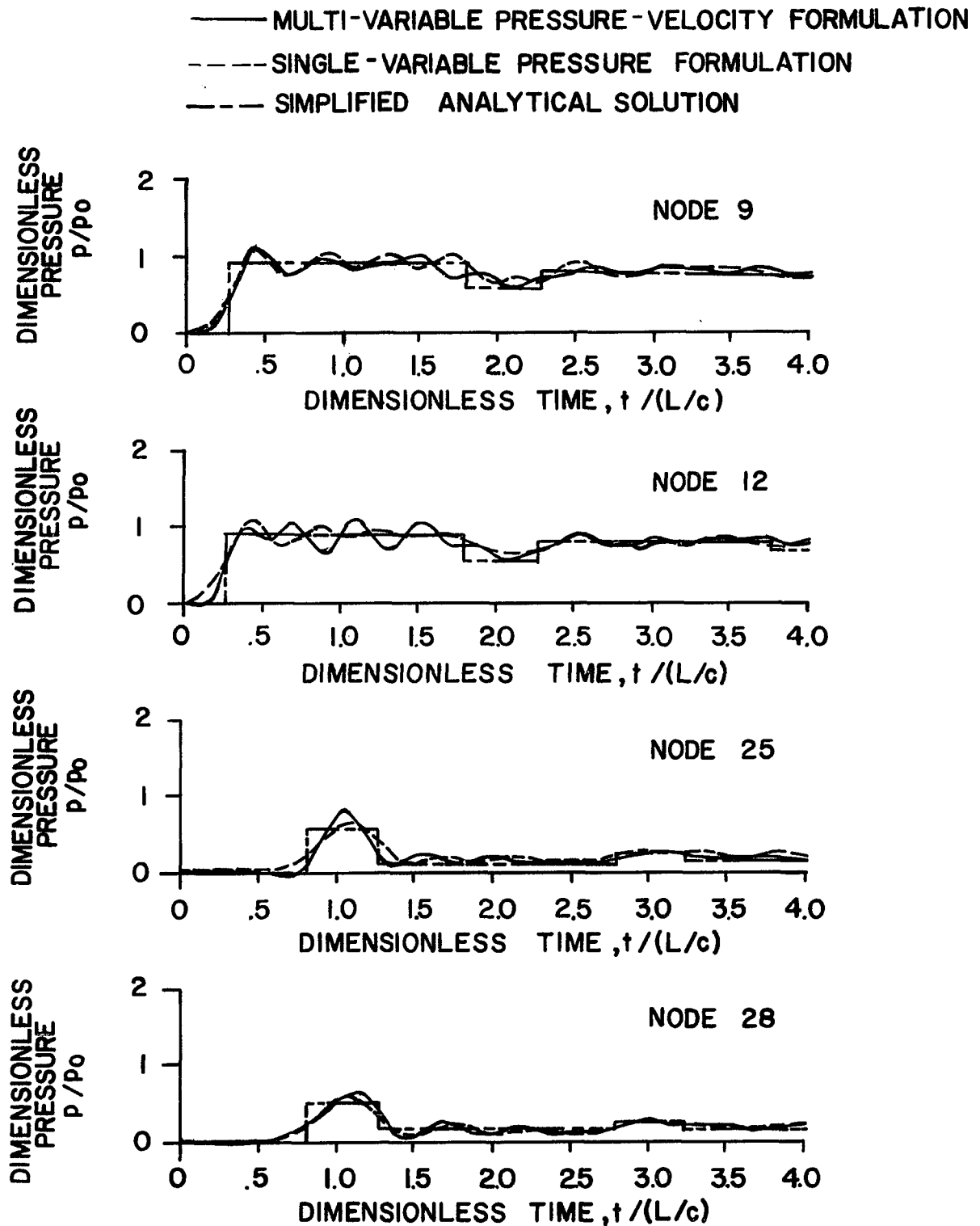


FIG. 11 A COMPARISON OF MULTI-VARIABLE AND SINGLE-VARIABLE PRESSURE TIME HISTORIES FOR HIGHLY VISCOUS CASE AT  $x = 6.9$  AND  $x = 23.7$  INCHES

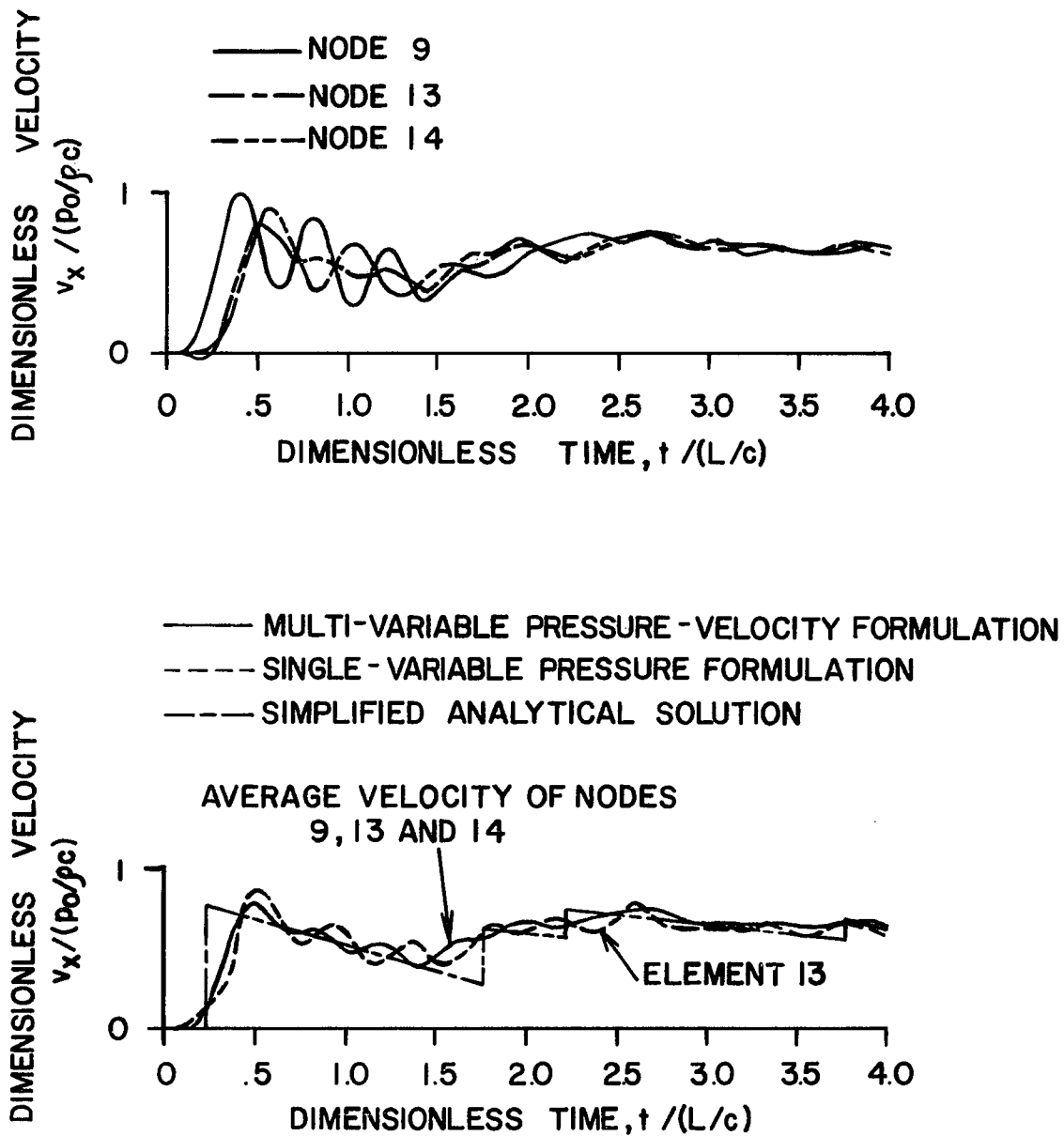


FIG. 12 A COMPARISON OF MULTI-VARIABLE AND SINGLE-VARIABLE VELOCITY TIME HISTORIES FOR HIGHLY VISCOUS CASE FOR ELEMENT 13

## 5. CONCLUSIONS

A multi-variable technique for the finite element analysis of wave propagation problems in fluids is presented. The main distinctive features of this technique are:

- 1) The mathematical formulation is based on the pressure-velocity formulation which facilitates the implementation of boundary conditions in terms of pressure and velocity components. This is in contrast with stream function, vorticity and pressure formulation for which realistic boundary conditions cannot be readily implemented.
- 2) The elemental matrices are used directly in the numerical solution. This feature results in a considerable saving in computer storage and running time -- in contrast with most schemes that the assembly and storage of system global matrices are essential to the numerical solution.

Based on this multi-variable pressure-velocity formulation, a plane triangular finite element fluid model for wave propagation phenomena in a two-dimensional flow field is developed. This model is verified by solving a wave propagation flow problem and comparing the results with a previous study based on a single-variable pressure formulation considering pressure as the only dependent variable. The agreement between the two models are confirmed with a parametric study using inviscid, slightly viscous and highly viscous flows.



PART TWO

DEVELOPMENT AND RESULTS OF FINITE ELEMENT MODEL FOR THE

ELASTIC WALL CASE

## 1. INTRODUCTION

Flow induced vibration is frequently encountered in the operation of many reactor systems and components. Vibratory stresses and dynamic instabilities of reactor fuel bundle and heat exchanger tubes are a few examples of flow induced vibration phenomena which have been studied extensively both experimentally and analytically. State of the art reviews of flow induced problems have also been undertaken [17,1,2].

Four types of vibratory patterns are generally involved:

- 1) Turbulent excitation which is independent of the structural motion and has a broad frequency spectrum.
- 2) Discrete frequency excitation or vortex shedding which is also independent of structural motion and has a definite period. This phenomenon is observed in cross-flow past heat exchanger tube banks. Vortices are periodically shed from alternate sides of the tubes, causing a wavy flow pattern in the wake.
- 3) Acoustic oscillations normal to both flow direction and tube or rod axis which in a rectangular duct has a wave length equal to twice the duct width for its lowest frequency. This oscillation is also unrelated to the tube motion.
- 4) Structural natural frequency oscillations which is mechanically related to the tube or rod motion and is a function of the structural rigidity, density, geometry and support boundary conditions.

Flow induced vibration in reactor system components occurs when two or more of the above vibratory patterns coincide with one another as described in the following situations.

- 1) A natural frequency of the structure falls within the frequency spectrum of turbulent pressure fluctuations giving rise to resonance referred to as "buffeting".
- 2) The frequency of vortex shedding at a particular flow rate coincides with the natural acoustic frequency of the component. The two systems thus couple, the kinetic energy in the flow stream is converted into acoustic pressure waves.
- 3) A structural natural frequency may be near the vortex shedding frequency. The tube or rod will then start to vibrate and reinforce the vortex shedding causing severe noise and structural fatigue failures. This is referred to as forced vibration.
- 4) The position of the structure with respect to the incident stream may cause a transverse fluid force on the structure producing instability and self-excited vibration characterized by continual lateral displacements. The forces causing this instability are affected by the deflection of the structure from its undeformed state. This is referred to as fluid elastic excitation, flutter, or galloping. A study of fluid elastic excitations requires the consideration of both solid and fluid motions including their interactive forces and constraints. Mathematically, this poses a more difficult problem than the other flow-induced vibration patterns enumerated above.

The purpose of this study is to examine the problem of fluid elastic excitation by developing a mathematical model for interaction between an elastic solid and a fluid medium using a finite element approach. A previous study of these problems employed the solid displacements and the fluid pressure as the only nodal degrees of freedom[11] in which the fluid finite element was based on the discretization of the two-dimensional

wave equation. This fluid element, referred to as single-variable pressure formulation does not provide a convenient means for the implementation of boundary conditions involving velocity components. The objective of this study is to employ the solid displacement and the fluid pressure and velocity components as the nodal degrees of freedom. In this approach the fluid finite element will be based on the discretization of the two-dimensional continuity and momentum equations.

The distinctive features of this study are that it provides a means for the implementation of both pressure and velocity boundary conditions and lays the foundation for the ultimate coupling between a structure represented by the matrix equations of motion and a flow field simulated by the continuity and Navier-Stokes equations.

Specifically, this part presents a plane triangular finite element solid-fluid model for wave propagation phenomena in a two-dimensional flow field employing the matrix pressure-velocity formulation for the fluid and the matrix displacement formulation for the solid. This solid-fluid model is verified by solving a wave propagation problem consisting of water, between two elastic parallel plates, initially at rest and accelerated suddenly by applying a step pressure at one end. The results obtained are compared with previous fluid elastic studies [11] based on the fluid finite element discretization of the two-dimensional wave equation with a single-variable pressure formulation as well as with previous wave propagation studies between two rigid parallel plates described in part one.

## 2. MATHEMATICAL FORMULATION

The simplifying assumptions employed in this study are as follows:

- 1) The solid continuum is assumed to be perfectly elastic and the fluid flow is compressible and isothermal.
- 2) The solid and fluid continua are considered to be two dimensional. The main dependent variables of the solid are two components of displacement in x and y directions and those of the fluid are the pressure and the two components of velocity in x and y directions.
- 3) The solid continuum undergoes small in-plane deformations while the fluid continuum experiences density changes of small magnitude. This allows the simplification of the flow momentum equations by the weak wave approximation.
- 4) Structural damping is considered by introducing damping matrices proportional to stiffness and/or mass matrices. Fluid friction is taken into account by assuming that the components of the fluid shear stress is proportional to their respective velocity components.
- 5) The momentum flux terms in the equations of motion is neglected.

The above assumptions permit the verification of the results with previous solid-fluid interaction studies based on a two-dimensional wave equation[11]. The finite element model is presented in the following sections entitled fluid element, solid element, and solid-fluid super-element and detailed further in Appendices 1 through 4.

### Fluid Element

The fluid finite element, used in this study, is developed by

employing the method of weighted residuals. The two-dimensional momentum and continuity equations in terms of the fluid pressure and velocity components are discretized on finite element subdivisions of the fluid region, as shown in the Appendices 1 and 2, leading to the following matrix differential equation for each fluid element shown in Fig.2.

$$[D_e] \dot{\{Z_e\}} + [E_e] \{Z_e\} = 0 \quad (25)$$

where  $[D_e]$  and  $[E_e]$  are the unsymmetric fluid inertia and fluidity matrices for the element,  $\{Z_e\}$  is the elemental array involving nodal degrees of freedom (pressure, x-component of velocity, and y-component of velocity), and  $\dot{\{Z_e\}}$  is the time derivative of  $\{Z_e\}$ .

It should be noted that the pressure-velocity formulation, employed above, permits the introduction of nodal pressure and velocity boundary values into  $\{Z_e\}$  and  $\dot{\{Z_e\}}$  arrays. This is in contrast with the pressure formulation, based on the discretization of the two-dimensional wave equation, expressed by [11]

$$[G_e] \ddot{\{p_e\}} + [L_e] \{\dot{p}_e\} + [H_e] \{p_e\} = \{F_e\} \quad (26)$$

in which the velocity boundary conditions can be implemented indirectly only if they can be expressed in terms of pressure.

### Solid Element

The solid finite element is obtained by applying the principle of virtual work to the solid [ 23, 16, 7 ]. This procedure yields the matrix differential equation for the nodal displacements of the solid element shown in Fig. 13.

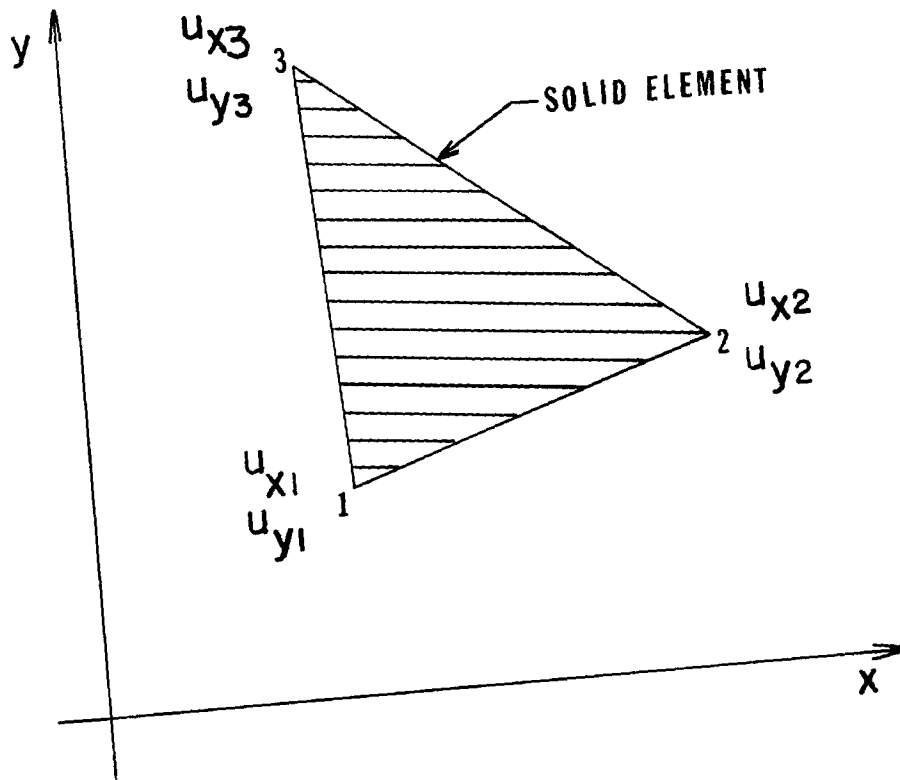


FIG. 13 PLANE TRIANGULAR SOLID FINITE ELEMENT

$$[M_e] \{\ddot{U}_e\} + [C_e] \{\dot{U}_e\} + [K_e] \{U_e\} = \{R_e\} + \{R'_e\} \quad (27)$$

This formulation permits the application of boundary conditions that can be represented by specified nodal displacements.

### Solid-Fluid Superelement

The solid-fluid superelement, shown in Fig.14, is constructed by combining the solid and fluid element while at the same time including the interaction between the two elements. For the solid part, the interactive term is the pressure force acting normal to the moving solid boundary. For the fluid part, the interaction is expressed by making the fluid nodal velocity components equal to the solid velocity components. The matrix differential equation for the solid-fluid superelement, shown in Fig. 14, becomes

$$\begin{bmatrix} M_e & 0 \\ 0 & 0 \end{bmatrix} \begin{Bmatrix} \ddot{U}_e \\ \ddot{Z}_e \end{Bmatrix} + \begin{bmatrix} C_e & 0 \\ 0 & D_e \end{bmatrix} \begin{Bmatrix} \dot{U}_e \\ \dot{Z}_e \end{Bmatrix} + \begin{bmatrix} K_e & 0 \\ 0 & E_e \end{bmatrix} \begin{Bmatrix} U_e \\ Z_e \end{Bmatrix} = \begin{Bmatrix} [S_e] \{p_e\} \\ 0 \end{Bmatrix} + \begin{Bmatrix} R'_e \\ 0 \end{Bmatrix} \quad (28)$$

together with a constraint that for nodal points on the solid-fluid boundary

$$\{v_{ye}\} = \{\dot{u}_{ye}\} \quad (29)$$

The boundary conditions applicable to equation (28) are those indicated for the solid and fluid parts.

The elemental matrices for the fluid element and the solid-fluid superelement are non-symmetric. This precludes the application of the



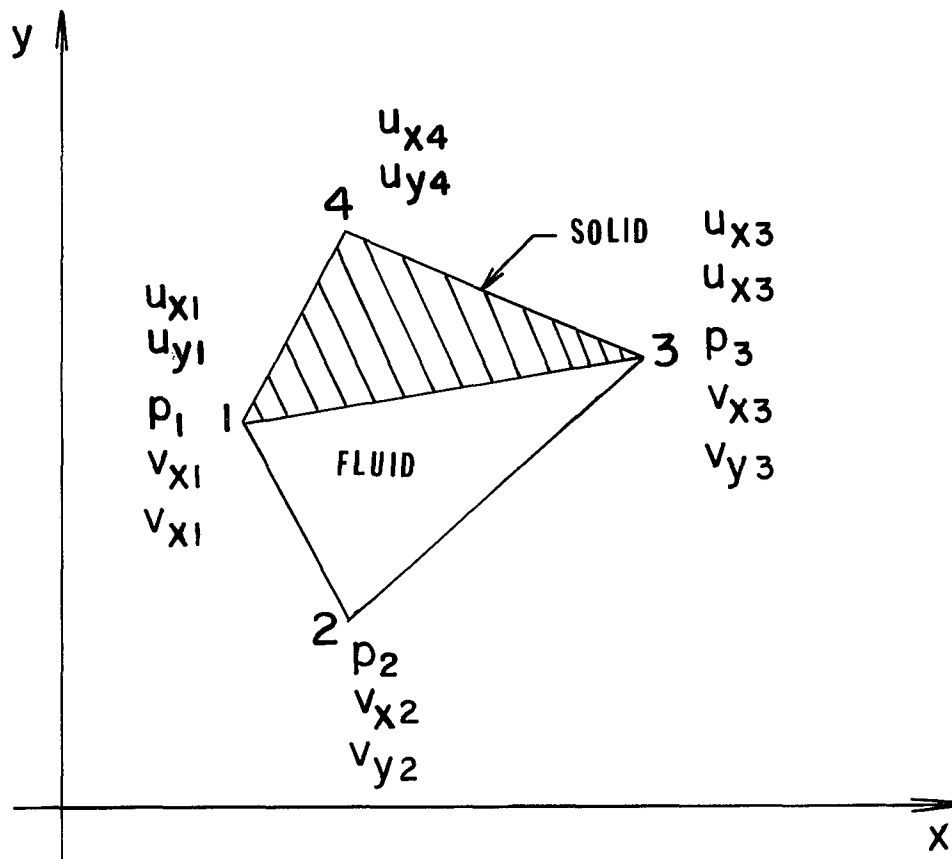


FIG. 14 PLANE QUADRILATERAL SOLID-FLUID SUPERELEMENT

modal superposition technique to the numerical solution of the problem. A direct numerical integration would require excessive computer memory and running time for the storage and algebraic manipulation of the global matrices. For these reasons, the numerical solution is obtained by a combination of matrix decomposition, analytical integration and iterative scheme discussed in the next section.

### 3. NUMERICAL SOLUTION

The elemental matrix equation, equations (25), (27), and (28) for the fluid, solid and solid-fluid elements are all in the following general form

$$[\bar{M}_e] \{\ddot{X}_e\} + [\bar{C}_e] \{\dot{X}_e\} + [\bar{K}_e] \{X_e\} = \{F_e\} \quad (30)$$

For the fluid element and the fluid part of the solid-fluid superelement, the contribution of  $[\bar{M}_e]$  is zero as indicated by equations (25) and (28) respectively. The numerical solution is achieved by breaking each of the elemental matrices  $[\bar{M}_e]$ ,  $[\bar{C}_e]$  and  $[\bar{K}_e]$  into two submatrices -- one diagonal matrix and one off-diagonal matrix such that equation (30) can be expressed by

$$[\bar{M}'_{e_j}] \{\ddot{X}_e\} + [\bar{C}'_{e_j}] \{\dot{X}_e\} + [\bar{K}'_{e_j}] \{X_e\} = \{F_e\} - [\bar{M}''_e] \{\ddot{X}_e\} - [\bar{C}''_e] \{\dot{X}_e\} - [\bar{K}''_e] \{X_e\} \quad (31)$$

in which  $[\bar{M}'_{e_j}]$ ,  $[\bar{C}'_{e_j}]$  and  $[\bar{K}'_{e_j}]$  are three diagonal matrices whose terms are the diagonal terms of  $[\bar{M}_e]$ ,  $[\bar{C}_e]$  and  $[\bar{K}_e]$  respectively, while  $[\bar{M}''_e]$ ,  $[\bar{C}''_e]$  and  $[\bar{K}''_e]$  are off-diagonal matrices with zeros along their diagonal and off-diagonal terms equal to those of  $[\bar{M}_e]$ ,  $[\bar{C}_e]$  and  $[\bar{K}_e]$  respectively. Furthermore,  $\{F_e\}$  represent the array of interactive forces exerted by the fluid on the solid in addition to the external forces acting on the solid, if any. It should be noted that, in contrast with the single-variable pressure formulation [11] where the interaction of solid on the fluid appears as inertial forces, in the multi-variable pressure-velocity formulation equation (29) expresses the constraint imposed by the solid on the fluid. Employing temporarily the past values of  $\{\ddot{X}_e\}$ ,

$\{\dot{X}_e\}$  and  $\{X_e\}$  for the right hand of equation(31), this equation becomes completely uncoupled and the elemental matrix equation becomes

$$\overline{M}'_{e_j} \{\ddot{X}_e\} + \overline{C}'_{e_j} \{\dot{X}_e\} + \overline{K}'_{e_j} \{X_e\} = \{F'_e\} \quad (32)$$

where

$$\{F'_e\} = \{F_e\} - [\overline{M}''_e] \{\ddot{X}_e\}_o - [\overline{C}''_e] \{\dot{X}_e\}_o - [\overline{K}''_e] \{X_e\}_o \quad (33)$$

in which the diagonal matrices  $\overline{M}'_{e_j}$ ,  $\overline{C}'_{e_j}$  and  $\overline{K}'_{e_j}$  as well as the forcing function  $\{F'_e\}$  can be conveniently stored in four separate arrays. This feature results in significant saving in computational storage and time requirement.

Assembling the above elemental equations for all n system elements, the global matrix differential equations for the discretized solid-fluid continua is obtained

$$\overline{M}'_j \{\ddot{X}\} + \overline{C}'_j \{\dot{X}\} + \overline{K}'_j \{X\} = \{\overline{F}'\} \quad (34)$$

where

$$\begin{aligned} \overline{M}'_j &= \sum_{e=1}^{e=n} \overline{M}'_{e_j} \\ \overline{C}'_j &= \sum_{e=1}^{e=n} \overline{C}'_{e_j} \\ \overline{K}'_j &= \sum_{e=1}^{e=n} \overline{K}'_{e_j} \\ \{\overline{F}'\} &= \sum_{e=1}^{e=n} \{F'_e\} \end{aligned} \quad (35)$$

Equation(34) constitutes a set of uncoupled second order differential

equations with time varying forcing function each having the following form

$$\lambda \ddot{x} + \sigma \dot{x} + \mu x = f(t) \quad (36)$$

in which  $\lambda$ ,  $\sigma$  and  $\mu$  are constants representing the diagonal terms of  $[\bar{M}]_j$ ,  $[\bar{C}]_j$  and  $[\bar{K}]_j$  respectively. Equation (36) can be readily integrated within each small time increment  $\Delta t$  by assuming a linear variation of  $f(t)$  given by

$$\bar{f}(t) = \frac{1}{2} ( f_j + f_{j-1} ) \quad (37)$$

in which  $f_{j-1}$  refers to the value of  $f(t)$  at time  $t$  and  $f_j$  refers to the value of  $f(t)$  at time  $t+\Delta t$  to be determined by an iterative procedure as will be described later.

Case (1) : Values of  $\lambda$ ,  $\sigma$  and  $\mu$  are nonzero. For this case which occurs for solid nodes, equation (36) may be written as follows:

$$\ddot{x} + 2 \xi \omega_n \dot{x} + \omega_n^2 x = \frac{\bar{f}}{\lambda} \quad (38)$$

where

$$\omega_n = \sqrt{\frac{\mu}{\lambda}} \quad \xi = \frac{1}{2\omega_n} \frac{\sigma}{\lambda} \quad (39)$$

If  $\xi < 1$ , the undamped solution is given by

$$x_j = e^{-\xi \omega_n \Delta t} ( A_1 \cos \omega_d \Delta t + A_2 \sin \omega_d \Delta t ) + \frac{\bar{f}}{\mu} \quad (40)$$

where

$$A_1 = x_{j-1} - \frac{\bar{f}}{\mu}$$

$$A_2 = \frac{1}{\omega_d} \left[ \dot{x}_{j-1} + \xi \omega_n \left( x_{j-1} - \frac{\bar{f}}{\mu} \right) \right]$$

$$\omega_d = \omega_n \sqrt{1 - \xi^2} \quad (41)$$

If  $\xi = 1$ , the critically damped solution is given by

$$x_j = (A_1 + A_2' \Delta t) e^{-\omega_n \Delta t} + \frac{\bar{f}}{\mu} \quad (42)$$

where

$$A_2' = \dot{x}_{j-1} + \omega_n \left( x_{j-1} - \frac{\bar{f}}{\mu} \right) \quad (43)$$

If  $\xi > 1$ , the overdamped solution is given by

$$x_j = B_1 e^{r_1 \Delta t} + B_2 e^{r_2 \Delta t} + \frac{\bar{f}}{\mu} \quad (44)$$

where

$$r_1 = \omega_n \left( -\xi + \sqrt{\xi^2 - 1} \right)$$

$$r_2 = \omega_n \left( -\xi - \sqrt{\xi^2 - 1} \right)$$

$$B_1 = - \frac{\dot{x}_{j-1} - r_2 [x_{j-1} - (\bar{f}/\mu)]}{r_2 - r_1}$$

$$B_2 = \frac{\dot{x}_{j-1} - r_1 [x_{j-1} - (\bar{f}/\mu)]}{r_2 - r_1} \quad (45)$$

Case (2): Values of  $\sigma$  and  $\mu$  are nonzero but  $\lambda = 0$ . For this case which occurs for fluid nodes with viscous effect, equation (36) may be integrated:

$$x_j = x_{j-1} e^{-(\mu/\sigma) \Delta t} + \frac{\bar{f}}{\mu} [1 - e^{-(\mu/\sigma) \Delta t}] \quad (46)$$

Case (3): Values of  $\sigma$  and  $\mu$  are zero but  $\lambda \neq 0$ . For this case which occurs for fluid nodes without viscous effects, the integration of equation (36) gives

$$x_j = x_{j-1} + \frac{\bar{f}}{\sigma} \Delta t \quad (47)$$

The first and second time derivatives of  $x_j$  needed for the calculation of  $\bar{f}$ , can be readily computed by analytically differentiating the above expressions as necessary. It should be further noted that since the updated value of  $f_j$  in  $\bar{f}$  used in the above equation are not yet known, an iterative procedure would be necessary. First, the values of  $f_j$  are set equal to  $f_{j-1}$  and the first trial values  $x_j^1$ ,  $\dot{x}_j^1$  and  $\ddot{x}_j^1$  are calculated from equation (40), (42), (44), (46) and (47), as the case may be. Substituting these values into equation (33), the first updated values are computed and used in equation (37) and in expressions for  $x_j$  to calculate the second trial values  $x_j^2$ ,  $\dot{x}_j^2$  and  $\ddot{x}_j^2$ . This iterative procedure is continued until the values of  $x_j$  converge within a prescribed error.

The above combined analytical and iterative solution is repeated for successive time increments (with the origin of time at the beginning of each time interval conveniently set equal to zero) until the entire problem time is covered.

#### 4. PRESENTATION OF RESULTS

The finite element model developed in this study (designated as multi - variable pressure-velocity formulation) is verified for a two-dimensional channel flow with elastic walls shown in Fig. 15. The results obtained are compared with a previous study based on a finite element model with pressure considered as the only dependent variable in the fluid region (referred to as the single - variable pressure formulation [11]). The results are also compared with wave propagation studies between two rigid parallel plates described in part one. Water initially at rest is accelerated suddenly by applying a step pressure,  $p_0$  at the left end while maintaining a zero pressure at the right end. A 72 element grid model, shown in Fig. 16, is used in this analysis. Elements 6, 15, 24, 33, 42, 51, 60 and 69 are modeled using the solid-fluid quadrilateral superelements. Elements located below and above these elements are modeled employing fluid and solid triangular finite elements respectively. Two values of fluid viscous damping are studied: 1) Inviscid case,  $k_f=0.$ , and 2) Highly viscous case,  $k_f=3062.467 \text{ sec}^{-1}$ .

The FASINT digital program, described in part 3, is employed to solve the problem. Response time histories are obtained numerically for the cases indicated above. Typical nodal pressure and velocity components for the fluid and the nodal displacement components for the solid for one position upstream and one position downstream are plotted for the present study employing the multi-variable pressure-velocity formulation and compared with two previous studies: 1) single-variable



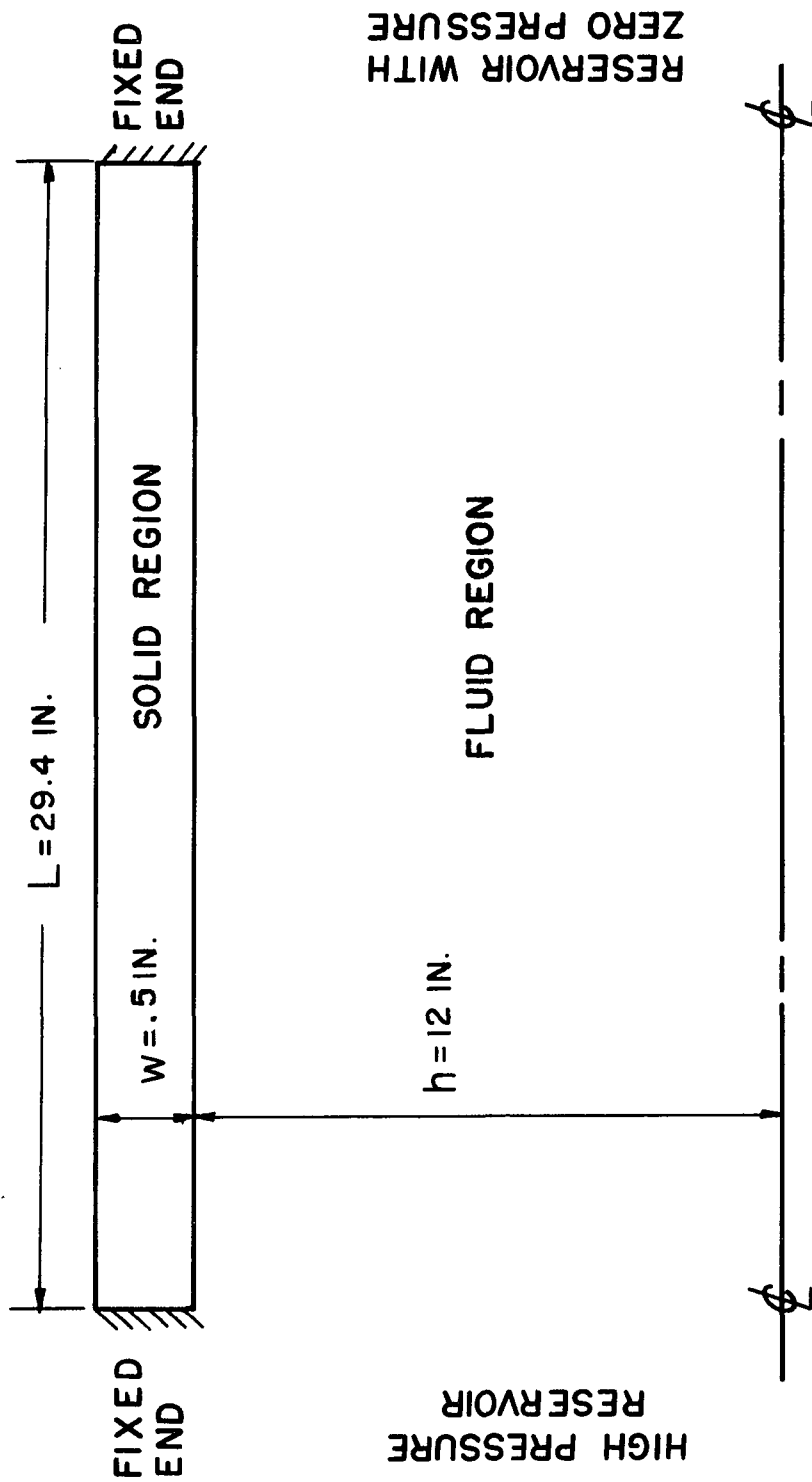


FIG. 15 FLOW CONFIGURATION

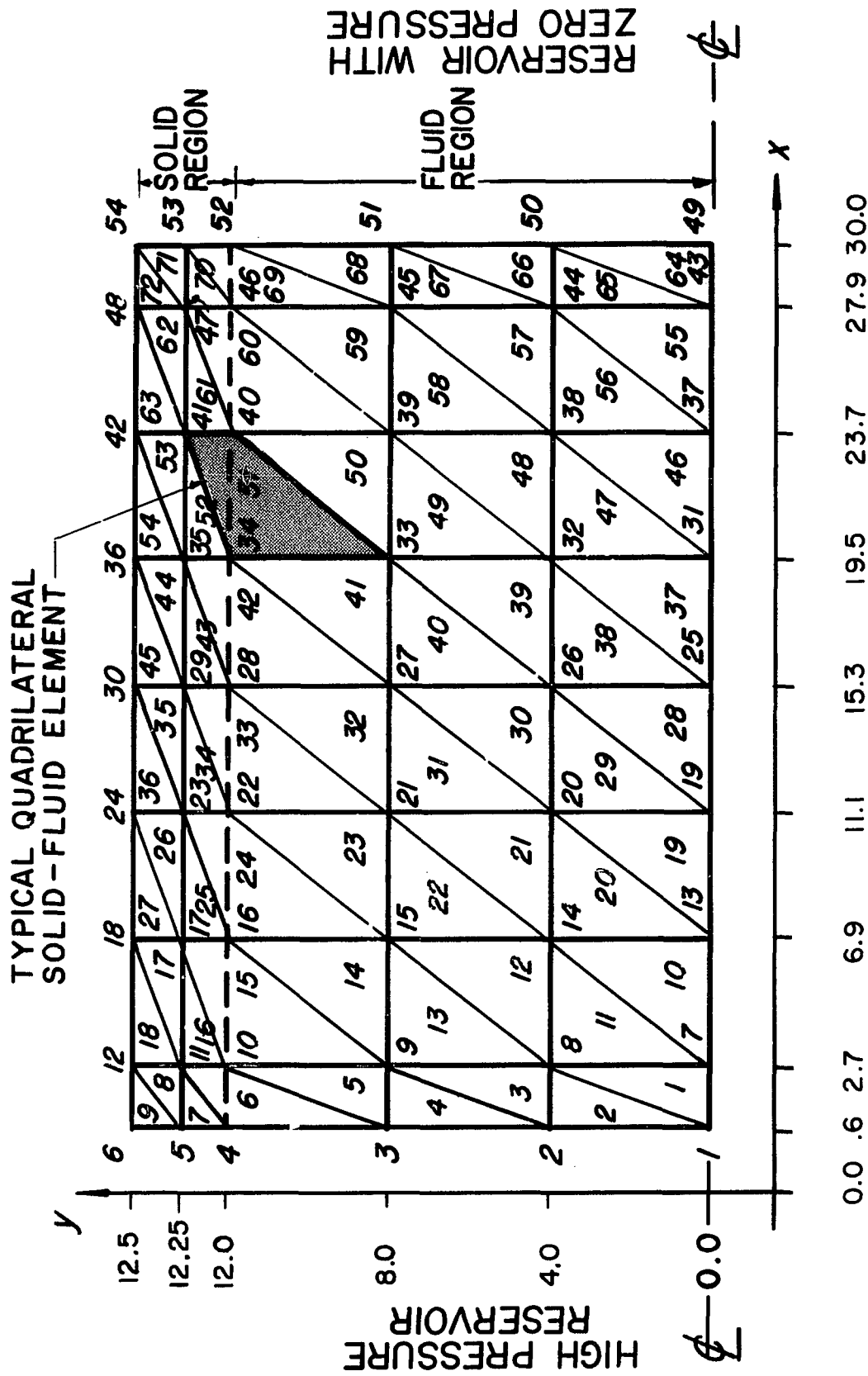


FIG. 16 72 ELEMENT SOLID-FLUID MODEL

pressure-formulation based on two-dimensional wave propagation between elastic walls ( see Figs.17 and 18 ) ; and 2) multi-variable pressure-velocity formulation for two-dimensional wave propagation between rigid walls and simplified one-dimensional analytical solution for channel flow with rigid walls ( see Figs.19 through 25 ). The positions and variables selected for plotting are marked on each figure and the physical data are summarized in Table 3 .

To establish the convergence of the numerical solution, the minimum period associated with the smallest length increment is calculated from

$$T_{\min} = 2 \pi \frac{l_{\min}}{c}$$

Since the speed of sound in the solid is much larger than that of the fluid and the solid length increments are much smaller than that of the fluid, the minimum period will correspond to the solid element with the smallest length. For  $l_{\min} = 0.25$  inches and  $c = 2.0276 \times 10^5$  in/sec,  $T_{\min}$  becomes equal to  $7.75 \times 10^{-6}$  sec. Examination of the solid displacements (not shown) indicates that this period is indeed present in the nodal time histories on the elements close to the solid element with the smallest length . To ascertain the convergence of the solution, the integration time step was set less than  $\frac{1}{50}$ th of this minimum period at  $t = 1.5 \times 10^{-7}$  seconds. This time increment led to a convergent solution for all cases studied. The convergence of the solution was established when doubling the time interval produced no significant change in the model time histories.

Figures 17 and 18 show a comparison of the multi-variable

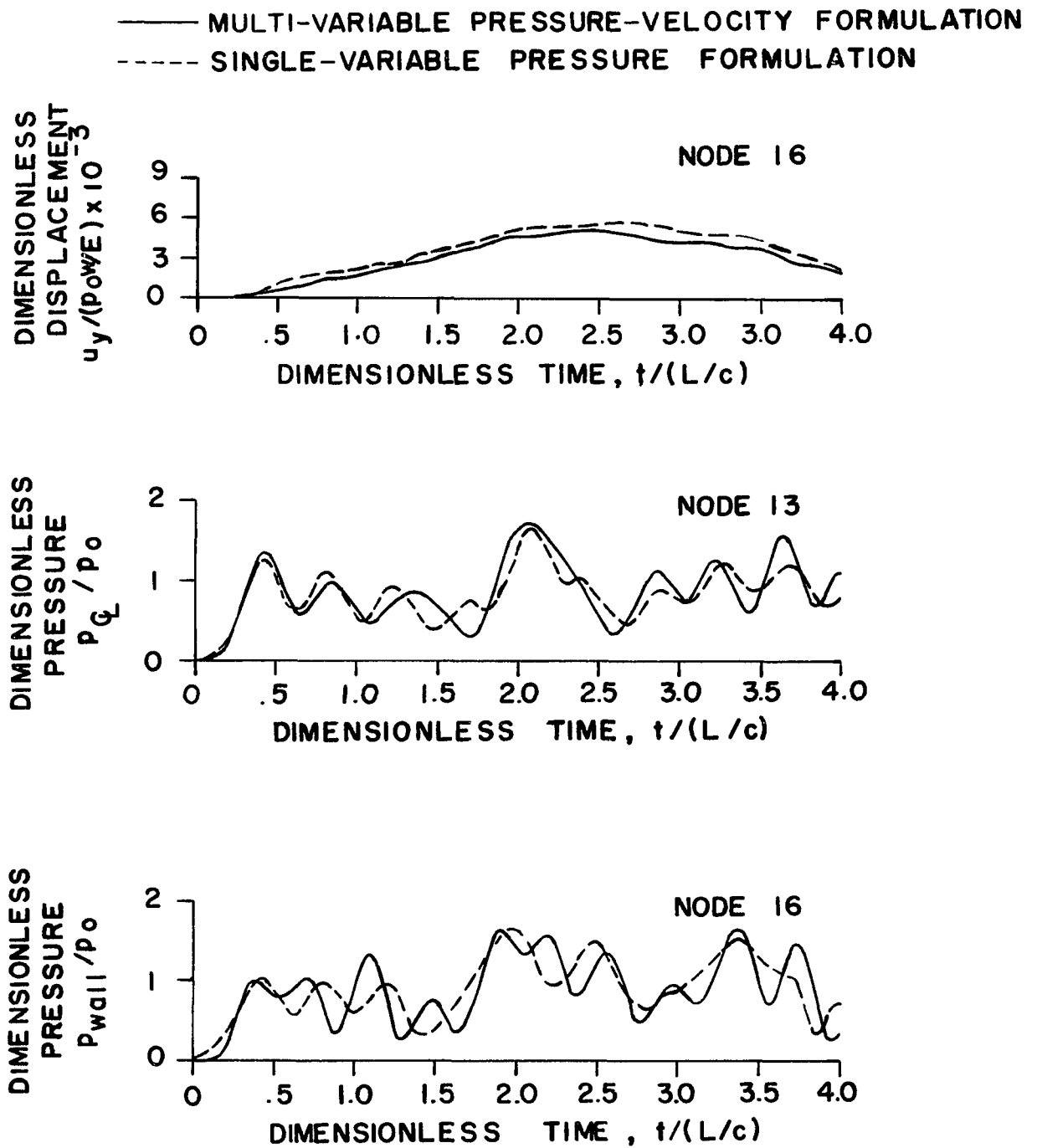


FIG. 17 A COMPARISON OF MULTI- AND SINGLE-VARIABLE PRESSURE AND DISPLACEMENT TIME HISTORIES FOR ELASTIC WALL CASE WITH INVISCID FLOW AT ( $x = 6.9$  IN.)

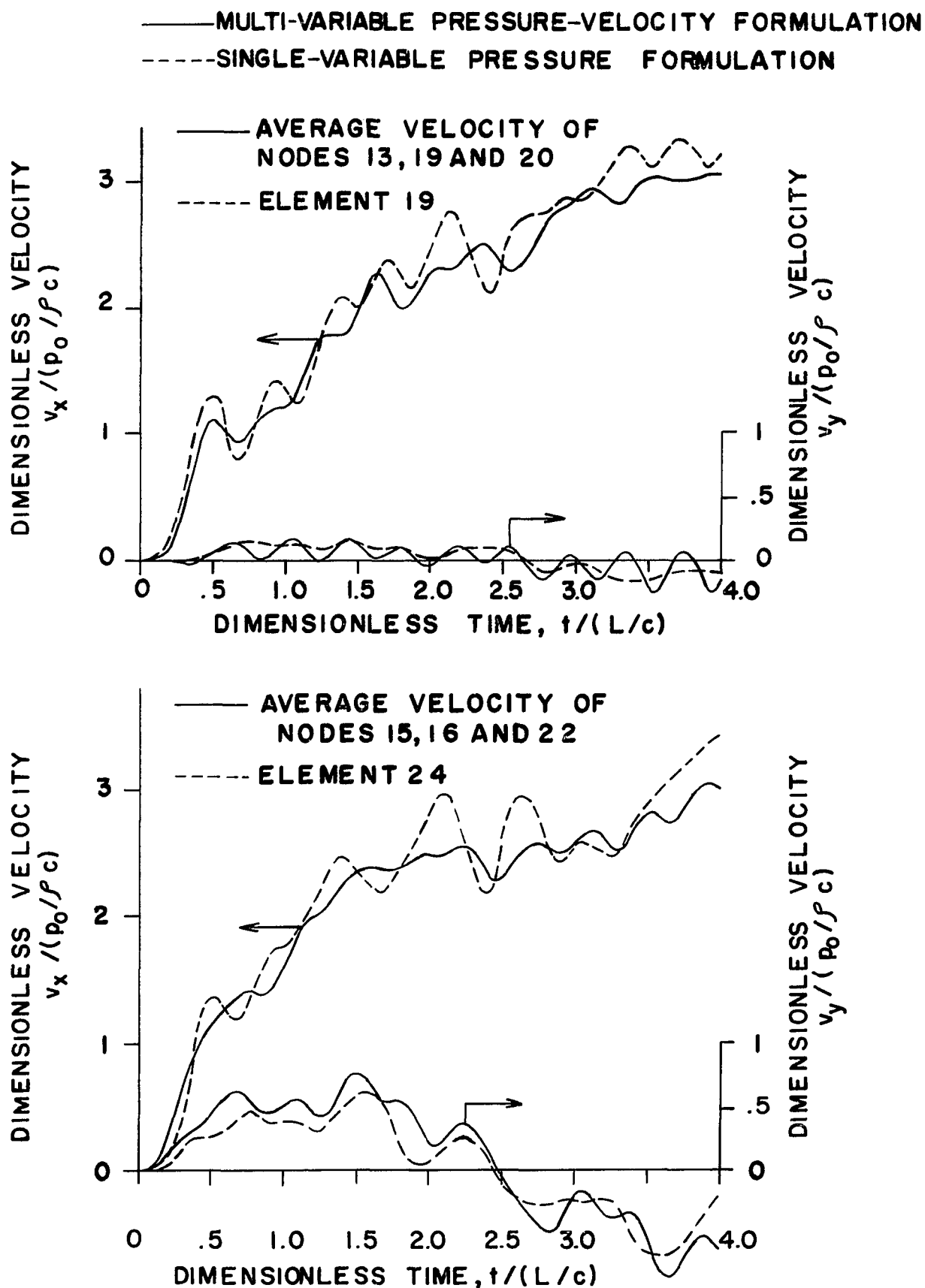


FIG. 18 A COMPARISON OF MULTI- AND SINGLE- VARIABLE FLUID VELOCITY TIME HISTORIES FOR ELASTIC WALL CASE WITH INVISCID FLOW ( AT  $x = 6.9$  IN.)

Table 3. Physical Data for the Elastic Wall Case

<u>Parameters</u>	<u>British Unit</u>	<u>SI Unit</u>
Fluid density	$9.35521 \times 10^{-5} \text{ lbf-sec}^2/\text{in}^4$	$999.78 \text{ N sec}^2/\text{m}^4$
Solid density	$7.297 \times 10^{-4} \text{ lbf-sec}^2/\text{in}^4$	$7798.2 \text{ N sec}^2/\text{m}^4$
Speed of sound in fluid	$6.0 \times 10^4 \text{ in/sec}$	$1524.0 \text{ m/sec}$
Speed of sound in solid	$2.0276 \times 10^5 \text{ in/sec}$	$5150.1 \text{ m/sec}$
Solid Young Modulus	$30.0 \times 10^6 \text{ psi}$	$20.68 \times 10^7 \text{ kPa}$
Solid Poisson Ratio	0.3	0.3
Pressure at channel inlet	10 psia	68948.0 Pa
Channel length, L	29.4 in	0.747 m
Channel height, h	24.0 in	0.610 m
Wall thickness, w	0.5 in	0.0127 m
Fluid damping coefficient, k:		
Inviscid	$0. \text{ sec}^{-1}$	$0. \text{ sec}^{-1}$
Highly viscous	$3062.467 \text{ sec}^{-1}$	$3062.467 \text{ sec}^{-1}$

pressure-velocity formulation, employed in this study, with single-variable pressure-formulation from reference [11] based on the two-dimensional wave equation. The two solutions are generally in reasonable agreement. However, since the velocity components are not among the system degrees of freedom in the single-variable pressure formulation, the associated time responses cannot be expected to be as accurate as the present multi-variable pressure - velocity formulation.

It should be remembered that the velocity time responses, shown in Fig.18, are the distinctive features of the multi-variable pressure-velocity formulation presented herein since the single-variable pressure formulation can provide only an elemental velocity calculated from the nodal pressures. A comparison between the multi-variable and single-variable velocity time histories has been made possible by averaging the nodal velocities from the multi-variable study and comparing the result with the elemental velocity from the single-variable approach which show a good agreement. This verification provides the confidence needed to initiate parametric studies and to present a detailed description of the system behavior as follows.

The solid vertical displacement, fluid pressure, and axial and transversal fluid velocity time histories at the centerline of the channel and at the wall are presented at one upstream and one downstream location for inviscid and highly viscous cases in Figs. 19 through 25 . These curves are representative of the response of the solid and the fluid, obtained in this study, at other locations along the channel. Superimposed on these curves are two rigid wall (no solid-fluid interaction) curves for comparison. The first is a finite element solution

for the wave propagation problem with rigid walls using multi-variable pressure-velocity formulation described in part one. The second is the analytic solution to the one-dimensional wave equation for the rigid wall problem[12].

In Fig. 19 , the pressure time history for the multi-variable pressure-velocity formulation in the rigid wall case oscillate about the simplified one-dimensional analytically-calculated rectangular wave form. However, the simplified one-dimensional analytical solution allows only axial motion or pressure variation and, therefore, cannot be expected to be accurate for a two-dimensional flow field under consideration. The multi-variable pressure-velocity formulation with rigid walls allows a two-dimensional pressure and velocity variation and for this reason, the pressure response is more oscillatory. This oscillatory behavior has been observed by other investigators both experimentally and analytically [3,22,9,20]. For the elastic wall case, the pressure surge in the channel results in a gradual deflection of the wall leading to a reduction of the axial pressure surge which is initially more pronounced near the wall than at the center. This situation creates a transverse flow, as shown in Fig. 20 , until the wall deflection reaches a maximum and no longer permits a transverse flow leading to a transversal water hammer and pressure surge about  $tL/c = 2$  which is distinctly opposed to the zero pressure dip for the rigid wall case. The transversal pressure surge occurs first at the wall and then travels backward to the centerline. Following the transverse surge phenomenon, the elastic energy stored in the wall forces the wall to move back toward its initial position and reverses the transverse flow direction with a subsequent gradual pressure rise toward the end of the cycle. The axial flow, for the elastic



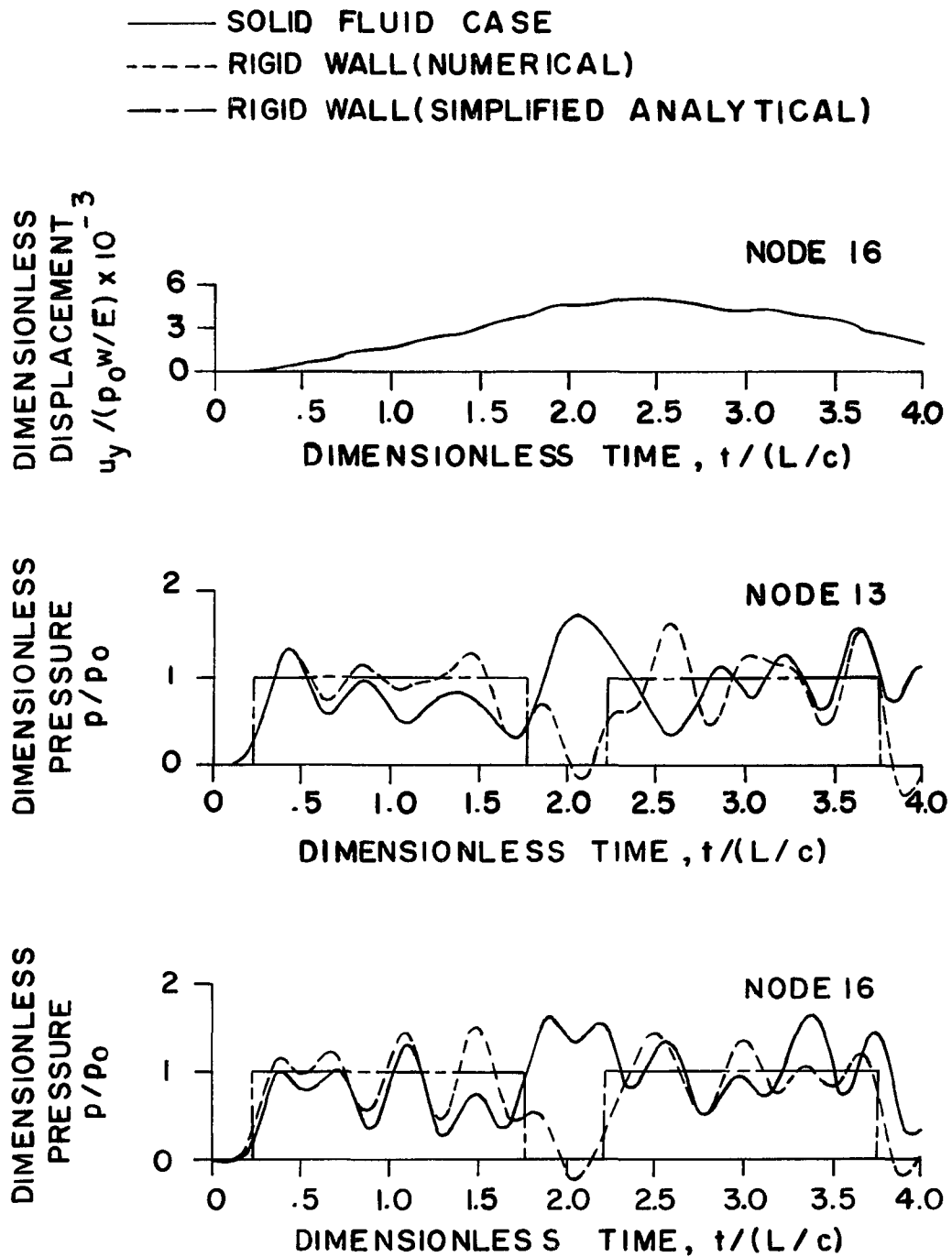


FIG. 19 A COMPARISON OF PRESSURE AND DISPLACEMENT TIME HISTORIES FOR ELASTIC AND RIGID WALL CASES WITH INVISCID FLOW ( AT  $x = 6.9$  IN.)

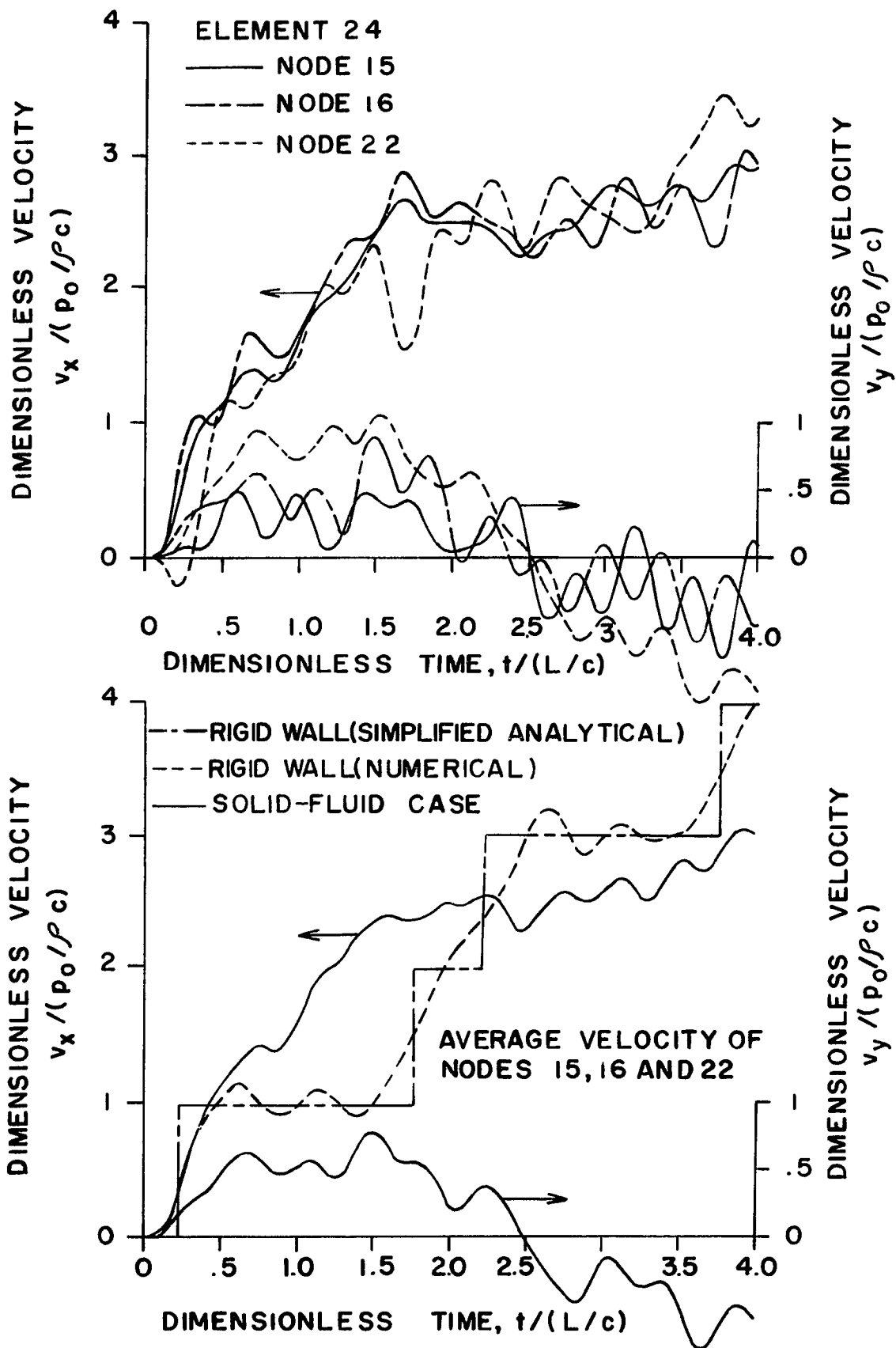


FIG. 20 A COMPARISON OF FLUID VELOCITY TIME HISTORIES FOR ELASTIC AND RIGID WALL CASES WITH INVISCID FLOW ( AT  $x = 6.9$  IN. NEAR THE WALL )

wall case, is larger than that of the rigid wall as the wall deflects outward and is smaller as the wall moves inward. This behavior is more pronounced near the wall (element 24 in Fig. 20 ) than near the channel centerline (element 19 in Fig. 21 ). The same characteristics are observable at the downstream position shown in Fig. 22 and 23 .

The effect of damping is shown in Figs. 24 and 25 for the highly viscous flow conditions. In comparison with the inviscid flow case, the pressure, velocity and displacement amplitudes in the highly viscous flow case are lower and the curves are smoother as expected. The transverse surge is not as large and the solution tends toward a steady-state value corresponding to the rigid wall case because of the highly viscous flow conditions.

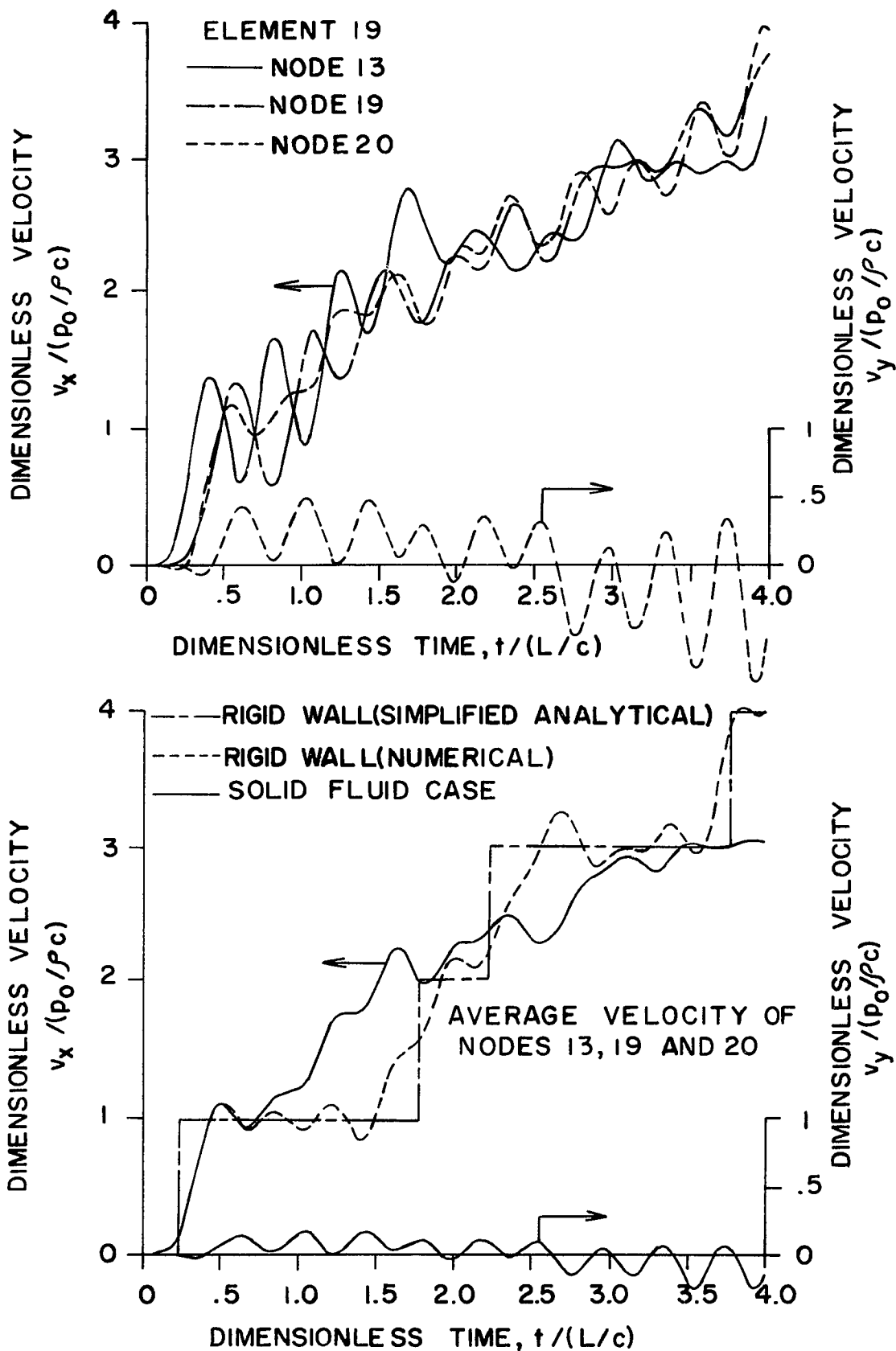


FIG. 21 A COMPARISON OF FLUID VELOCITY TIME HISTORIES FOR ELASTIC AND RIGID WALL CASES WITH INVISCID FLOW ( AT  $x = 6.9$  IN. NEAR THE CHANNEL CENTERLINE )

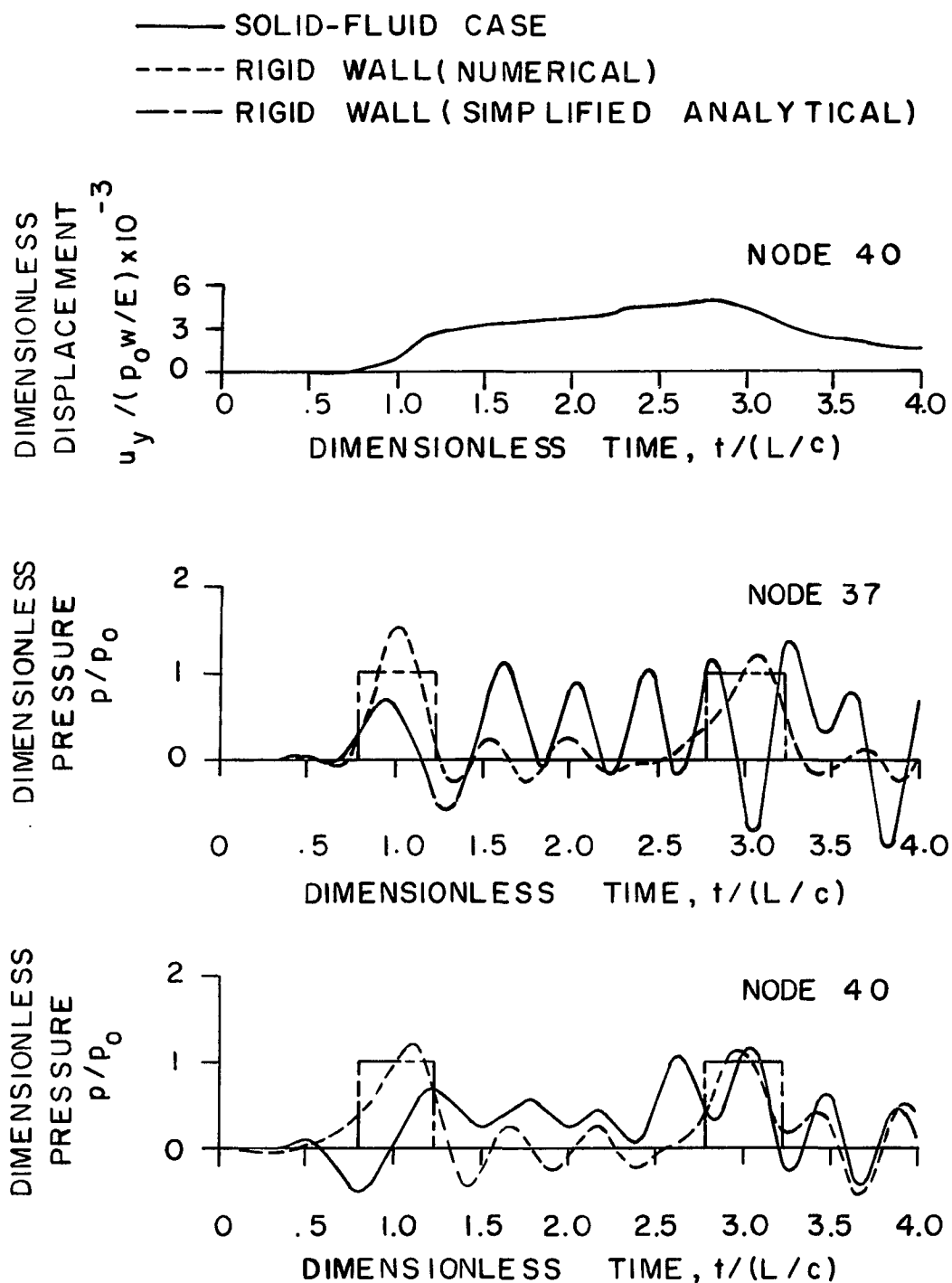


FIG. 22 A COMPARISON OF PRESSURE AND DISPLACEMENT TIME HISTORIES FOR ELASTIC AND RIGID WALL CASES WITH INVISCID FLOW ( AT  $x = 23.7$  IN.)

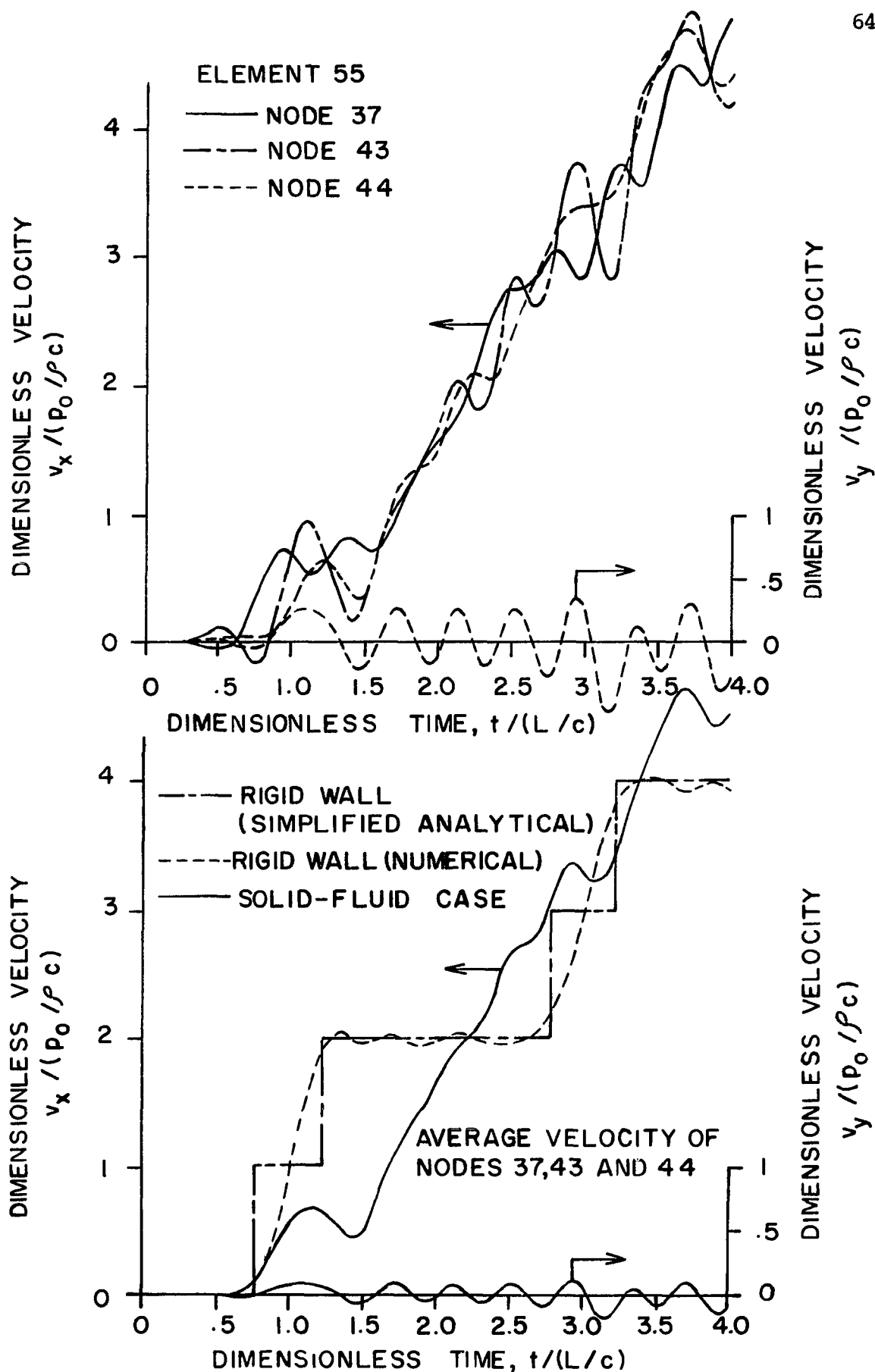


FIG. 23 A COMPARISON OF FLUID VELOCITY TIME HISTORIES FOR ELASTIC AND RIGID WALL CASES WITH INVISCID FLOW ( AT  $x = 23.7$  IN. NEAR THE CHANNEL CENTERLINE )

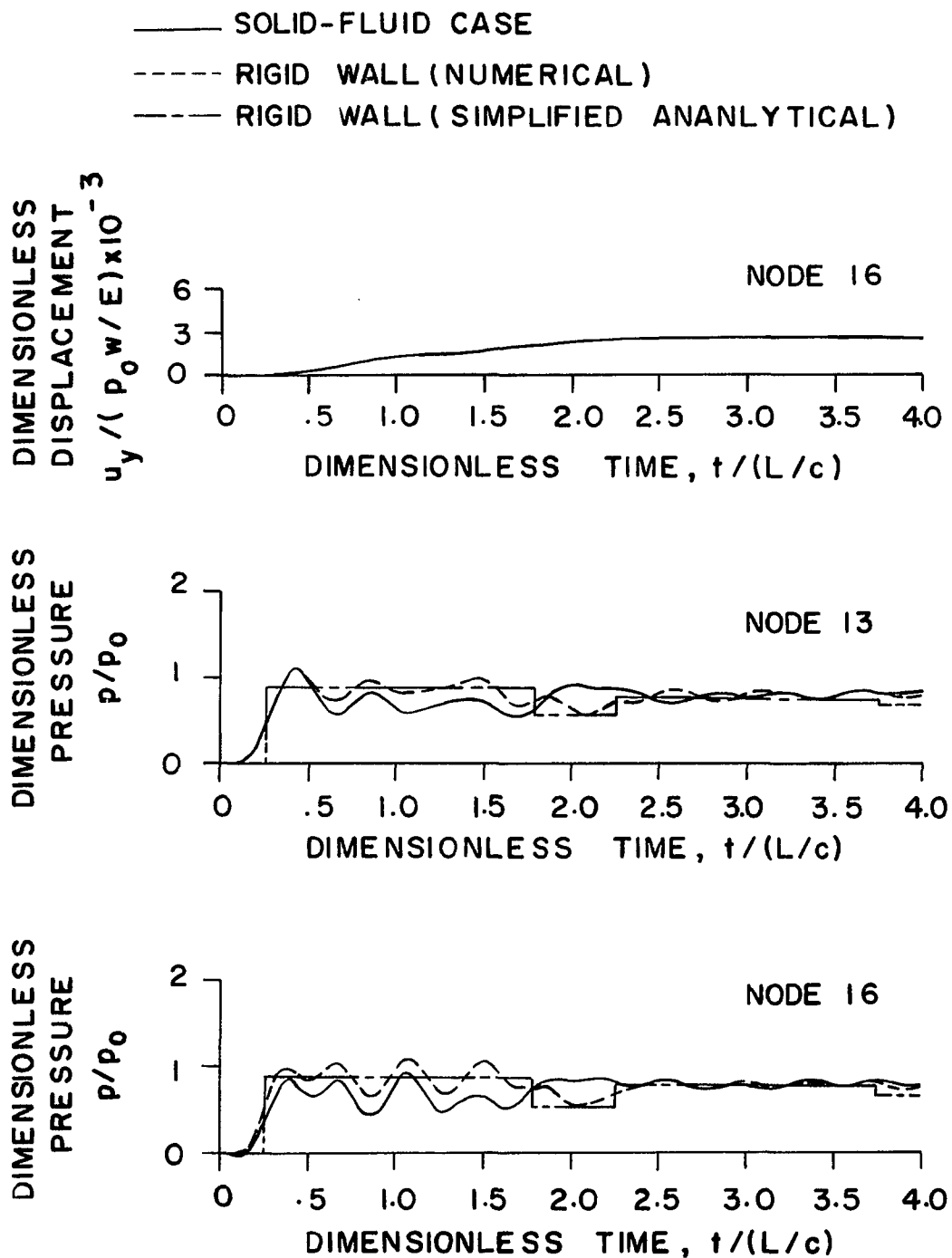


FIG. 24 A COMPARISON OF PRESSURE AND DISPLACEMENT TIME HISTORIES FOR ELASTIC AND RIGID WALL CASES WITH HIGHLY VISCOUS FLOW ( AT  $x = 6.9$  IN.)

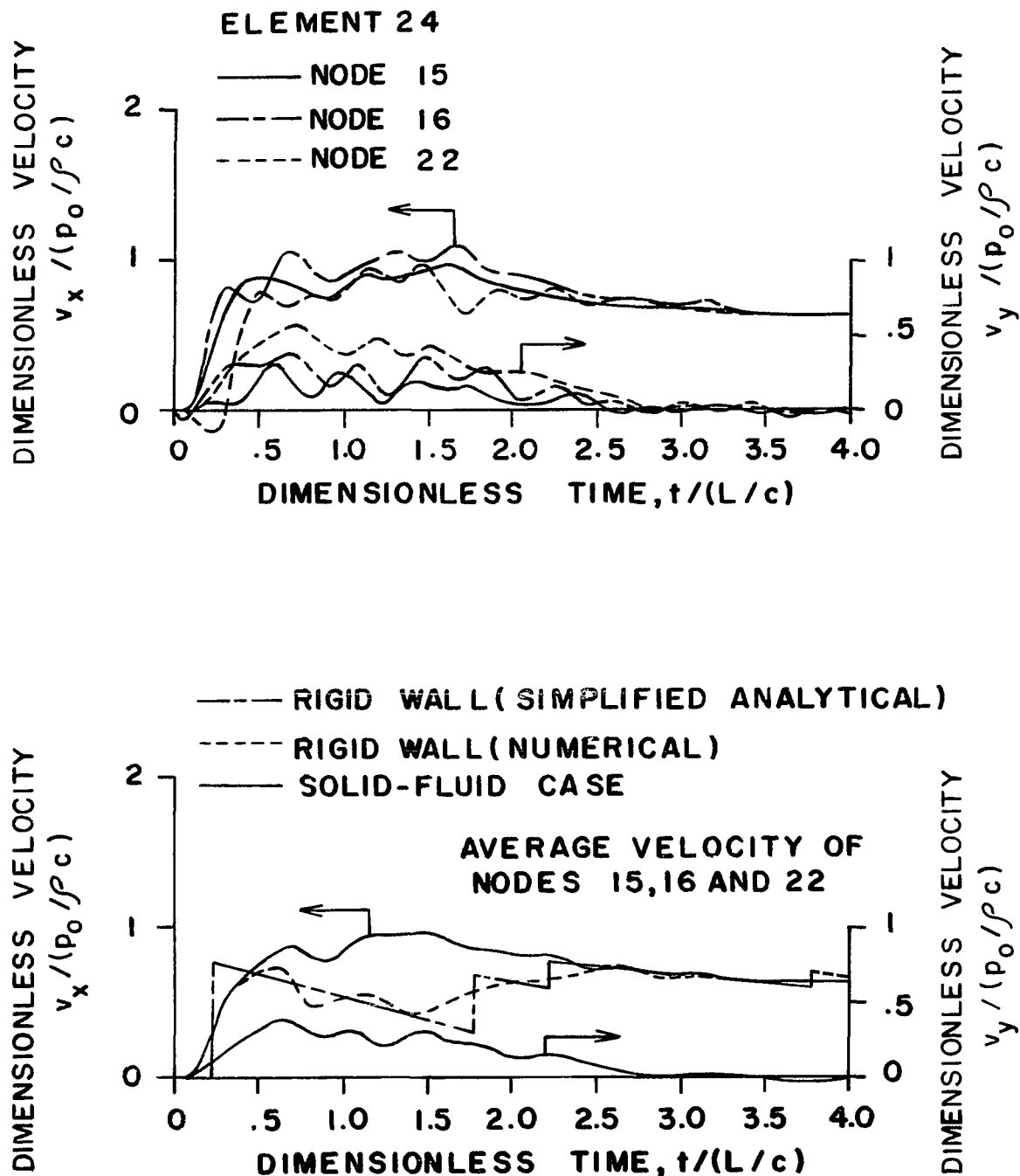


FIG. 25 A COMPARISON OF FLUID VELOCITY TIME HISTORIES FOR ELASTIC AND RIGID WALL CASES WITH HIGHLY VISCOUS FLOW ( AT  $x = 6.9$  IN. )



## 5. CONCLUSIONS

A finite element model for the study of solid-fluid interaction is presented. This finite element model may be used to analyze two-dimensional solid-fluid interaction problems involving complex geometries and loadings. The model is based on the discretization of the solid equation of motion and the fluid continuity and momentum equations. It employs the solid displacements together with the fluid pressure and velocity components as the nodal degrees of freedom. This facilitates the implementation of realistic boundary conditions, in contrast with formulations using stream function, vorticity and pressure as the only fluid field variables.

The elemental matrices are used directly in the numerical solution. This feature results in a considerable saving in computer storage and running time, in contrast with most schemes that the assembly and storage of system global matrices are essential to the numerical solution.

The model was tested for a flow configuration consisting of water, between two elastic parallel plates, subjected to a step pressure at one end. Verification of the model was achieved by comparing the results with a previous study based on the finite element discretization of the two-dimensional wave equation. Further comparison with flow between two rigid parallel plates demonstrated the development of a transversal water hammer phenomenon and pressure surge caused by the wall deformation and the fluid transversal flow. This transversal

water hammer has a substantial effect on the response characteristics and may have important implications in the design of fluid systems. Parametric studies , conducted to observe the effect of fluid damping, demonstrated that damping can effectively reduce the amplitude of the pressure surge caused by the transversal water hammer.

## NOMENCLATURE

A	Finite element area
$A_1, A_2, A_2', B_1, B_2$	Integration constants defined in the text
$a_i, b_i, c_i$	Quantities defined by equations (A-5)
$[B]_i^i$	Strain-Displacement matrix
c	Speed of sound in continuum under consideration
$[C]$	Damping or equivalent damping matrix depending upon superscript
$[C']$	Diagonal matrix with diagonal terms equal to diagonal terms of $[C]$
$[C'']$	Off-diagonal matrix with off-diagonal terms equal to off-diagonal terms of $[C]$ and zeros along the diagonal
$[D]$	Inertia matrix in fluid multi-variable pressure-velocity formulation
$[D']$	Diagonal matrix with diagonal terms equal to diagonal terms of $[D]$
$[D'']$	Off-diagonal matrix with off-diagonal terms equal to off-diagonal terms of $[D]$ and zeros along the diagonal
e	Element index number
$[E]$	Fluidity matrix in fluid multi-variable pressure-velocity formulation
$[E']$	Diagonal matrix with diagonal terms equal to diagonal terms of $[E]$
$[E'']$	Off-diagonal matrix with off-diagonal terms equal to off-diagonal terms of $[E]$ and zeros along the diagonal
E	Young's modulus
$\{F\}$	Boundary integral array in fluid single-variable pressure formulation

$\{F'\}$	Forcing function array defined by equations (15),(17), (33) or (35) depending upon subscript and superscript
$f$	Individual terms of $\{F'\}$
$[G]$	Inertia matrix in fluid single-variable pressure formulation
$h$	Channel height
$\tilde{h}$	Constant value of $\tilde{h}$ used in eqs.(D-13) and (D-15)
$[H]$	Fluidity matrix in fluid single-variable pressure formulation
$i, j$	Node number
$[I]$	Identity matrix
$I_1, I_6$	Integrals defined by eqs.(B-8) and (B-11)
$k_f, k_s$	Viscous or damping parameter
$k$	$=\mu/\sigma$ in equation (19)
$k_{ij}$	Terms of stiffness matrix $[K]$
$[K]$	Stiffness or equivalent stiffness matrix depending upon superscript
$\overline{K}'$	Diagonal matrix with diagonal terms equal to diagonal terms of $[K]$
$[K'']$	Off-diagonal matrix with off-diagonal terms equal to off-diagonal terms of $[K]$ and zeros along the diagonal
$L$	Channel length
$[L]$	Viscous damping matrix in fluid single-variable pressure formulation
$\lambda_{\min}$	Smallest length increment
$m$	Slope of solid-fluid boundary
$[M]$	Mass or equivalent mass matrix depending upon superscript
$\overline{M}'$	Diagonal matrix with diagonal terms equal to diagonal terms of $[M]$
$[M'']$	Off-diagonal matrix with off-diagonal terms equal to off-diagonal terms of $[M]$ and zeros along the diagonal
$[N]$	Element shape function defined by equations (A-4),(A-5), (C- 2) and (C-3 )

$n$	Maximum number of elements
$p$	Fluid pressure
$P_0$	Fluid pressure at channel entrance
$\{p\}$	Elemental array of nodal pressures
$\{R\}$	Elemental array of loads on the solid due to fluid pressure
$\{R'\}$	Elemental or global array of applied nodal loads
$r_1, r_2$	Characteristic roots defined by equations (45)
$S$	Solid-fluid boundary
$S_{i,j}$	Terms of coupling matrix $[S_e]$
$[S_e]$	Solid-fluid coupling matrix defined by eq.(D-11)
$[R], [S], [T]$	Matrices defined by equations(A-13),(A-14) and (A-15) with terms $R_{ij}, S_{ij}$ and $T_{ij}$ , respectively
$T_{min}$	Minimum period associated with smallest length increment
$t$	Time
$U$	Array of elemental freedom for the solid ( $x$ and $y$ components of displacements )
$u_x, u_y$	Solid displacements in $x$ and $y$ directions respectively
$v_x, v_y$	Fluid velocity components in $x$ and $y$ directions respectively
$w$	Channel wall thickness
$W$	Work
$x, y$	Cartesian coordinate system
$x', y'$	Cartesian coordinate system passing through the centroid
$x_o, x_f$	Abscissa of first and last node of solid-fluid boundary, respectively
$\{X\}$	Array of elemental or global freedoms ( $x$ -component of solid displacement, $y$ -component of solid displacement, fluid pressure, $x$ -component of fluid velocity and $y$ -component of fluid velocity )
$x_1, x_2, x_3$	Abscissa of nodes 1,2,3 respectively
$x$	Individual terms of $X$
$y_o, y_f$	Ordinate of first and last nodes of solid-fluid boundary
$y_1, y_2, y_3$	Ordinates of nodes 1,2,3 respectively
$\{Z\}$	Array of elemental or global freedoms for the fluid ( fluid pressure, $x$ -component of fluid velocity and $y$ -component of fluid velocity )

z Nodal freedoms (pressure, x-component of velocity or y-component of velocity)

### Greek Symbols

$\alpha_i, \alpha_j, \alpha_k$  Coefficients used in equations (A-1), (A-2) and (C-14) for finite element discretization  
 $\alpha$  Angle of solid-fluid boundary with x-axis  
 $\delta$  Virtual displacement  
 $\Delta t$  Time increment

$[\Delta]$  Stress-strain matrix

$\lambda$  Individual terms of  $\bar{M}_j$   
 $\mu$  Individual terms of  $\bar{K}_j$  or  $\bar{E}_j$ , whichever applies  
 $\xi$  Pseudo damping ratio defined by equation (39)  
 $\nu$  Poisson's ratio for solid  
 $\rho$  Continuum density depending upon subscript  
 $\sigma$  Individual terms of  $\bar{C}_j$  or  $\bar{D}_j$ , whichever applies  
 $\tau$  Time within the interval  $t$  and  $t+\Delta t$   
 $\omega_n$  Pseudo natural frequency defined by equation (39)  
 $\omega_d$  Pseudo damped natural frequency defined by equation (41)

### Superscripts

., .. First and second time derivatives

1,2 First and second trial values

T Matrix transpose

- Global matrices and arrays

= Solid-fluid boundary

### Subscripts

c Refers to the centroid of the triangular element

e Elemental matrices and arrays ( without e refers to global matrices and arrays )

f Fluid

i Node number

j Updated time

j-1 Present time

N	Normal
s	Entropy constant or solid
T	Tangential
o	Past values
x	x-direction
y	y-direction

Operators

d	Virtual
---	---------

APPENDIX 1 - DERIVATION OF THE FLUID FINITE ELEMENT EQUATIONS

A plane triangular fluid finite element, shown in Figure 2, is used as the basis for the fluid finite element formulation. It is assumed that the fluid pressure and velocity components at any point in the triangular fluid element may be expressed as linear polynomials in  $x$  and  $y$ :

$$\begin{aligned} p &= \alpha_1 + \alpha_2 x + \alpha_3 y \\ v_x &= \alpha_4 + \alpha_5 x + \alpha_6 y \\ v_y &= \alpha_7 + \alpha_8 x + \alpha_9 y \end{aligned} \quad (A-1)$$

or generally

$$z = \alpha_i + \alpha_j x + \alpha_k y \quad (A-2)$$

in which the coefficients  $\alpha$  are functions of time. Employing the above equations, it is shown in Appendix 2 that

$$z = [N_f(x,y)] \{z_e(t)\} \quad (A-3)$$

in which the shape function  $[N_f]$  is given by

$$[N_f] = [N_{f1} \quad N_{f2} \quad N_{f3}] \quad (A-4)$$

where

$$N_{fi} = \frac{1}{2A_f} (a_i + b_i x + c_i y) \quad i = 1, 2, 3$$



$$\begin{aligned}
a_1 &= x_2 y_3 - x_3 y_2 & b_1 &= y_2 - y_3 & c_1 &= x_3 - x_2 \\
a_2 &= x_3 y_1 - x_1 y_3 & b_2 &= y_3 - y_1 & c_2 &= x_1 - x_3 \\
a_3 &= x_1 y_2 - x_2 y_1 & b_3 &= y_1 - y_2 & c_3 &= x_2 - x_1
\end{aligned} \tag{A-5}$$

and  $A_f$  is the area of the triangular fluid element

$$A_f = (a_1 + a_2 + a_3)/2 \tag{A-6}$$

Employing the Galerkin method of weighted residuals, equations (5), (6), and (7) become

$$\iint_A [N_f]^T \left\{ \frac{1}{c} \frac{\partial p}{\partial t} + \rho_f \left( \frac{\partial v_x}{\partial x} + \frac{\partial v_y}{\partial y} \right) \right\} dx dy = 0 \tag{A-7}$$

$$\iint_A [N_f]^T \left\{ \frac{\partial v_x}{\partial t} + \frac{1}{\rho_f} \frac{\partial p}{\partial x} + k_f v_x \right\} dx dy = 0 \tag{A-8}$$

$$\iint_A [N_f]^T \left\{ \frac{\partial v_y}{\partial t} + \frac{1}{\rho_f} \frac{\partial p}{\partial y} + k_f v_y \right\} dx dy = 0 \tag{A-9}$$

Substituting eq. (A-3) into eqs. (A-7), (A-8) and (A-9), one obtains

$$\begin{aligned}
&\iint_A \frac{1}{c^2} [N_f]^T [N_f] \{ \dot{p}_e \} dx dy + \iint_A \rho_f [N_f]^T \frac{\partial [N_f]}{\partial x} \{ v_{xe} \} dx dy \\
&\quad + \iint_A \rho_f [N_f]^T \frac{\partial [N_f]}{\partial y} \{ v_{ye} \} dx dy = 0
\end{aligned} \tag{A-10}$$

$$\begin{aligned}
& \iint_A [N_f]^T [N_f] \{\dot{v}_{xe}\} \, dx \, dy + \iint_A \frac{1}{\rho_f} [N_f]^T \frac{\partial [N_f]}{\partial x} \{p_e\} \, dx \, dy \\
& + \iint_A k_f [N_f]^T [N_f] \{v_{xe}\} \, dx \, dy = 0 \quad (A-11)
\end{aligned}$$

$$\begin{aligned}
& \iint_A [N_f]^T [N_f] \{\dot{v}_{ye}\} \, dx \, dy + \iint_A \frac{1}{\rho_f} [N_f]^T \frac{\partial [N_f]}{\partial y} \{p_e\} \, dx \, dy \\
& + \iint_A k_f [N_f]^T [N_f] \{v_{ye}\} \, dx \, dy = 0 \quad (A-12)
\end{aligned}$$

The above equations involve calculation of the following three types of matrices

$$[R] = \iint_A [N_f]^T [N_f] \, dx \, dy \quad (A-13)$$

$$[S] = \iint_A [N_f]^T \frac{\partial [N_f]}{\partial x} \, dx \, dy \quad (A-14)$$

$$[T] = \iint_A [N_f]^T \frac{\partial [N_f]}{\partial y} \, dx \, dy \quad (A-15)$$

Performing the integration, as shown in Appendix 2, one obtains

$$[R] = \frac{A_f}{12} \begin{bmatrix} 2 & 1 & 1 \\ 1 & 2 & 1 \\ 1 & 1 & 2 \end{bmatrix} \quad (A-16)$$

$$[S] = \frac{1}{6} \begin{bmatrix} b_1 & b_2 & b_3 \\ b_1 & b_2 & b_3 \\ b_1 & b_2 & b_3 \end{bmatrix} \quad (A-17)$$

$$[T] = \frac{1}{6} \begin{bmatrix} c_1 & c_2 & c_3 \\ c_1 & c_2 & c_3 \\ c_1 & c_2 & c_3 \end{bmatrix} \quad (A-18)$$

Substituting equations (A-16) through (A-18) into equations (A-10) through (A-12), combining the resulting equations into one matrix equation after dividing the pressure equation by  $\rho_f$  and multiplying the velocity equations by  $\rho_f$ , one obtains

$$[D_e] \{\dot{Z}_e\} + [E_e] \{Z_e\} = 0 \quad (A-19)$$

where

$$\{ \dot{z}_e \} = \begin{Bmatrix} \dot{p}_1 \\ \dot{v}_{x1} \\ \dot{v}_{y1} \\ \dot{p}_2 \\ \dot{v}_{x2} \\ \dot{v}_{y2} \\ \dot{p}_3 \\ \dot{v}_{x3} \\ \dot{v}_{y3} \end{Bmatrix} \quad \{ z_e \} = \begin{Bmatrix} p_1 \\ v_{x1} \\ v_{y1} \\ p_2 \\ v_{x2} \\ v_{y2} \\ p_3 \\ v_{x3} \\ v_{y3} \end{Bmatrix} \quad (\text{A-20})$$

$$[D_e] = A_f \begin{bmatrix} \frac{1}{6c^2 \rho_f} & 0 & 0 & \frac{1}{12c^2 \rho_f} & 0 & 0 & \frac{1}{12c^2 \rho_f} & 0 & 0 \\ 0 & \frac{\rho_f}{6} & 0 & 0 & \frac{\rho_f}{12} & 0 & 0 & \frac{\rho_f}{12} & 0 \\ 0 & 0 & \frac{\rho_f}{6} & 0 & 0 & \frac{\rho_f}{12} & 0 & 0 & \frac{\rho_f}{12} \\ \frac{1}{12c^2 \rho_f} & 0 & 0 & \frac{1}{6c^2 \rho_f} & 0 & 0 & \frac{1}{12c^2 \rho_f} & 0 & 0 \\ 0 & \frac{\rho_f}{12} & 0 & 0 & \frac{\rho_f}{6} & 0 & 0 & \frac{\rho_f}{12} & 0 \\ 0 & 0 & \frac{\rho_f}{6} & 0 & 0 & \frac{\rho_f}{6} & 0 & 0 & \frac{\rho_f}{12} \\ \frac{1}{12c^2 \rho_f} & 0 & 0 & \frac{1}{12c^2 \rho_f} & 0 & 0 & \frac{1}{6c^2 \rho_f} & 0 & 0 \\ 0 & \frac{\rho_f}{12} & 0 & 0 & \frac{\rho_f}{12} & 0 & 0 & \frac{\rho_f}{6} & 0 \\ 0 & 0 & \frac{\rho_f}{12} & 0 & 0 & \frac{\rho_f}{12} & 0 & 0 & \frac{\rho_f}{6} \end{bmatrix}$$

(A-21)

$$[E_e] = \begin{bmatrix} 0 & \frac{b_1}{6} & \frac{c_1}{6} & 0 & \frac{b_2}{6} & \frac{c_2}{6} & 0 & \frac{b_3}{6} & \frac{c_3}{6} \\ \frac{b_1}{6} & \frac{\rho_f k_f A_f}{6} & 0 & \frac{b_2}{6} & \frac{\rho_f k_f A_f}{12} & 0 & \frac{b_3}{6} & \frac{\rho_f k_f A_f}{12} & 0 \\ \frac{c_1}{6} & 0 & \frac{\rho_f k_f A_f}{6} & \frac{c_2}{6} & 0 & \frac{\rho_f k_f A_f}{12} & \frac{c_3}{6} & 0 & \frac{\rho_f k_f A_f}{12} \\ 0 & \frac{b_1}{6} & \frac{c_1}{6} & 0 & \frac{b_2}{6} & \frac{c_2}{6} & 0 & \frac{b_3}{6} & \frac{c_3}{6} \\ \frac{b_1}{6} & \frac{\rho_f k_f A_f}{12} & 0 & \frac{b_2}{6} & \frac{\rho_f k_f A_f}{6} & 0 & \frac{b_3}{6} & \frac{\rho_f k_f A_f}{12} & 0 \\ \frac{c_1}{6} & 0 & \frac{\rho_f k_f A_f}{12} & \frac{c_2}{6} & 0 & \frac{\rho_f k_f A_f}{6} & \frac{c_3}{6} & 0 & \frac{\rho_f k_f A_f}{12} \\ 0 & \frac{b_1}{6} & \frac{c_1}{6} & 0 & \frac{b_2}{6} & \frac{c_2}{6} & 0 & \frac{b_3}{6} & \frac{c_3}{6} \\ \frac{b_1}{6} & \frac{\rho_f k_f A_f}{12} & 0 & \frac{b_2}{6} & \frac{\rho_f k_f A_f}{12} & 0 & \frac{b_3}{6} & \frac{\rho_f k_f A_f}{6} & 0 \\ \frac{c_1}{6} & 0 & \frac{\rho_f k_f A_f}{12} & \frac{c_2}{6} & 0 & \frac{\rho_f k_f A_f}{12} & \frac{c_3}{6} & 0 & \frac{\rho_f k_f A_f}{6} \end{bmatrix}$$

(A-22)

APPENDIX 2 - DEVELOPMENT OF FLUID SHAPE FUNCTION AND MATRICES

As stated earlier, the fluid pressure and velocity components at any point in triangular fluid element are given by equation (A-2). Expressing this equation for points 1, 2, and 3 in Fig. 2, and eliminating  $\alpha_i$ ,  $\alpha_j$ , and  $\alpha_k$  among the resulting equations yields

$$\alpha_i = \frac{1}{2A_f} \begin{vmatrix} z_1 & x_1 & y_1 \\ z_2 & x_2 & y_2 \\ z_3 & x_3 & y_3 \end{vmatrix}$$

$$\alpha_j = \frac{1}{2A_f} \begin{vmatrix} 1 & z_1 & y_1 \\ 1 & z_2 & y_2 \\ 1 & z_3 & y_3 \end{vmatrix}$$

$$\alpha_k = \frac{1}{2A_f} \begin{vmatrix} 1 & x_1 & z_1 \\ 1 & x_2 & z_2 \\ 1 & x_3 & z_3 \end{vmatrix} \tag{B-1}$$

where

$$A_f = \frac{1}{2} \begin{vmatrix} 1 & x_1 & y_1 \\ 1 & x_2 & y_2 \\ 1 & x_3 & y_3 \end{vmatrix} = (\text{Area of triangle 123}) \tag{B-2}$$

Substituting the values of  $\alpha_i$ ,  $\alpha_j$ , and  $\alpha_k$  into equation (A-2) and

factoring nodal{z}array gives

$$\{z\} = \frac{1}{2A_f} \left[ \begin{array}{ccc} (a_1 + b_1x + c_1y) & (a_2 + b_2x + c_2y) & (a_3 + b_3x + c_3y) \end{array} \right] \begin{Bmatrix} z_1 \\ z_2 \\ z_3 \end{Bmatrix} \quad (\text{B-3})$$

where  $a_i$ ,  $b_i$ ,  $c_i$  and  $A_f$  are defined in Appendix 1. A comparison of the above equation with equation (A-3) yields the shape function given by equation (A-4). Substituting the shape function  $N_f$  into equation (A-13) through (A-15) yields

$$[R] = \frac{1}{4A_f^2} \iint_A \begin{bmatrix} (a_1 + b_1x + c_1y)^2 & (a_1 + b_1x + c_1y)(a_2 + b_2x + c_2y) & (a_1 + b_1x + c_1y)(a_3 + b_3x + c_3y) \\ \text{Symmetric} & (a_2 + b_2x + c_2y)^2 & (a_2 + b_2x + c_2y)(a_3 + b_3x + c_3y) \\ & & (a_3 + b_3x + c_3y)^2 \end{bmatrix} dx dy \quad (\text{B-4})$$

$$[S] = \frac{1}{4A_f^2} \iint_A \begin{bmatrix} b_1(a_1 + b_1x + c_1y) & b_2(a_1 + b_1x + c_1y) & b_3(a_1 + b_1x + c_1y) \\ b_1(a_2 + b_2x + c_2y) & b_2(a_2 + b_2x + c_2y) & b_3(a_2 + b_2x + c_2y) \\ b_1(a_3 + b_3x + c_3y) & b_2(a_3 + b_3x + c_3y) & b_3(a_3 + b_3x + c_3y) \end{bmatrix} dx dy \quad (\text{B-5})$$

$$[T] = \frac{1}{4A_f^2} \iint_A \begin{bmatrix} c_1(a_1 + b_1x + c_1y) & c_2(a_1 + b_1x + c_1y) & c_3(a_1 + b_1x + c_1y) \\ c_1(a_2 + b_2x + c_2y) & c_2(a_2 + b_2x + c_2y) & c_3(a_2 + b_2x + c_2y) \\ c_1(a_3 + b_3x + c_3y) & c_2(a_3 + b_3x + c_3y) & c_3(a_3 + b_3x + c_3y) \end{bmatrix} dx dy \quad (\text{B-6})$$

To determine the fluid matrices R, S, and T, twenty seven integrations indicated by equations (B-4), (B-5) and (B-6) should be performed. To demonstrate this lengthy process, it suffices here to show the procedure involved in the evaluation of  $R_{11}$ ,  $S_{11}$ , and  $T_{11}$  given by

$$R_{11} = \frac{1}{4A_f^2} \iint_A (a_1 + b_1x + c_1y)^2 dx dy$$

$$S_{11} = \frac{1}{4A_f^2} \iint_A b_1(a_1 + b_1x + c_1y) dx dy$$

$$T_{11} = \frac{1}{4A_f^2} \iint_A c_1(a_1 + b_1x + c_1y) dx dy \quad (B-7)$$

The integration of the above terms involve the calculation of the following integrals

$$I_1 = \iint_A dx dy \quad I_2 = \iint_A x dx dy \quad I_3 = \iint_A x^2 dx dy$$

$$I_4 = \iint_A y dx dy \quad I_5 = \iint_A y^2 dx dy \quad I_6 = \iint_A xy dx dy$$

$$(B-8)$$

Performing transformation of coordinates, involving a pure translation, from point (0,0) to the centroid of the triangle  $(x_c, y_c)$  such that

$$x = x' + x_c$$

$$y = y' + y_c \quad (B-9)$$

where



$$x_c = \frac{1}{3} (x_1 + x_2 + x_3) \quad y_c = \frac{1}{3} (y_1 + y_2 + y_3) \quad (\text{B-10})$$

The above integrals are calculated as follows by noting that the first moment with respect to the centroid vanishes.

$$\begin{aligned} I_1 &= \iint_A dx dy = \iint_A dx' dy' = A_f \\ I_2 &= \iint_A x dx dy = \iint_A (x' + x_c) dx' dy' = x_c A_f \\ I_3 &= \iint_A x^2 dx dy = \iint_A (x' + x_c)^2 dx' dy' = \frac{A_f}{12} (x_1^2 + x_2^2 + x_3^2) + \frac{3}{4} x_c^2 A_f \\ I_4 &= \iint_A y dx dy = y_c A_f \\ I_5 &= \iint_A y^2 dx dy = \frac{A_f}{12} (y_1^2 + y_2^2 + y_3^2) + \frac{3}{4} y_c^2 A_f \\ I_6 &= \iint_A xy dx dy = \frac{A_f}{12} (x_1 y_1 + x_2 y_2 + x_3 y_3) + \frac{3}{4} x_c y_c A_f \end{aligned} \quad (\text{B-11})$$

Employing the above integrals, expressions for  $S_{11}$  reduces to

$$S_{11} = \frac{1}{4A_f^2} (a_1 b_1 A_f + b_1^2 x_c A_f + b_1 c_1 A_f) = \frac{b_1}{4A_f} (a_1 + b_1 x_c + c_1 y_c) \quad (\text{B-12})$$

Substituting for  $a_1$ ,  $b_1$ ,  $c_1$ ,  $x_c$  and  $y_c$  from equations (A-5) and (B-10), one obtains

$$\begin{aligned} S_{11} &= \frac{b_1}{4A_f} \left[ (x_2 y_3 - x_3 y_2) + (y_2 - y_3) \left( \frac{x_1 + x_2 + x_3}{3} \right) \right. \\ &\quad \left. + (x_3 - x_2) \left( \frac{y_1 + y_2 + y_3}{3} \right) \right] \end{aligned} \quad (\text{B-13})$$

Upon further simplification

$$S_{11} = \frac{b_1}{4A_f} \left( \frac{a_1 + a_2 + a_3}{3} \right) = \frac{b_1}{6} \quad (\text{B-14})$$

Similarly, it can be shown that

$$T_{11} = \frac{c_1}{6} \quad (\text{B-15})$$

Proceeding in a similar manner, the expression for  $R_{11}$  becomes

$$\begin{aligned} R_{11} = & (a_1^2/4A_f) + (b_1^2/16A_f) \left[ \frac{1}{3}(x_1^2 + x_2^2 + x_3^2) + 3x_c^2 \right] \\ & + (c_1^2/16A_f) \left[ \frac{1}{3}(y_1^2 + y_2^2 + y_3^2) + 3y_c^2 \right] + a_1 b_1 x_c / 2A_f \\ & + (b_1 c_1 / 8A_f) \left[ \frac{1}{3}(x_1 y_1 + x_2 y_2 + x_3 y_3) + 3x_c y_c \right] + a_1 c_1 y_c / 2A_f \end{aligned} \quad (\text{B-16})$$

Substituting for  $a_1$ ,  $b_1$ ,  $c_1$ ,  $x_c$ , and  $y_c$  from equation (A-5) and (B-10) one obtains

$$R_{11} = \frac{1}{72A_f} (6a_1^2 + 6a_2^2 + 12a_1 a_2 + 12a_1 a_3 + 12a_2 a_3) \quad (\text{B-17})$$

Upon further simplification

$$R_{11} = A_f / 6 \quad (\text{B-18})$$

APPENDIX 3 - DERIVATION OF SOLID FINITE ELEMENT EQUATIONS

The solid finite element used in this study is developed based on the method of virtual work. This method equates the work and change in strain energy in a system generated during a virtual displacement. This procedure is well known and has been documented [16,23,15,4,21].

A plane triangular solid finite element, as shown in Fig. 13, is used as the basis for the solid finite element formulation. It is assumed that the displacement components at any point in the triangular solid element,  $u_x$  and  $u_y$ , may be expressed as a polynomial in  $x$  and  $y$ . In this case

$$u_x = \alpha_{10} + \alpha_{11}x + \alpha_{12}y \quad u_y = \alpha_{13} + \alpha_{14}x + \alpha_{15}y \quad (C-1)$$

Employing the above equations in the same fashion as the pressure and velocity components in the fluid finite element, it can be shown that

$$\begin{Bmatrix} u_x \\ u_y \end{Bmatrix} = [N_s] \{u_e\} = \begin{bmatrix} N_{s1} & 0 & N_{s2} & 0 & N_{s3} & 0 \\ 0 & N_{s1} & 0 & N_{s2} & 0 & N_{s3} \end{bmatrix} \{u_e\} \quad (C-2)$$

where  $\{u_e\}$  is the array of time-dependent nodal displacements and  $[N_s]$  is the solid shape function given by

$$N_{si} = \frac{1}{2A_s} (a_i + b_i x + c_i y) \quad i = 1,2,3 \quad (C-3)$$

in which all the terms are defined as for the fluid element in Appendix 1.  $A_s$  is the area of the triangular solid element.

$$A_s = ( a_1 + a_2 + a_3 ) / 2 \quad (C-4)$$

The relationship in eq. ( C -2) is used in conjunction with the principle of virtual work and the theory of elasticity to yield the matrix differential equation for the nodal displacements of the solid finite element.

The discretization procedure is well documented [16,23,15,7,18 ] and yields

$$[M_e] \{\ddot{U}_e\} + [C_e] \{\dot{U}_e\} + [K_e] \{U_e\} = \{R'_e\} \quad (C-5)$$

where

$$\text{Solid mass matrix} \quad [M_e] = \iint_A [N_s]^T \rho_s [N_s] dA$$

$$\text{Solid damping matrix} \quad [C_e] = k_s [M_e] \quad (C-6)$$

$$\text{Solid stiffness matrix} \quad [K_e] = \iint_A [B]^T [\Delta] [B] dA$$

$\{R'_e\}$  is the external forcing function acting on the solid,  $\rho_s$  is density of the solid,  $[C_e]$  is the proportional damping matrix related to the mass matrix by the damping parameter  $k_s^{-1}$ , matrix  $[B]$  is the strain-displacement matrix and  $[\Delta]$  is the elasticity matrix. The boundary conditions which may be applied to eq. (C-5) are specified nodal displacements.

---

1

The damping matrices used throughout this study are proportional to mass matrix only.

The mass and damping matrices may be evaluated by directly substituting in the solid shape function (eq.(C -2 ) and (C -3 ))into eqs.(C-6) and performing the required integration. This yields the consistent mass matrix[15].

$$[M_e] = \frac{\rho_s A_s}{3} \begin{bmatrix} \frac{1}{2} & 0 & \frac{1}{4} & 0 & \frac{1}{4} & 0 \\ 0 & \frac{1}{2} & 0 & \frac{1}{4} & 0 & \frac{1}{4} \\ \frac{1}{4} & 0 & \frac{1}{2} & 0 & \frac{1}{4} & 0 \\ 0 & \frac{1}{4} & 0 & \frac{1}{2} & 0 & \frac{1}{4} \\ \frac{1}{4} & 0 & \frac{1}{4} & 0 & \frac{1}{2} & 0 \\ 0 & \frac{1}{4} & 0 & \frac{1}{4} & 0 & \frac{1}{2} \end{bmatrix} \quad (C-7)$$

Two types of mass matrices may be employed. The first is the consistent mass matrix given above. It is called consistent because it results directly from the finite element formulation. The second is the lumped mass matrix. In earlier solutions of structural dynamics problems, the mass of the element was arbitrarily lumped or concentrated at the nodes. This results in a mass matrix of the form [15]

$$[M_e] = \frac{\rho_s A_s}{3} [I_6] \quad (C-8)$$

in which  $[I_6]$  is the 6 x 6 identity matrix. The consistent mass matrix is more appealing from the point of view that it is a direct product of the mathematical formulation. It has also been observed that the off-diagonal terms in the consistent mass matrix produce sufficient numerical noise to obscure the actual results[15]. It has been demonstrated that for a given number of degrees of freedom, the lumped-mass representation is less accurate than the consistent mass; however, in many practical applications it is still preferable to use the lumped-mass matrices because of the significant computational advantage derived from the fact that such matrices are diagonal[23]. For these reasons, lumped mass matrices have been used throughout this study.

The stiffness matrix for the plane triangular linear finite element is a 6 x 6 symmetric matrix as follows [15].

$$[K_e] = \frac{E}{4 A_s (1 - \nu^2)} \begin{bmatrix} k_{11} & k_{12} & k_{13} & k_{14} & k_{15} & k_{16} \\ & k_{22} & k_{23} & k_{24} & k_{25} & k_{26} \\ & & k_{33} & k_{34} & k_{35} & k_{36} \\ & & & k_{44} & k_{45} & k_{46} \\ \text{Symmetric} & & & & k_{55} & k_{56} \\ & & & & & k_{66} \end{bmatrix} \quad (\text{C-9})$$

in which

$$\begin{aligned} k_{11} &= b_1^2 + \frac{1-\nu}{2} c_1^2 & k_{33} &= b_2^2 + \frac{1-\nu}{2} c_2^2 \\ k_{12} &= \frac{1+\nu}{2} b_1 c_1 = k_{21} & k_{34} &= \frac{1+\nu}{2} b_2 c_2 = k_{43} \\ k_{13} &= b_1 b_2 + \frac{1-\nu}{2} c_1 c_2 = k_{31} & k_{35} &= b_2 b_3 + \frac{1-\nu}{2} c_2 c_3 = k_{53} \\ k_{14} &= \nu b_1 c_2 + \frac{1-\nu}{2} b_2 c_1 = k_{41} & k_{36} &= \nu b_2 c_3 + \frac{1-\nu}{2} b_3 c_2 = k_{63} \\ k_{15} &= b_1 b_3 + \frac{1-\nu}{2} c_1 c_3 = k_{51} & k_{44} &= c_2^2 + \frac{1-\nu}{2} b_2^2 \\ k_{16} &= \nu b_1 c_3 + \frac{1-\nu}{2} b_3 c_1 = k_{61} & k_{45} &= \nu b_3 c_2 + \frac{1-\nu}{2} b_2 c_3 = k_{54} \\ k_{22} &= c_1^2 + \frac{1-\nu}{2} b_1^2 & k_{46} &= c_2 c_3 + \frac{1+\nu}{2} b_2 b_3 = k_{64} \\ k_{23} &= \nu b_2 c_1 + \frac{1-\nu}{2} b_1 c_2 = k_{32} & k_{55} &= b_3^2 + \frac{1-\nu}{2} c_3^2 \\ k_{24} &= c_1 c_2 + \frac{1-\nu}{2} b_1 b_2 = k_{42} & k_{56} &= \frac{1+\nu}{2} b_3 c_3 = k_{65} \\ k_{25} &= \nu b_3 c_1 + \frac{1-\nu}{2} b_1 c_3 = k_{52} & k_{66} &= c_3^2 + \frac{1-\nu}{2} b_3^2 \\ k_{26} &= c_1 c_3 + \frac{1-\nu}{2} b_1 b_3 = k_{62} \end{aligned}$$

APPENDIX 4. DERIVATION OF THE SOLID-FLUID SUPERELEMENT EQUATIONS

The finite element formulation of the solid-fluid superelement (i.e., equation (28) ) is based on the solid and fluid elements matrix equations as well as the interaction forces between the two elements.

The matrix equation for the solid-fluid superelement is obtained by combining equations (A-19) and (C-5) and including the interactive forces

$$\begin{Bmatrix} M_e & 0 \\ 0 & 0 \end{Bmatrix} \begin{Bmatrix} \ddot{U}_e \\ \ddot{Z}_e \end{Bmatrix} + \begin{Bmatrix} C_e & 0 \\ 0 & D_e \end{Bmatrix} \begin{Bmatrix} \dot{U}_e \\ \dot{Z}_e \end{Bmatrix} + \begin{Bmatrix} K_e & 0 \\ 0 & E_e \end{Bmatrix} \begin{Bmatrix} U_e \\ Z_e \end{Bmatrix} = \begin{Bmatrix} R_e \\ 0 \end{Bmatrix} + \begin{Bmatrix} R'_e \\ 0 \end{Bmatrix}$$

(D-1)

where  $\{R_e\}$  and  $\{R'_e\}$  are the fluid pressure force exerted on the solid representing the coupling force and the external forcing function acting on the solid respectively.

The contribution of the fluid pressure loading  $\{R_e\}$  is determined by calculating the work done by the pressure force during the virtual displacement as detailed hereunder.

Computation of the Solid-Fluid Coupling Matrix

The solid-fluid finite element, as shown in Fig. 14, is a quadrilateral composed of a solid and a fluid finite element. The equations for the nodal displacement components, pressure and velocity components of the quadrilateral solid-fluid element are obtained from the separate fluid and solid parts with the addition of the interactive forces. For the solid part, the interactive force is the pressure force acting normal to the moving boundary. For the fluid part, the interactive term is established by the solid-fluid boundary constraint given in eq.(29).

The interactive force due to pressure load on the solid is determined by calculating the work done by the pressure force during the virtual displacement as follows [11,15]:

$$dW_p = \int_S (du_N)^T p dS \quad (D-2)$$

The virtual displacement is given by

$$d\delta = d \begin{Bmatrix} u_x \\ u_y \end{Bmatrix} = [N_S] d\{u_e\} \quad (D-3)$$

Resolving it into its normal and tangential components by a coordinate transformation one obtains

$$d \begin{Bmatrix} u_T \\ u_N \end{Bmatrix} = \begin{bmatrix} \cos \alpha & \sin \alpha \\ -\sin \alpha & \cos \alpha \end{bmatrix} d \begin{Bmatrix} u_x \\ u_y \end{Bmatrix} \quad (D-4)$$

where  $\alpha$  is the angle the solid-fluid boundary makes with the horizontal axis, measured counterclockwise. The normal component of the virtual displa-



cement is given by

$$du_N = \begin{bmatrix} -\sin \alpha & \cos \alpha \end{bmatrix} [N_s] d\{u_e\} = [\bar{N}_s] d\{u_e\} \quad (D-5)$$

in which

$$[\bar{N}_s] = \begin{bmatrix} -\sin \alpha & \cos \alpha \end{bmatrix} [N_s] \quad (D-6)$$

$[\bar{N}_s]$  is the solid boundary shape function. Substituting eq. (D-6) into eq. (D-2) yields

$$dW_p = d\{u_e\}^T \int_S [\bar{N}_s]^T p \, dS \quad (D-7)$$

Substituting eq. (A - 3) for pressure into eq. (D-7) gives

$$dW_p = d\{u_e\}^T \int_S [\bar{N}_s]^T [N_f] \, dS \{p_e\} \quad (D-8)$$

The fluid pressure force on the solid-fluid boundary is

$$\{R_e\} = \int_S [\bar{N}_s]^T [N_f] \, dS \{p_e\} \quad (D-9)$$

or simply

$$\{R_e\} = [S_e] \{p_e\} \quad (D-10)$$

where

$$[S_e] = \int_S [\bar{N}_s]^T [N_f] dS \quad (D-11)$$

is the solid-fluid coupling matrix in which  $S$  is the line defining the solid-fluid boundary. Substituting eq.(D-10) into eq.(D-1), the final matrix equation for the superelement is obtained(i.e.eq.28). It shows clearly that the solid nodal displacements,  $u_x$  and  $u_y$ , and fluid nodal pressure,  $p$ , have been coupled. The boundary conditions for eq.(D-1) are the same as those indicated for the solid and the fluid parts.

Evaluation of the solid-fluid coupling matrix, eq. (D-11), for the case of a horizontal boundary ( i.e.,  $y = \hat{h}$ , a constant, and  $\alpha = 0$ ) yields a 6 x 3 matrix

$$[S_e] = \frac{1}{4A_s A_f} \begin{bmatrix} 0 & 0 & 0 \\ s_{21} & s_{22} & s_{23} \\ 0 & 0 & 0 \\ s_{41} & s_{42} & s_{43} \\ 0 & 0 & 0 \\ s_{61} & s_{62} & s_{63} \end{bmatrix} \quad (D-12)$$

in which

$$\begin{aligned} s_{2I,J} = & (a_i a_j + (a_i c_j + a_j c_i) h + c_i c_j \hat{h}^2)(x_f - x_o) + \\ & (a_i b_j + a_j b_i + (b_i c_j + b_j c_i) \hat{h}) (x_f^2 - x_o^2)/2 + \\ & b_i b_j (x_f^3 - x_o^3)/3 \end{aligned} \quad (D-13)$$

where  $i$  refers to the  $i^{\text{th}}$  node of the solid portion of the solid-fluid element and  $j$  refers to the  $j^{\text{th}}$  node of the fluid portion of the solid-fluid element, and  $x_o$  and  $x_f$  refer to the abscissa of the nodes defining the solid-fluid boundary. The coupling matrix may also be calculated for a vertical wall and the generalized case of a sloped wall, yielding similar results. For the vertical wall (i.e.,  $x = \hat{h}$ , a constant, and  $\alpha = \pi/2$ ) the coupling matrix is

$$[S_e] = \frac{1}{4A_s A_f} \begin{bmatrix} -s_{11} & -s_{12} & -s_{13} \\ 0 & 0 & 0 \\ -s_{31} & -s_{32} & -s_{33} \\ 0 & 0 & 0 \\ -s_{51} & -s_{52} & -s_{53} \\ 0 & 0 & 0 \end{bmatrix} \quad (\text{D-14})$$

in which

$$\begin{aligned} s_{(2I-1),J} = & (a_i a_j + (a_i b_j + a_j b_i) \hat{h} + b_i b_j \hat{h}^2)(y_f - y_o) \\ & + (a_i c_j + a_j c_i + (b_i c_j + b_j c_i) \hat{h})(y_f^2 - y_o^2)/2 \\ & + c_i c_j (y_f^3 - y_o^3)/3 \end{aligned} \quad (\text{D-15})$$

in which all terms are defined as before and  $y_o$  and  $y_f$  are the ordinates the nodes defining the solid-fluid boundary. For the general case of a sloped wall, the relationship along the boundary given by

$$y = \frac{y_f - y_o}{x_f - x_o} (x - x_o) + y_o = m (x - x_o) + y_o \quad (\text{D-16})$$

is used. This results in the coupling matrix

$$[S_e] = \frac{1}{4A_s A_f} \begin{bmatrix} -s_{11} \sin \alpha & -s_{12} \sin \alpha & -s_{13} \sin \alpha \\ s_{11} \cos \alpha & s_{12} \cos \alpha & s_{13} \cos \alpha \\ -s_{31} \sin \alpha & -s_{32} \sin \alpha & -s_{33} \sin \alpha \\ s_{31} \cos \alpha & s_{32} \cos \alpha & s_{33} \cos \alpha \\ -s_{51} \sin \alpha & -s_{52} \sin \alpha & -s_{53} \sin \alpha \\ s_{51} \cos \alpha & s_{52} \cos \alpha & s_{53} \cos \alpha \end{bmatrix} \quad (\text{D-17})$$

in which

$$\begin{aligned}
 s_{(2I-1),J} = & (a_i a_j - (a_i c_j + a_j c_i)(m x_o - y_o) + \\
 & c_i c_j (m x_o - y_o)^2)(x_f - x_o) + (a_i b_j + a_j b_i + \\
 & (a_i c_j + a_j c_i) m - (b_i c_j + b_j c_i)(m x_o - y_o) - \\
 & 2 c_i c_j m (m x_o - y_o))(x_f^2 - x_o^2)/2 + (b_i b_j + \\
 & (b_i c_j + b_j c_i) m + c_i c_j m)(x_f^3 - x_o^3)/3
 \end{aligned} \tag{D-18}$$

$$\alpha = \tan^{-1} \frac{y_f - y_o}{x_f - x_o} \tag{D-19}$$

and all other quantities are defined as before.

REFERENCES

- [1] Chen, S.S., "Flow-Induced Vibration of Circular Cylindrical Structures, Part I: Stationary Fluids and Parallel Flow", The Shock and Vibration Digest, vol. 9, No. 10, pp. 25-38, October 1977.
- [2] Chen, S.S., "Flow-Induced Vibration of Circular Cylindrical Structures, Part II: Cross-Flow Considerations", The Shock and Vibration Digest, vol. 9, No. 11, pp. 21-28, November 1977.
- [3] Conway, H.D. and Jakubowski, M., "Axial Impact of Short Cylindrical Bars", ASME publication 69-WA/APM-6 for meeting of November 16-20 1969.
- [4] Cook, R.D., Concepts and Applications of Finite Element Analysis, John Wiley and Sons, Inc., New York, 1974.
- [5] Feng, G.C., Kiefling, L., "Fluid-Structure Finite Element Vibrational Analysis", AIAA 74-102, AIAA 12th Aerospace Sciences Meeting, Washington, D.C., 1974.
- [6] Gallagher, R.H., Oden, J.T., Taylor, C. and Zienkiewicz, O.C., "Finite Elements in Fluids", volumes 1 and 2, John Wiley and Sons, 1975.
- [7] Gallagher, R.H., Finite Element Analysis Fundamentals, Prentice-Hall, Inc., New Jersey, 1975.
- [8] Greenspon, J.E., "Fluid-Solid Interaction", The American Society of Mechanical Engineers, New York, 1967.
- [9] Holmboe, E.L. and Rouleau, W.T., "The Effect of Viscous Shear on Transients in Liquid Lines", Transactions of ASME, Journal of Basic Engineering, vol. 89, No. 1, pp. 174-180, March 1967.
- [10] Huebner, K.H., "The Finite Element Methods for Engineers", John Wiley and Sons, 1975.
- [11] Nahavandi, A.N. and Pedrido, R.R., "An Analysis of Solid-Fluid Interaction Using the Finite Element Method", Dynamic Analysis of Pressure Vessel and Piping Components, ASME PVP-PB-022, pp. 75-93, 1977.
- [12] Nahavandi, A.N., Bohm, G.J. and Pedrido, R.R., "Structurally Compatible Fluid Finite Element for Solid-Fluid Interaction Studies", Nuclear Engineering and Design 35 (1975) 335-347.
- [13] Pettigrew, M.J. and Paidoussis, M.P., "Dynamics and Stability of Flexible Cylinders Subjected to Liquid and Two-Phase Axial Flow in Confined Annuli," 3rd Intl. Conf. Struc. Mech. Reactor Tech., London, vol. 1, Part D (sept. 1-5, 1975).

- [14] Paidoussis, M.P., "Vibration of Cylindrical Structures Induced by axial Flow", J. Engr. Indus., Trans., ASME, 96, pp. 547-553 (1974).
- [15] Pedrido, R.R., "Dynamic Analysis of Structures with Solid-Fluid Interaction", Dr. Eng. Sc. Dissertation, New Jersey Institute of Technology, Newark, New Jersey (1977).
- [16] Przemieniecki, J.S., Theory of Matrix Structural Analysis, New York: McGraw-Hill, 1968.
- [17] Savkar, S.D., "A Survey of Flow Induced Vibrations of Cylindrical Arrays in Cross-Flow", ASME publication 76-WA/FE-21 for meeting of Dec. 5, 1976.
- [18] Segerlind, L.J., Applied Finite Element Analysis, John Wiley and Sons, Inc., New Jersey, 1976.
- [19] Szilard, R., Hydrodynamically Loaded Shells, Honolulu: The University Press of Hawaii, 1973.
- [20] Tarantine, F.J. and Rouleau, W.T., "Fluid Pressure Transients in a Tapered Transmission Line", Transactions of ASME, Journal of Basic Engineering, vol. 89, No. 1, pp. 181-190, March 1967.
- [21] Wang, C.K., Computer Methods in Advanced Structural Analysis, Intext Educational Publishers, New York, 1973.
- [22] Zielke, W., "Frequency-Dependent Friction in Transient Pipe Flow", Transactions of ASME, Journal of Basic Engineering, March 1968, pp. 109-115.
- [23] Zienkiewicz, O.C., The Finite Element Method in Engineering Science, London: McGraw-Hill, 1971.

PART THREE

USER'S MANUAL

### 1. DESCRIPTION OF FASINT DIGITAL COMPUTER PROGRAM

The program FASINT(Fluid And Solid Interaction), developed for the analysis of interaction between an elastic solid and a fluid medium having pressure and velocity components in the fluid as well as solid displacements as the main dependent variables, consists of a main program and several subroutines. At the user's option, the program may also be used to analyze totally solid or totally fluid continua. A tabular outline of the MAIN program and its subroutines together with their functions are given below and followed by a more detailed description. The flowchart of FASINT is shown in Fig.26.

<u>PROGRAM OR SUBROUTINE NAME</u>	<u>FUNCTIONS</u>
MAIN	Controls the calling sequence of subroutines, initialization of the problem, insertion of the specified freedoms and the normal termination of the program.
CLEAR	Initializes all labelled common blocks to zero.
GDATA	Reads in and prints out the input data and initializes time and iteration number.
LOAD	Reads in and assembles applied loads and specified freedoms(i.e., displacements, pressure and velocities).
STIFT1(N)	Finds mass, damping and stiffness matrices for solid element number N.



<u>PROGRAM OR SUBROUTINE NAME</u>	<u>FUNCTIONS</u>
STIFT2(N)	Finds the inertia and fluidity matrices for fluid element number N.
STIFT3(N)	Finds the equivalent mass, combined damping-inertia and combined stiffness-fluidity matrices for solid-fluid superelement number N.
FORMK	Assembles the diagonal terms of matrices in global arrays and stores the off-diagonal terms.
SF(I,J)	Function subroutine used to calculate solid-fluid coupling matrix.
FORCE	Finds generalized global force array.
AINTEG	Finds analytical solution to the uncoupled global differential equations.

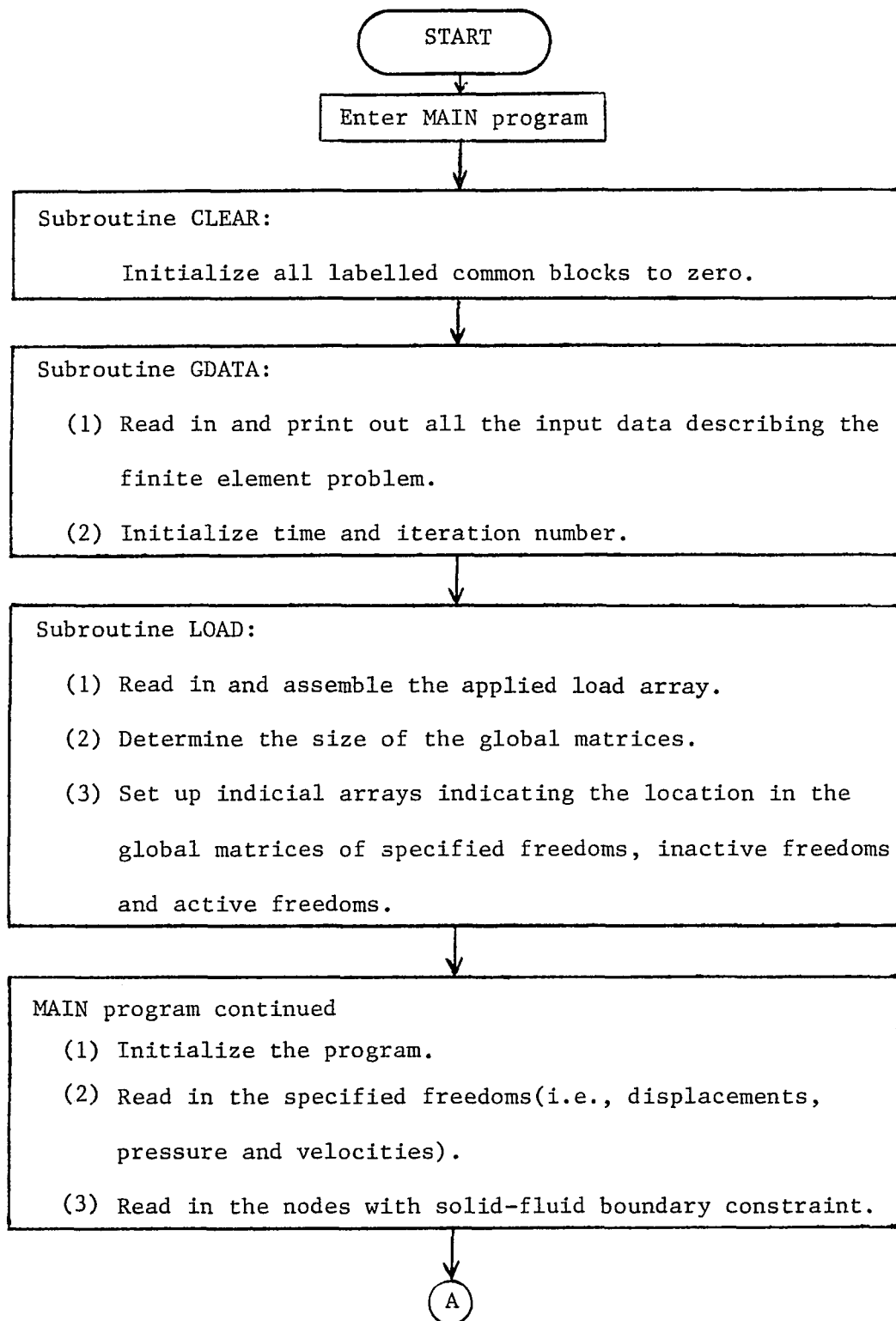


FIG. 26 SIMPLIFIED FLOWCHART OF FASINT PROGRAM

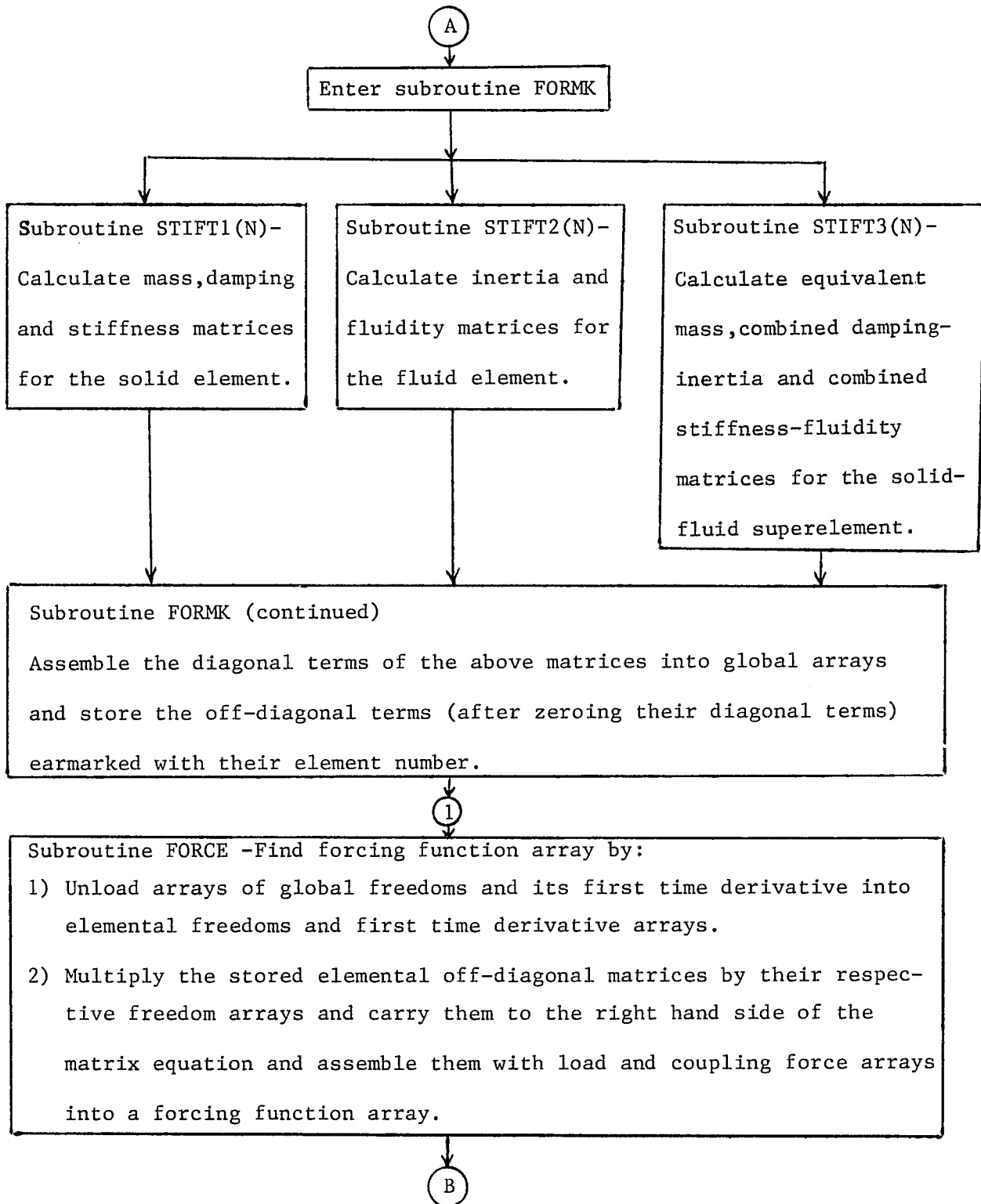


FIG. 26 SIMPLIFIED FLOWCHART OF FASINT PROGRAM ( CONTINUED )

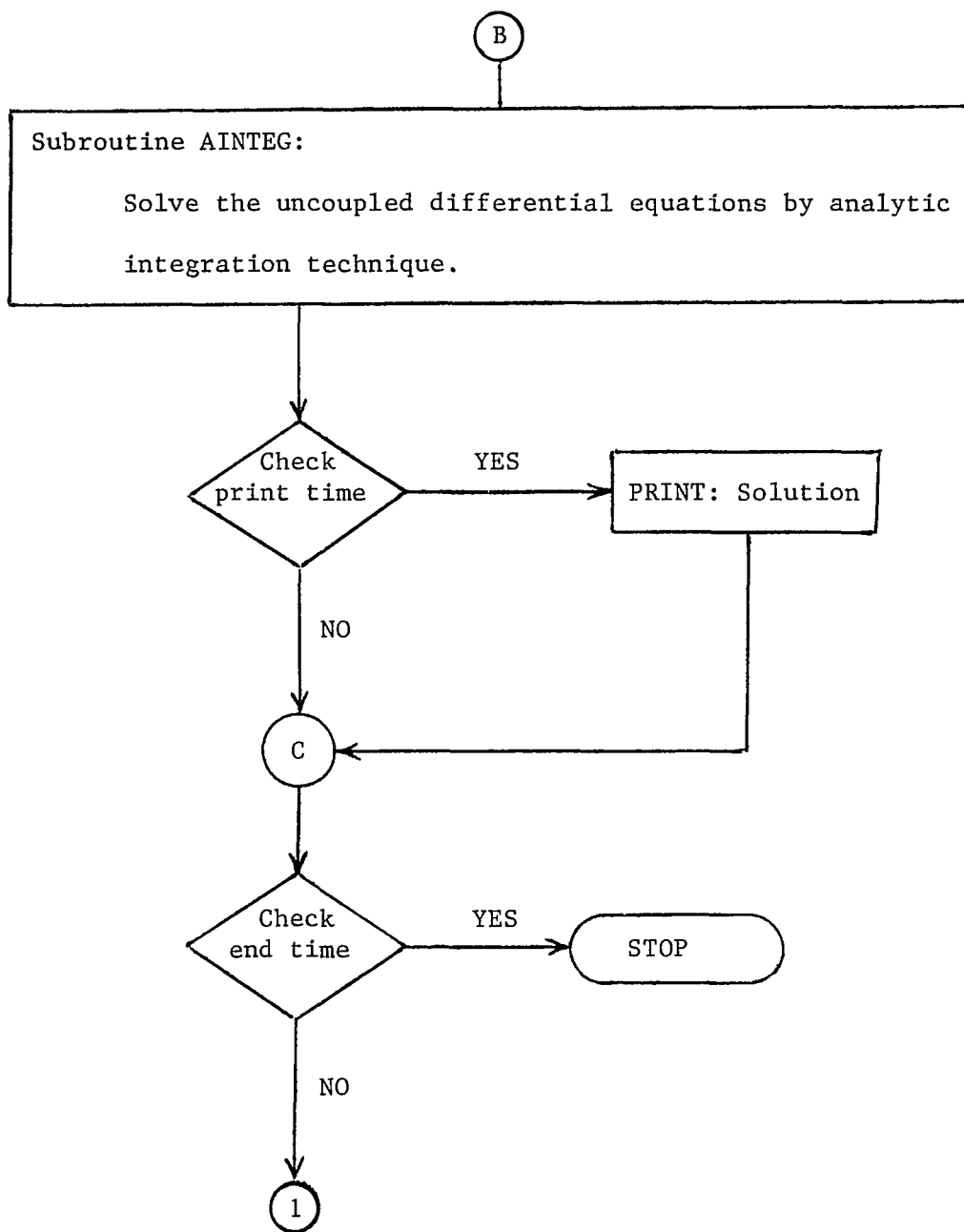


FIG. 26 SIMPLIFIED FLOWCHART OF FASINT PROGRAM ( CONTINUED )

### 1.1 MAIN Program

The MAIN program controls the calling sequence of subroutines, initialization of the problem, insertion of the specified freedoms and the normal termination of the program. The solution is obtained in an iterative loop based on the elapsed time of the problem. The program normally terminates when the iteration number(ITIME) is equal to the offline storage controller(IITIME) or the elapsed problem time is equal or greater than the final time.

### 1.2 CLEAR Subroutine

CLEAR subroutine initializes all variables in a labelled COMMON block equal to zero. Its calling sequence is

```
CALL CLEAR (AMEMBR, LENGTH)
```

in which AMEMBR is the name of the first variable in the COMMON block and LENGTH is the total number of variables occupying the COMMON block[15]. For example, if a COMMON block is of the form

```
COMMON/ITER/DIADIT(270),DIAK1(270)
```

the calling sequence for CLEAR would be

```
CALL CLEAR(DIADIT,540)
```

### 1.3 GDATA Subroutine

GDATA reads in and prints out all the input data describing the finite element problem. The data which are read in are described in section 2, DESCRIPTION OF INPUT DATA. GDATA also initializes the elapsed time and iteration number. Its calling sequence is

```
CALL GDATA
```

#### 1.4 LOAD Subroutine

This subroutine reads in and assembles the global applied load array and reads in the specified displacements, pressure and velocities. LOAD also functions as the system initialization routine. It determines the size of the global matrices and further sets up indicial arrays indicating the location in the global matrix of specified freedoms, inactive freedoms, and active freedoms for analytical solution. The calling statement for LOAD is

```
CALL LOAD
```

#### 1.5 FORMK Subroutine

Subroutine FORMK is entered only in the first iteration. Its function is to find and assemble the diagonal terms of mass, damping, stiffness, inertia, volumetric fluidity, combined damping-inertia and combined stiffness-volumetric fluidity matrices into global arrays and store their off-diagonal terms (after zeroing their diagonal terms) earmarked with their element number. FORMK calls the subroutines STIFT1, STIFT2 and STIFT3 to calculate the solid, fluid and solid-fluid matrices as described later. If the coupling matrix is to be calculated, FORMK calls STIFT3 which in turn calls SF Function to obtain this matrix. The calling sequence for this subroutine is

```
CALL FORMK
```

#### 1.6 STIFT1(N) Subroutine

Subroutine STIFT1(N) is called by FORMK to calculate the mass, damping and stiffness matrices for solid plane triangular finite element N. The calling statement for this subroutine is

```
CALL STIFT1(N)
```

in which the argument N is the solid element number.

### 1.7 STIFT2(N) Subroutine

Subroutine STIFT2(N) is called by FORMK to calculate the inertia and fluidity matrices for the fluid plane linear triangular finite element N. The calling statement for this subroutine is

```
CALL STIFT2(N)
```

in which the argument N is the fluid element number.

### 1.8 STIFT3(N) Subroutine

Subroutine STIFT3(N) is called by FORMK to calculate the combined damping-inertia and combined stiffness - fluidity matrices for the superelement plane linear quadrilateral solid-fluid finite element N. STIFT3(N) is also entered from FORMK to calculate the solid-fluid coupling matrix. The calling statement for this subroutine is

```
CALL STIFT3(N)
```

in which the argument N is the solid-fluid superelement number.

### 1.9 SF Function Subroutine

SF function is called by subroutine STIFT3 to calculate the terms of the 6 x 3 solid-fluid coupling matrix according to equations (D-13), (D-15) and (D-18). The subscripts I and J in these equations are indicial node numbers which refers to the node of the element being considered, i.e., first, second, or third. I refers to the solid nodes of the solid-fluid superelement, and J refers to the fluid nodes. This function is basically similar to the one presented by Pedrido [15].

### 1.10 FORCE Subroutine

FORCE prepares matrices for analytic solution by unloading global displacements, pressure, and velocities and their first and second time derivatives arrays into elemental arrays and multiplying the off-diagonal terms of matrices by these elemental arrays and assembling them with load and coupling force arrays into a generalized force array. The calling statement for this subroutine is

```
CALL FORCE
```

### 1.11 AINTEG Subroutine

AINTEG solves the uncoupled global matrix differential equations which results from the application of FORMK and FORCE subroutines described earlier , by analytic integration technique. Nodal displacement, pressure and velocities and their first and second time derivatives are determined analytically as function of time. The solution can be obtained for inviscid, slightly viscous and highly viscous or undamped and highly damped cases. The calling statement for this subroutine is

```
CALL AINTEG
```



## 2. DESCRIPTION OF INPUT DATA

In this section, the input data for FASINT is described in detail, followed by the printout of a sample data deck.

The format for each card description is as follows:

Card number. Title of Card

Purpose of Card

Format

Columns	Variable	Comments
---------	----------	----------

### FASINT Input Data

#### 1. Title Card

This card contains a 48-character descriptive title which is printed as a heading for the output data.

Format(12A4)

<u>Columns</u>	<u>Variable</u>	<u>Comments</u>
1-48	TITLE	If no title is desired, insert a blank card.

#### 2. Restart Card

IRUN, Restart Switch. This quantity controls the initialization of the program. When IRUN=0, program will start from initial condition. When IRUN=1, program will skip the initialization and will use previous output already stored on tape as initial values. The latter tape storage is achieved by setting IEND=1 in the previous run as discussed next.

IEND, Restart Controller. This quantity controls the

output at the completion of a dynamic run. When IEND = 1, the final program output will be stored on tape for restarting the run at a later date. When IEND = 0, no storage of the final output will be made.

Format(2I5)

<u>Columns</u>	<u>Variable</u>	<u>Comments</u>
1-5	IRUN	Restar switch
5-10	IEND	Restart controller

### 3. Program Control Card

This card reads two parameters. The first parameter, designated as offline storage controller(IITIME), controls the offline storage of output data for subsequent restart. At the appropriate iteration, indicated by IITIME, the output are stored on a disc, and recalled in the restart mode. The second parameter is the maximum number of iteration(LMAX) which may be needed for convergence of pressure and velocities.

Format(2I5)

<u>Columns</u>	<u>Variable</u>	<u>Comments</u>
1-5	IITIME	Offline storage controller
5-10	LMAX	Maximum number of iterations for convergence of pressure and velocities

### 4. Convergence Error Card

This card reads in the convergence error for convergence of pressure and velocities.

Format(I5)

<u>Columns</u>	<u>Variable</u>	<u>Comments</u>
1-5	ERRMAX	Convergence error

## 5. System Parameters Card

The data describing the system parameters, such as the number of nodes, elements, etc., are provided on this card.

Format(10I8)

<u>Columns</u>	<u>Variable</u>	<u>Comments</u>
1-8	NP	Number of nodes; $\leq 54$
9-16	NE	Number of elements; $\leq 72$
17-24	NB	Number of nodes with applied loads; $NB \geq 1$
25-32	NLD	Not used
33-40	NMAT	Number of materials, $\leq 2$
41-48	I1	Debug option, $0 \leq I1 \leq 3$  = 0 yields solution only = 3 yields maximum debug printout <sup>1</sup>
49-56	NPRINT	Frequency of printout; $\geq 1$
57-64	ND	Number of nodes with specified displacements, pressure and velocities; $1 \leq ND \leq 22$
65-72	NDF	Number of degrees of freedom of the system  = 3 for fluid system  = 2 for solid system  = 5 for solid-fluid system <sup>2</sup>

<sup>1</sup> In view of the voluminous amount of data resulting when  $I1 = 3$ , it is suggested that the user limit the duration of his runs when using a high debug option ( $I1 \geq 2$ ).

<sup>2</sup> Care must be taken that the product  $NP \times NDF$ , which represents the total global number of degrees of freedom, does not exceed 270.

<u>Columns</u>	<u>Variable</u>	<u>Comments</u>
73-80	NCON	Number of nodes with specified solid-fluid boundary constraints; $1 < \text{NCON} < 7$ .

#### 6. Time Card

This card reads in the parameters associated with the time history duration, as well as the angle between the solid-fluid boundary and the x-axis.  
Format(I10,3F10.6)

<u>Columns</u>	<u>Variable</u>	<u>Comments</u>
1-10	NIT	Number of iterations.
11-20	TBEG	Initial time of time history.
21-30	TEND	Final time of time history.
31-40	ALPHA	Angle between the solid-fluid boundary and the x-axis, measured counter-clockwise, radians.

#### 7. Material Properties Card

This card reads in the material properties for the number of materials specified in NMAT. One card is needed for each material.  
Format(I10,3E12.5)

<u>Columns</u>	<u>Variable</u>	<u>Comments</u>
1-10	N	Material type number; $\leq 2$
11-22	ORT(N,1)	= E, Young's modules for the solid. = c, Speed of sound for the fluid.
23-34	ORT(N,2)	= $\nu$ , Poisson's ratio for the solid. = $k_f$ , Viscous damping coefficient for the fluid.
35-46	ORT(N,3)	= $\rho$ , Density for the solid or the fluid.

#### 8. Damping Parameter Card

This card reads in the value of proportional damping to be used in the problem.  
Format(E12.5)

<u>Columns</u>	<u>Variable</u>	<u>Comments</u>
1-12	DAMP	= 0 for undamped system. = Nonzero for damped system.

#### 9. Nodal Point Data Card

This card reads in the x and y coordinates of each nodal point.

There must be one card for every node.

Format(I10,2F10.3)

<u>Columns</u>	<u>Variable</u>	<u>Comments</u>
1-10	N	Node number.
11-20	CORD(N,1)	x-coordinate of node.
21-30	CORD(N,2)	y-coordinate of node.

#### 10. Nodal Point Freedom Card

This card contains the number of degrees of freedom which exist at each node. There must be one card for each node.

Format(2I5)

<u>Columns</u>	<u>Variable</u>	<u>Comments</u>
1-5	N	Node number.
6-10	NTYPE(N)	Active degrees of freedom at node N.

#### 11. Element Connections Card

This card contains the node number associated with each element and the element material type number (see card 7). Element connections should be numbered in a consistent counter-clockwise fashion.

Solid-fluid elements are numbered listing the solid nodes first, and then the fluid nodes.

Format(8I5)

<u>Columns</u>	<u>Variable</u>	<u>Comments</u>
1-5	N	Element number.

<u>Columns</u>	<u>Variable</u>	<u>Comments</u>
6-10	NOP(N,1)	Nodes of fluid or solid finite element or
11-15	NOP(N,2)	solid nodes of solid-fluid finite element.
16-20	NOP(N,3)	
20-25	NOP(N,4)	Fluid nodes of solid-fluid finite element;
26-30	NOP(N,5)	blank for fluid or solid elements.
31-35	NOP(N,6)	
36-40	IMAT(N)	Material type number for finite element N. = 1 for totally solid problem. = 2 for totally fluid problem. For interactive problem. = 1 for solid element. = 2 for fluid element. = 3 for solid-fluid element.

## 12. Applied Load Type Card

This card contains the nodes at which applied loads act and the type of load which acts there. Even if no applied loads exist, a dummy load of zero must be applied at some arbitrary node. One card is needed for each applied load.

Format(2I5)

<u>Columns</u>	<u>Variable</u>	<u>Comments</u>
1-5	NBC	Node at which specified load acts.
6-10	NFIX	Code indication of direction of load = 01 load is in y-direction. = 10 load is in x-direction. = 11 load is in x and y-directions. = 0 dummy load.

### 13. Specified Freedom Type Card

This card contains the nodes at which specified freedoms (i.e., displacements, pressure and velocities) act and the type of specified freedoms which act there. At least one specified freedom must be given in order to restrain the system and remove rigid body modes. If a specified displacement and a specified pressure and velocity exist at a node, that node must be indicated twice, once for the specified displacements and once for the pressure and velocity.

Format(2I5)

<u>Columns</u>	<u>Variable</u>	<u>Comments</u>
1-5	NSD	Node at which specified freedoms act.
6-10	NDFIX	Code indication of direction of specified freedom. = 01 displacement in y-direction is given = 10 displacement in x-direction is given = 11 displacements in x and y-directions are given = 200 pressure is given = 20 velocity in x-direction is given = 2 velocity in y-direction is given = 22 velocities in x and y-directions are given = 220 pressure and x-direction velocity are given = 202 pressure and y-direction velocity are given = 222 pressure, x and y-direction velocities are given

## 14. Solid-Fluid Boundary Constraint Nodes

This card reads in the solid-fluid boundary constraint nodes in order to enforce eq.(29). There must be one card for every node.

Format(I5)

<u>Columns</u>	<u>Variable</u>	<u>Comments</u>
1-5	NSCON	Solid-fluid boundary constraint node.

## 15. Load Card

This card reads in the load information corresponding to card No. 12.

Format(F10.4)

<u>Columns</u>	<u>Variable</u>	<u>Comments</u>
1-10	PMAX	Magnitude of load.

## 16. Specified Freedom Card

This card contains the specified freedoms (i.e., displacements, pressure and velocities). One card is needed for each set of specified displacements and pressure and velocities corresponding to card No. 13.

Format(3F10.3)

<u>Columns</u>	<u>Variable</u>	<u>Comments</u>
1-10	DISP(N,1)	Specified pressure or specified displacement in x-direction.
11-20	DISP(N,2)	Specified velocity in x-direction or specified displacement in y-direction.
21-30	DISP(N,3)	Specified velocity in y-direction.



\*\*\*\*\* THIS IS A PRINTOUT OF A FASINT DATA DECK \*\*\*\*\*  
 72 ELEMENT FLUID-SOLID MODEL

54	72	1	3	2	700	21	5	7
0.01								
56000	0.	.002	0.					
1	.3E+08	.3E+00	.7297E-03					
2	.5E+05	0.0E+00	.0000935521					
0.								
1	.5	3.						
2	.5	4.						
3	.6	8.						
4	.5	12.						
5	.5	12.25						
6	.6	12.5						
7	2.7	0.						
8	2.7	4.						
9	2.7	8.						
10	2.7	12.						
11	2.7	12.25						
12	2.7	12.5						
13	5.9	0.						
14	5.9	4.						
15	5.9	8.						
16	5.9	12.						
17	5.9	12.25						
18	5.9	12.5						
19	11.1	0.						
20	11.1	4.						
21	11.1	8.						
22	11.1	12.						
23	11.1	12.25						
24	11.1	12.5						
25	15.3	0.						
26	15.3	4.						
27	15.3	8.						
28	15.3	12.						
29	15.3	12.25						
30	15.3	12.5						
31	19.5	0.						
32	19.5	4.						
33	19.5	8.						
34	19.5	12.						
35	19.5	12.25						
36	19.5	12.5						
37	23.7	0.						
38	23.7	4.						
39	23.7	8.						
40	23.7	12.						
41	23.7	12.25						
42	23.7	12.5						
43	27.9	0.						
44	27.9	4.						
45	27.9	8.						
46	27.9	12.						
47	27.9	12.25						
48	27.9	12.5						
49	30.	0.						
50	30.	4.						

	51	30.	3.	
	52	30.	12.	
	53	30.	12.25	
	54	30.	12.5	
1	3			
2	3			
3	3			
4	5			
5	2			
6	2			
7	3			
8	3			
9	3			
10	5			
11	2			
12	2			
13	3			
14	3			
15	3			
16	5			
17	2			
18	2			
19	3			
20	3			
21	3			
22	5			
23	2			
24	2			
25	3			
26	3			
27	3			
28	5			
29	2			
30	2			
31	3			
32	3			
33	3			
34	5			
35	2			
36	2			
37	3			
38	3			
39	3			
40	5			
41	2			
42	2			
43	3			
44	3			
45	3			
46	5			
47	2			
48	2			
49	3			
50	3			
51	3			
52	5			
53	2			
54	2			
1	1	7	3	2
2	1	8	2	2
3	2	3	2	2

4	2	9	3					2
5	3	9	10					2
5	4	10	11	3	10	4		3
7	4	11	5					1
9	5	11	12					1
9	5	12	6					1
10	7	13	14					2
11	7	14	3					2
12	8	14	15					2
13	8	15	9					2
14	9	15	15					2
15	10	16	17	9	15	10		3
15	10	17	11					1
17	11	17	13					1
18	12	13	12					1
19	13	19	20					2
20	13	20	14					2
21	14	20	21					2
22	14	21	15					2
23	15	21	22					2
24	15	22	23	15	22	15		3
25	15	23	17					1
26	17	23	24					1
27	17	24	13					1
28	19	25	25					2
29	19	25	20					2
30	20	25	27					2
31	20	27	21					2
32	21	27	29					2
33	22	28	29	21	23	22		3
34	22	29	23					1
35	23	29	30					1
35	23	30	24					1
37	25	31	32					2
38	25	32	25					2
39	25	32	33					2
40	25	33	27					2
41	27	33	34					2
42	23	34	35	27	31	23		3
43	23	35	29					1
44	23	35	35					1
45	29	36	30					1
45	31	37	31					2
47	31	33	32					2
48	32	38	39					2
49	32	39	33					2
50	33	39	40					2
51	34	40	41	33	31	34		3
52	34	41	35					1
53	35	41	42					1
54	35	42	35					1
55	37	43	44					2
56	37	44	38					2
57	38	44	45					2
58	38	45	39					2
59	39	45	45					2
50	40	45	47	39	45	40		3
51	40	47	41					1
62	41	47	43					1
53	41	48	42					1
64	45	49	50					2

55	43	50	44	2			
56	44	50	51	2			
67	44	51	45	2			
59	45	51	52	2			
69	45	52	43	45	52	45	3
70	45	53	47	1			
71	47	53	54	1			
72	47	54	43	1			
I	0						
1	202						
2	200						
3	200						
4	202						
4	11						
5	11						
6	11						
7	2						
13	2						
19	2						
25	2						
31	2						
37	2						
43	2						
49	202						
50	200						
51	200						
52	202						
52	11						
53	11						
54	11						
10							
15							
22							
28							
34							
40							
+5							

0.		
10.		0.
10.		
10.		0.
0.	0.	
0.	0.	
0.	0.	
		0.
		0.
		0.
		0.
		0.
		0.
		0.
0.		0.
0.		0.
0.		0.
0.		0.
0.	0.	
0.	0.	
0.	0.	

\*\*\*\*\* END OF SAMPLE DATA DECK \*\*\*\*\*

### 3. DESCRIPTION OF OUTPUT DATA

The output data are classified as follows:

#### 3.1 Output data not under debug option control

The output data which are not under the control of the debug option  $Il$  control are as follows:

<u>Subroutine</u>	<u>Output</u>
GDATA	Geometric and properties input data, the other parameters defined in the description of input data.
LOAD	Global degrees of freedom; specified freedoms; load input data; indicial arrays; global load array.
AINTEG	Time parameters such as time, iteration number, etc; numerical values of the results.

All the above data are printed out with suitable headings regardless of the debug printout discussed hereunder.

#### 3.2 Output data under the control of the debug option

When  $Il \geq 1$ , the following data is printed out.

<u>Subroutine</u>	<u>Output</u>
FORMK	Global arrays of assembled diagonal terms of matrices.
FORCE	Forcing function array.
AINTEG	Global arrays of displacements, pressure and velocities and their corresponding first and second derivatives excluding the specified freedoms; intermediate parameters such as damped frequency, natural frequency, etc.

When  $Il \geq 2$ , the following data is printed out.

<u>Subroutine</u>	<u>Output</u>
FORCE	Temporary arrays of elemental displacements, pressure and velocities and their corresponding first and second derivatives and indicial array; temporary elemental force array resulting from the off-diagonal terms of elemental mass, stiffness, inertia, fluidity, combined damping-inertia or combined stiffness-fluidity matrices.

When  $Il \geq 3$ , the following data is printed out.

<u>Subroutine</u>	<u>Output</u>
FORMK	Elemental indicial array; elemental off-diagonal terms of damping, stiffness, inertia, fluidity, combined damping-inertia, or combined stiffness-fluidity matrices.
STIFT1	Local coordinates; element connections; elemental mass, damping and stiffness matrices; area of finite element, etc.
STIFT2	Local coordinates; element connections; elemental inertia and fluidity matrices; area of finite element; etc.
STIFT3	Local coordinates, element connections, and areas of solid portion and fluid portion of quadrilateral solid-fluid element; elemental equivalent mass, combined damping-inertia and stiffness-fluidity matrices; elemental coupling matrices.

All of the above data are printed out with suitable headings. A working knowledge of the program is necessary to perform effective debugging.

### 3.3 Error Prinouts

If the user does not number either the nodes in an orderly fashion or the element connections in a consistently counter-clockwise manner, the following printout will occur.

#### Subroutine

#### Output

STIFT1,2 or 3    Number of element with bad connections - run is terminated.

### 3.4 Output Data Defining the Problem Solution

The program first prints out the heading " Finite Element Analytic Integration Solution " followed by the elapsed time, time increment, iteration number, printout iteration number, frequency of printout, and time at first iteration. The node number, freedom number and the numerical value of the result are then printed out as the problem solution.

#### 4 OPERATING PROCEDURE

To employ the FASINT computer program effectively, it is recommended that the user familiarizes himself with the formulation of finite element model and its numerical solution, presented in Part 1 and 2 as well as the organization of the program described in Part 3, before attempting to solve a solid-fluid interaction problem using FASINT.

In developing the finite element mesh the user should number the nodes in an orderly fashion and the element connections in a consistently counterclockwise manner. Failure to do so would result in a bad connection error message printout and abnormal termination of the run. Quadrilateral solid-fluid elements are numbered starting with the solid nodes first and then the fluid nodes. The input data is then punched and prepared in accordance with the format and description presented in Part 3, Section 2, DESCRIPTION OF INPUT DATA. These input data are then punched on cards and assembled with with FASINT source deck and the appropriate control cards. A sample of the deck assembling cards for UNIVAC SERIES 70 is given below:

```
/LOGON userid,acct. no. TIME=in second
/PARAM LIST=YES,MAP=YES,DEBUG=YES
/EXEC BGFOR
PROGRAM NAME
( FASINT Source Statement)
END
```



```
/FILE FASINT .RESTART1,LINK=DSET24,FCBTYPE=SAM1
/FILE FASINT .RESTART2,LINK=DSET25,FCBTYPE=SAM2
/EXEC *
      (FASINT data deck)
/LOGOFF
```

The following procedure is recommended for effective use of the FASINT program,

1) Input data check run

The user should make a run with the beginning time and final time of the run set equal to zero. The debug option should also be set equal to zero. The program will then print out all of the input data and all other problem data, such as sorted global load array, up to the problem solution. This enables the user to check the input data and the intermediate results for correctness. If the input data is incorrect, this run should be repeated until all user errors have been rectified. If the intermediate results appear incorrect, the program may be run with a higher debug option for several integration time steps to provide more debug printout to help the user determine the nature of the difficulty.

2) Test run

After the data has been debugged, the user may perform

---

<sup>1</sup>RESTART1 designates the input offline storage

<sup>2</sup>RESTART2 designates the output offline storage

a dynamic run using a time step on the basis of Section 4 in part one and part two.

### 3) Finite element mesh convergence run

The convergence of the finite element mesh is determined by making a run having a finer grid (more elements) than the desired grid. Convergence is achieved when there is no appreciable difference between the runs.

### 4) Time step convergence run

The convergence of the time step is determined by making a run having a time step that is twice the desired one. Convergence is reached when there is no appreciable difference between the runs. If there is a discrepancy, the time step should be halved and this run repeated until convergence is established.

### 5) Restart Capability

Restart switch, IRUN, controls the initialization of the program. When IRUN = 0, program will start from initial condition. When IRUN = 1, program will skip the initialization and will use previous output already stored on tape as initial values. The latter tape storage is achieved by setting IEND=1 in the previous run as discussed next. Restart controller, IEND, controls the output at the completion of a dynamic run. When IEND = 1, the final program output will be stored on tape for restarting the run at a later date. When IEND = 0, no storage of the final output will be made. This procedure may be used for any desired offline storage controller iteration

number, IITIME, at which the output will be stored on tape for restarting the run at a later date.

The runs made for the completion of part one required 68k bytes of storage and was executed on the INTERDATA 7/32 mini-computer. The computations for part two required 318k bytes of storage and was executed on IBM 370/168 digital computer.

## 5. FASINT NOMENCLATURE

The variables used in FASINT are listed, defined, and cross-referenced with the analysis notation, to aid the user in understanding the program.

### 5.1 Subscripted Variables

<u>Program Notation</u>	<u>Analysis Notation</u>	<u>Subroutine</u>	<u>Description</u>
AO(3),AM(3)	a	STIFT2,STIFT3	Local area coordinates of fluid and solid triangles, respectively, in <sup>2</sup> .
AK(20,20)	$[K_e]$ , $[H_e]$ , $[\bar{K}_e]$	STIFT1,STIFT2, STIFT3	In STIFT1, stiffness matrix In STIFT2, fluidity matrix In STIFT3, combined stiffness-fluidity matrix
BO(3),BM(3)	b	STIFT1,STIFT2, STIFT3	Local y-coordinate of fluid and solid triangles, respectively, in.
CO(3),CM(3)	c	STIFT1,STIFT2, STIFT3	Local x-coordinate of fluid and solid triangles, respectively, in.
CORD(54,2)	x,y	GDATA	Array of nodal coordinates, in.
DISPL(20)	$\{Z_e\}$ , $\{X_e\}$	FORCE	Array of elemental freedoms(i.e., pressure, x-component of velocity and y-component of velocity, and displacements).

<u>Program Notation</u>	<u>Analysis Notation</u>	<u>Subroutine</u>	<u>Description</u>
DISP(22,3)	-	LOAD	Matrix of specified freedoms (i.e., displacements, pressure and velocities).
GM(20,20)	$[M_e], [\bar{M}_e]$	STIFT1, STIFT3	In STIFT1, mass matrix  In STIFT3, equivalent mass matrix
DIAAC(270)	$\{\ddot{X}\}$	FORCE,AINTEG	Updated array of global freedoms second time derivative
DIAACC(270)	$\{\ddot{X}\}_o$	FORCE,AINTEG	Array of global freedoms (i.e., displacements, pressure and velocities) second time derivative.
DIADI(270)	$\{\bar{X}\}$	FORCE,AINTEG	Updated array of global freedoms (i.e., displacements, pressure and velocities).
DIADIS(270)	$\{\bar{X}\}_o$	FORCE,AINTEG	Array of global freedoms (i.e., displacements, pressure and velocities).
DIAVE(270)	$\{\dot{X}\}$	FORCE,AINTEG	Updated array of global freedoms (i.e., displacements, pressure and velocities) first time derivative.
DIAVEL(270)	$\{\dot{X}\}_o$	FORCE,AINTEG	Array of global freedoms (i.e., displacements, pressure and

<u>Program Notation</u>	<u>Analysis Notation</u>	<u>Subroutine</u>	<u>Description</u>
DIAGC(270)	$\bar{C}'_i$	FORCE,AINTEG	Diagonal matrix with diagonal terms equal to diagonal terms of $[\bar{C}]$ .
DIAGK(270)	$\bar{K}'_i$	FORCE,AINTEG	Diagonal matrix with diagonal terms equal to diagonal terms of $[\bar{K}]$ .
DIAGM(270)	$\bar{M}'_i$	FORCE,AINTEG	Diagonal matrix with diagonal terms equal to diagonal terms of $[\bar{M}]$ .
DIAK(270)	$\{\bar{F}'\}_o$	FORCE,AINTEG	Forcing function array.
DIAK1(270)	$\{\bar{F}'\}$	FORCE,AINTEG	Updated forcing function array.
FORCEC(20)	$[\bar{C}''_e] \cdot \{\dot{x}_e\}$	FORCE	Elemental forcing function array resulting from the multiplication of the stored elemental off-diagonal damping, inertia or combined damping-inertia matrices by their respective freedom array.
FORCEK(20)	$[\bar{K}''_e] \cdot \{x_e\}$	FORCE	Elemental forcing function array resulting from the multiplication of the stored elemental off-diagonal stiffness, fluidity or combined stiffness-fluidity matrices by their respective freedom array.
IMAT(72)	-	GDATA,FORMK, STIFT1,2 and 3	Array of element material type numbers.
INACT(115)	-	LOAD	Indicial array of rows which contain inactive freedoms.
INDEX(32)	-	LOAD	Indicial array of rows at which specified freedoms act.

<u>Program Notation</u>	<u>Analysis Notation</u>	<u>Subroutine</u>	<u>Description</u>
NACT(32)	-	LOAD	Indicial array of active row numbers in sequence.
NBC(1)	-	GDATA,LOAD	Array of nodes at which specified loads act.
NDFIX(22)	-	GDATA,LOAD	Array of code indicators of direction of specified freedoms.
NFIX(1)	-	GDATA,LOAD	Array of code indicators of direction of applied loads.
NOP(72,6)	-	STIFT1,2 and 3	Matrix of element connections.
NSCON(7)	-	GDATA	Nodes with solid-fluid boundary constraints.
NSD(22)	-	GDATA,LOAD	Array of nodes at which specified freedoms act.
NSDF(270)	-	AINTEG	Indicator of specified freedoms: = 0 for free freedoms = 1 for specified freedoms
NTYPE(54)	-	GDATA,FORMK	Array of nodal degrees of freedom.
ORT(2,3)	-	GDATA,STIFT1, STIFT2,STIFT3	Matrix of material properties.
R(5)	$\{R'_e\}$	LOAD	Elemental applied load array.
R4(270)	$\{R'\}$	LOAD,FORCE	Array of applied loads.
S(6,3)	$[S_e]$	STIFT3	Elemental solid-fluid coupling matrix.
STOREC(20,20,72)	$[\bar{C}''_e]$	FORMK,FORCE	Damping, inertia or combined damping-inertia matrices with zeroes along their diagonals.

<u>Program Notation</u>	<u>Analysis Notation</u>	<u>Subroutine</u>	<u>Description</u>
STOREK(20,20,72)	$[\bar{K}_e'']$	FORMK, FORCE	Stiffness, fluidity, and combined stiffness-fluidity matrices with zeroes along their diagonal.
VELOC(20)	$\{\dot{\bar{X}}_e\}$	FORCE	Array of elemental freedoms (i.e., displacements, pressure and velocities) first time derivative.
XM(20,20)	$[C_e], [L_e], [\bar{C}_e]$	STIFT1, STIFT2,	In STIFT1, elemental damping matrix.
		STIFT3	In STIFT2, elemental inertia matrix.
			In STIFT3, elemental combined damping-inertia matrix.



## 5.2 Nonsubscripted Variables

<u>Program Notation</u>	<u>Analysis Notation</u>	<u>Subroutine</u>	<u>Description</u>
ALPHA	$\alpha$	STIFT3	Angle of solid-fluid boundary with longitudinal x-axis, radians.
AH	$\tilde{h}$	STIFT3	Constant value of x or y used in the computation of solid-fluid coupling matrix for vertical or horizontal wall, respectively.
AREAO,AREAM	$A_f, A_s$	STIFT1,2 and 3	Area of fluid and solid triangles respectively.
DAMP	$k_s$	STIFT1,STIFT3	Damping factor based on mass, $\text{sec}^{-1}$ .
DELT	$\Delta t$	FORMK	Time step, sec.
DOF	-	LOAD	Degrees of freedom.
ERRMAX	-	FORCE	Convergence error.
I1	-	GDATA	Debug option.
IEND	-	GDATA	Restart controller.
IITIME	-	GDATA	Off-line storage controller.
I,J,K	-	STIFT1,2 and 3	Element connections.
IRUN	-	GDATA	Restart switch.
ITIME	-	GDATA	Iteration number.
LMAX	-	GDATA	Maximum number of iterations for convergence of freedoms.
MDF	-	FORMK	Dummy degree of freedom.
NB	-	GDATA,LOAD	Number of nodes with applied loads.
NCN	-	MAIN	Number of nodes per element.
NCON	-	GDATA	Number of nodes with specified solid-fluid boundary constraints.
NQ	-	LOAD	Node at which load acts.
ND	-	GDATA,LOAD	Number of nodes with specified freedoms.

<u>Program Notation</u>	<u>Analysis Notation</u>	<u>Subroutine</u>	<u>Description</u>
NDF	-	GDATA,SF	Nodal degree of freedom.
NE	-	GDATA,FORMK	Number of elements.
NIT	-	GDATA	Number of iterations.
NLD	-	GDATA	Not used.
NMAT	-	GDATA	Number of material types.
NP	-	GDATA,SF	Number of nodes.
NPRINT	-	GDATA	Frequency of printout.
NSZF	-	SF,GDATA	Size of global arrays.
NTIME	-	FORMK	Printout control parameter.
T	t	FORMK	Elapsed problem time, sec.
TBEG	-	GDATA	Time at beginning of time history.
TEND	-	GDATA	Time at end of time history.
T1	-	FORMK	Time at first iteration.

## 6. PROGRAM LISTING AND SAMPLE RUN

In this section, the FORTRAN program listing of FASINT together with the output of a sample run for an undamped system are presented. The model being used to illustrate the behaviour of the program is a 72 element solid-fluid model, similar to Fig.13 . To reduce the bulk of computer printout, the output data are supplied for iteration number 0, 1, and 700 corresponding to 0.00000E+00, 0.35714E-07 and 0.24999E-04 seconds, respectively.



```

C
3270 IFC IRUN .EQ. 11 GO TO 10
3281 GO TO 11
3282 CONTINUE
C
3283 READ ID
3284 READ(20) T, DELT, TIME, NTIME, PRINT, IS, II
3285 CONTINUE, 7201, DELT, TIME, NTIME, PRINT, II, II
3286 CONTINUE
3287 WRITE(5, 5001)
3288 DO 11 J=1, 450, 5
3289 IF(J=4)
3290 READ(30) (DIVIDIS(K), DIAMEL(K), DIAC2(K), I<=IJ, IL)
3291 WRITE(5, 5002)
3292 CONTINUE, 5001, 5002, DIAC2(K), I<=IJ, IL)
3293 CONTINUE
3294 WRITE(5, 5003)
3295 CONTINUE
C
C-----END OF DISC OUTPUT -----
3296 CONTINUE
3297 CONTINUE
C
C-----FOR ALL FREE DMS
3298 DO 200 J=1, 450
C
C INCLUDE SPECIFIED DISPLACEMENTS AND SOLID-FLUID BOUNDARY
C CONSTRAINTS
3299 READ(10) ND
3300 IFC(ND=1) GO TO 40
3301 WRITE(5, 5004)
3302 IFC(ND=2) GO TO 30
3303 IFC(ND=3) GO TO 41
3304 IFC(ND=4) GO TO 52
3305 IFC(ND=5) GO TO 52
3306 IFC(ND=6) GO TO 52
3307 IFC(ND=7) GO TO 52
3308 IFC(ND=8) GO TO 52
3309 IFC(ND=9) GO TO 52
3310 IFC(ND=10) GO TO 52
3311 IFC(ND=11) GO TO 52
3312 IFC(ND=12) GO TO 52
3313 IFC(ND=13) GO TO 52
3314 IFC(ND=14) GO TO 52
3315 IFC(ND=15) GO TO 52
3316 IFC(ND=16) GO TO 52
3317 IFC(ND=17) GO TO 52
3318 IFC(ND=18) GO TO 52
3319 IFC(ND=19) GO TO 52
3320 IFC(ND=20) GO TO 52
3321 IFC(ND=21) GO TO 52
3322 IFC(ND=22) GO TO 52
3323 IFC(ND=23) GO TO 52
3324 IFC(ND=24) GO TO 52
3325 IFC(ND=25) GO TO 52
3326 IFC(ND=26) GO TO 52
3327 IFC(ND=27) GO TO 52
3328 IFC(ND=28) GO TO 52
3329 IFC(ND=29) GO TO 52
3330 IFC(ND=30) GO TO 52
3331 IFC(ND=31) GO TO 52
3332 IFC(ND=32) GO TO 52
3333 IFC(ND=33) GO TO 52
3334 IFC(ND=34) GO TO 52
3335 IFC(ND=35) GO TO 52
3336 IFC(ND=36) GO TO 52
3337 IFC(ND=37) GO TO 52
3338 IFC(ND=38) GO TO 52
3339 IFC(ND=39) GO TO 52
3340 IFC(ND=40) GO TO 52
3341 IFC(ND=41) GO TO 52
3342 IFC(ND=42) GO TO 52
3343 IFC(ND=43) GO TO 52
3344 IFC(ND=44) GO TO 52
3345 IFC(ND=45) GO TO 52
3346 IFC(ND=46) GO TO 52
3347 IFC(ND=47) GO TO 52
3348 IFC(ND=48) GO TO 52
3349 IFC(ND=49) GO TO 52
3350 IFC(ND=50) GO TO 52
3351 IFC(ND=51) GO TO 52
3352 IFC(ND=52) GO TO 52
3353 IFC(ND=53) GO TO 52
3354 IFC(ND=54) GO TO 52
3355 IFC(ND=55) GO TO 52
3356 IFC(ND=56) GO TO 52
3357 IFC(ND=57) GO TO 52
3358 IFC(ND=58) GO TO 52
3359 IFC(ND=59) GO TO 52
3360 IFC(ND=60) GO TO 52
3361 IFC(ND=61) GO TO 52
3362 IFC(ND=62) GO TO 52
3363 IFC(ND=63) GO TO 52
3364 IFC(ND=64) GO TO 52
3365 IFC(ND=65) GO TO 52
3366 IFC(ND=66) GO TO 52
3367 IFC(ND=67) GO TO 52
3368 IFC(ND=68) GO TO 52
3369 IFC(ND=69) GO TO 52
3370 IFC(ND=70) GO TO 52
3371 IFC(ND=71) GO TO 52
3372 IFC(ND=72) GO TO 52
3373 IFC(ND=73) GO TO 52
3374 IFC(ND=74) GO TO 52
3375 IFC(ND=75) GO TO 52
3376 IFC(ND=76) GO TO 52
3377 IFC(ND=77) GO TO 52
3378 IFC(ND=78) GO TO 52
3379 IFC(ND=79) GO TO 52
3380 IFC(ND=80) GO TO 52
3381 IFC(ND=81) GO TO 52
3382 IFC(ND=82) GO TO 52
3383 IFC(ND=83) GO TO 52
3384 IFC(ND=84) GO TO 52
3385 IFC(ND=85) GO TO 52
3386 IFC(ND=86) GO TO 52
3387 IFC(ND=87) GO TO 52
3388 IFC(ND=88) GO TO 52
3389 IFC(ND=89) GO TO 52
3390 IFC(ND=90) GO TO 52
3391 IFC(ND=91) GO TO 52
3392 IFC(ND=92) GO TO 52
3393 IFC(ND=93) GO TO 52
3394 IFC(ND=94) GO TO 52
3395 IFC(ND=95) GO TO 52
3396 IFC(ND=96) GO TO 52
3397 IFC(ND=97) GO TO 52
3398 IFC(ND=98) GO TO 52
3399 IFC(ND=99) GO TO 52
3400 IFC(ND=100) GO TO 52

```



PAGE 0001

11/53/39

DATE = 78232

CLEAR

FURIRAN IV 5 LEVEL 21

```
0001 SUBROUTINE CLEAR(AMVER,LENGTH)
0002   DIMENSION REZR(LENGTH)
0003   DO 10 I=1,LENGTH
0004     REZR(I)=0.0
0005   10 CONTINUE
0006   RETURN
0007   END
```







```

0001      SUBROUTINE L3AD
0002      DIMENSION P(NT,LEI2),QRI(2,2,3),VSCOV(7),UDR(54,2),WDP(72,6)
0003      IF(NT*(2)+4*LEI2 > 1) WRITE(*,*) 'ERROR: INSUFFICIENT SPACE FOR P'
0004      CALL L3ADQ(NT,LEI2,NDIR,NDP,NDIR(1:NDP),VACT(1:NDP),VACT(1:NDP))
0005      CALL L3ADP(NT,LEI2,NDIR,NDP,NDIR(1:NDP),VACT(1:NDP))
0006      IF(NT*(2)+4*LEI2 > 1) WRITE(*,*) 'ERROR: INSUFFICIENT SPACE FOR Q'
0007      DIMENSION WDP(72,6),VACT(1:NDP),VACT(1:NDP)
0008      WDP(1:72,6) = 0.0
0009      WDP(1:72,6) = WDP(1:72,6) + VACT(1:NDP)
0010      WDP(1:72,6) = WDP(1:72,6) + VACT(1:NDP)
0011      WDP(1:72,6) = WDP(1:72,6) + VACT(1:NDP)
0012      WDP(1:72,6) = WDP(1:72,6) + VACT(1:NDP)
0013      WDP(1:72,6) = WDP(1:72,6) + VACT(1:NDP)
0014      WDP(1:72,6) = WDP(1:72,6) + VACT(1:NDP)
0015      WDP(1:72,6) = WDP(1:72,6) + VACT(1:NDP)
0016      WDP(1:72,6) = WDP(1:72,6) + VACT(1:NDP)
0017      WDP(1:72,6) = WDP(1:72,6) + VACT(1:NDP)
0018      WDP(1:72,6) = WDP(1:72,6) + VACT(1:NDP)
0019      WDP(1:72,6) = WDP(1:72,6) + VACT(1:NDP)
0020      WDP(1:72,6) = WDP(1:72,6) + VACT(1:NDP)
0021      WDP(1:72,6) = WDP(1:72,6) + VACT(1:NDP)
0022      WDP(1:72,6) = WDP(1:72,6) + VACT(1:NDP)
0023      WDP(1:72,6) = WDP(1:72,6) + VACT(1:NDP)
0024      WDP(1:72,6) = WDP(1:72,6) + VACT(1:NDP)
0025      WDP(1:72,6) = WDP(1:72,6) + VACT(1:NDP)
0026      WDP(1:72,6) = WDP(1:72,6) + VACT(1:NDP)
0027      WDP(1:72,6) = WDP(1:72,6) + VACT(1:NDP)
0028      WDP(1:72,6) = WDP(1:72,6) + VACT(1:NDP)
0029      WDP(1:72,6) = WDP(1:72,6) + VACT(1:NDP)
0030      WDP(1:72,6) = WDP(1:72,6) + VACT(1:NDP)
0031      WDP(1:72,6) = WDP(1:72,6) + VACT(1:NDP)
0032      WDP(1:72,6) = WDP(1:72,6) + VACT(1:NDP)
0033      WDP(1:72,6) = WDP(1:72,6) + VACT(1:NDP)
0034      WDP(1:72,6) = WDP(1:72,6) + VACT(1:NDP)
0035      WDP(1:72,6) = WDP(1:72,6) + VACT(1:NDP)
0036      WDP(1:72,6) = WDP(1:72,6) + VACT(1:NDP)
0037      WDP(1:72,6) = WDP(1:72,6) + VACT(1:NDP)
0038      WDP(1:72,6) = WDP(1:72,6) + VACT(1:NDP)
0039      WDP(1:72,6) = WDP(1:72,6) + VACT(1:NDP)
0040      WDP(1:72,6) = WDP(1:72,6) + VACT(1:NDP)
0041      WDP(1:72,6) = WDP(1:72,6) + VACT(1:NDP)
0042      WDP(1:72,6) = WDP(1:72,6) + VACT(1:NDP)
0043      WDP(1:72,6) = WDP(1:72,6) + VACT(1:NDP)
0044      WDP(1:72,6) = WDP(1:72,6) + VACT(1:NDP)
0045      WDP(1:72,6) = WDP(1:72,6) + VACT(1:NDP)

```









```

0001      SUBROUTINE STIFFI(N)
0002      COMMON/ST/IT(2,2),RTT(2,3),VSCDN(7),CDRO(5),Z1,NDP(72,6)
0003      I(18,7),SCCL(1,8),X(1,1),XSO(22),VDFIX(22),NI(PE(54)
0004      CDS(6),X(1,1),X(2,2),X(3,3),X(4,4),X(5,5),X(6,6),X(7,7),X(8,8),X(9,9),X(10,10),
0005      I,AREA,XI,XP,SLJDE,Y2
0006      COMMON/PARAM/ITIME,ITEND,VCN,      TRUN,ITMD,ITIME,ITMAX
0007      I(18,7),X(1,1),X(2,2),X(3,3),X(4,4),X(5,5),X(6,6),X(7,7),X(8,8),X(9,9),X(10,10),
0008      I(18,7),X(1,1),X(2,2),X(3,3),X(4,4),X(5,5),X(6,6),X(7,7),X(8,8),X(9,9),X(10,10),
0009      I(18,7),X(1,1),X(2,2),X(3,3),X(4,4),X(5,5),X(6,6),X(7,7),X(8,8),X(9,9),X(10,10),
0010      I(18,7),X(1,1),X(2,2),X(3,3),X(4,4),X(5,5),X(6,6),X(7,7),X(8,8),X(9,9),X(10,10),
0011      I(18,7),X(1,1),X(2,2),X(3,3),X(4,4),X(5,5),X(6,6),X(7,7),X(8,8),X(9,9),X(10,10),
0012      I(18,7),X(1,1),X(2,2),X(3,3),X(4,4),X(5,5),X(6,6),X(7,7),X(8,8),X(9,9),X(10,10),
0013      I(18,7),X(1,1),X(2,2),X(3,3),X(4,4),X(5,5),X(6,6),X(7,7),X(8,8),X(9,9),X(10,10),
0014      I(18,7),X(1,1),X(2,2),X(3,3),X(4,4),X(5,5),X(6,6),X(7,7),X(8,8),X(9,9),X(10,10),
0015      I(18,7),X(1,1),X(2,2),X(3,3),X(4,4),X(5,5),X(6,6),X(7,7),X(8,8),X(9,9),X(10,10),
0016      I(18,7),X(1,1),X(2,2),X(3,3),X(4,4),X(5,5),X(6,6),X(7,7),X(8,8),X(9,9),X(10,10),
0017      I(18,7),X(1,1),X(2,2),X(3,3),X(4,4),X(5,5),X(6,6),X(7,7),X(8,8),X(9,9),X(10,10),
0018      I(18,7),X(1,1),X(2,2),X(3,3),X(4,4),X(5,5),X(6,6),X(7,7),X(8,8),X(9,9),X(10,10),
0019      I(18,7),X(1,1),X(2,2),X(3,3),X(4,4),X(5,5),X(6,6),X(7,7),X(8,8),X(9,9),X(10,10),
0020      I(18,7),X(1,1),X(2,2),X(3,3),X(4,4),X(5,5),X(6,6),X(7,7),X(8,8),X(9,9),X(10,10),
0021      I(18,7),X(1,1),X(2,2),X(3,3),X(4,4),X(5,5),X(6,6),X(7,7),X(8,8),X(9,9),X(10,10),
0022      I(18,7),X(1,1),X(2,2),X(3,3),X(4,4),X(5,5),X(6,6),X(7,7),X(8,8),X(9,9),X(10,10),
0023      I(18,7),X(1,1),X(2,2),X(3,3),X(4,4),X(5,5),X(6,6),X(7,7),X(8,8),X(9,9),X(10,10),
0024      I(18,7),X(1,1),X(2,2),X(3,3),X(4,4),X(5,5),X(6,6),X(7,7),X(8,8),X(9,9),X(10,10),
0025      I(18,7),X(1,1),X(2,2),X(3,3),X(4,4),X(5,5),X(6,6),X(7,7),X(8,8),X(9,9),X(10,10),
0026      I(18,7),X(1,1),X(2,2),X(3,3),X(4,4),X(5,5),X(6,6),X(7,7),X(8,8),X(9,9),X(10,10),
0027      I(18,7),X(1,1),X(2,2),X(3,3),X(4,4),X(5,5),X(6,6),X(7,7),X(8,8),X(9,9),X(10,10),
0028      I(18,7),X(1,1),X(2,2),X(3,3),X(4,4),X(5,5),X(6,6),X(7,7),X(8,8),X(9,9),X(10,10),
0029      I(18,7),X(1,1),X(2,2),X(3,3),X(4,4),X(5,5),X(6,6),X(7,7),X(8,8),X(9,9),X(10,10),
0030      I(18,7),X(1,1),X(2,2),X(3,3),X(4,4),X(5,5),X(6,6),X(7,7),X(8,8),X(9,9),X(10,10),
0031      I(18,7),X(1,1),X(2,2),X(3,3),X(4,4),X(5,5),X(6,6),X(7,7),X(8,8),X(9,9),X(10,10),
0032      I(18,7),X(1,1),X(2,2),X(3,3),X(4,4),X(5,5),X(6,6),X(7,7),X(8,8),X(9,9),X(10,10),
0033      I(18,7),X(1,1),X(2,2),X(3,3),X(4,4),X(5,5),X(6,6),X(7,7),X(8,8),X(9,9),X(10,10),
0034      I(18,7),X(1,1),X(2,2),X(3,3),X(4,4),X(5,5),X(6,6),X(7,7),X(8,8),X(9,9),X(10,10),
0035      I(18,7),X(1,1),X(2,2),X(3,3),X(4,4),X(5,5),X(6,6),X(7,7),X(8,8),X(9,9),X(10,10),
0036      I(18,7),X(1,1),X(2,2),X(3,3),X(4,4),X(5,5),X(6,6),X(7,7),X(8,8),X(9,9),X(10,10),
0037      I(18,7),X(1,1),X(2,2),X(3,3),X(4,4),X(5,5),X(6,6),X(7,7),X(8,8),X(9,9),X(10,10),
0038      I(18,7),X(1,1),X(2,2),X(3,3),X(4,4),X(5,5),X(6,6),X(7,7),X(8,8),X(9,9),X(10,10),
0039      I(18,7),X(1,1),X(2,2),X(3,3),X(4,4),X(5,5),X(6,6),X(7,7),X(8,8),X(9,9),X(10,10),
0040      I(18,7),X(1,1),X(2,2),X(3,3),X(4,4),X(5,5),X(6,6),X(7,7),X(8,8),X(9,9),X(10,10),
0041      I(18,7),X(1,1),X(2,2),X(3,3),X(4,4),X(5,5),X(6,6),X(7,7),X(8,8),X(9,9),X(10,10),
0042      I(18,7),X(1,1),X(2,2),X(3,3),X(4,4),X(5,5),X(6,6),X(7,7),X(8,8),X(9,9),X(10,10),
0043      I(18,7),X(1,1),X(2,2),X(3,3),X(4,4),X(5,5),X(6,6),X(7,7),X(8,8),X(9,9),X(10,10),
0044      I(18,7),X(1,1),X(2,2),X(3,3),X(4,4),X(5,5),X(6,6),X(7,7),X(8,8),X(9,9),X(10,10),
0045      I(18,7),X(1,1),X(2,2),X(3,3),X(4,4),X(5,5),X(6,6),X(7,7),X(8,8),X(9,9),X(10,10),
0046      I(18,7),X(1,1),X(2,2),X(3,3),X(4,4),X(5,5),X(6,6),X(7,7),X(8,8),X(9,9),X(10,10),
0047      I(18,7),X(1,1),X(2,2),X(3,3),X(4,4),X(5,5),X(6,6),X(7,7),X(8,8),X(9,9),X(10,10)

```















6

6

6

6

6

6

6

6

6

6

F03TRAN IV G LEVEL 2L STIFF3 DATE = 78202 14/58/39 PAGE 0033

```

0096      B0(I)=C0R0(J,2)-C0R3(K,2)
0097      A0(B3-C0R0(I,1)+C0R0(J,2)-C0R0(K,1)+C0R0(L,2))
0098      A0(I2)=C0R0(K,2)+C0R0(L,2)-C0R0(I,1)+C0R0(J,2)
0099      A0(I1)=C0R0(J,1)+C0R0(K,2)-C0R0(L,1)+C0R0(I,2)
0100      IFEIIG(2)RRIIE(6,1,0)IL,N,(80)I),C(I1),A0(I),I=1,NCN)
0101      AREA0=C0R0(3)+B0(I2)-C0(2)+B0(3))/2.
          C      ERROR EXIT FOR BAD CONNECTIONS
          C      ITRARIQ,LE,J,33 TO 22)
          C      CALCULATE FLUIDITY MATRIK
0102      TERP1=B0(I1)/5.
0103      TERM2=C0(I1)/5.
0104      TERM3=(JRIIL(3)+JRIIL(2)+AREAO)/5.
0105      TERM4=FERM3/2.
0106      TERM5=B(2)/5.
0107      TERM6=C(2)/5.
0108      FERW7=B(3)/5.
0109      TERW8=C(3)/5.
0110      AK(I,4)=FERW7
0111      AK(I,5)=FERW8
0112      AK(I,2)=FERM3
0113      AK(I,10)=FERM6
0114      AK(I,19)=FERM1
0115      AK(I,19)=FERM1
0116      AK(I,20)=TERM2
0117      AK(I,4)=FERW7
0118      AK(I,4)=FERW7
0119      AK(I,4,3)=FERM4
0120      AK(I,4,9)=FERM4
0121      AK(I,19)=FERM1
0122      AK(I,19)=FERM1
0123      AK(I,5)=FERM4
0124      AK(I,5)=FERM4
0125      AK(I,8)=FERM6
0126      AK(I,10)=FERM4
0127      AK(I,19)=FERM1
0128      AK(I,20)=FERM3
0129      AK(I,4)=FERW7
0130      AK(I,5)=FERM4
0131      AK(I,9)=FERM4
0132      AK(I,10)=FERM4
0133      AK(I,19)=FERM1
0134      AK(I,20)=FERM2
0135      AK(I,9)=FERM7
0136      AK(I,9)=FERM4
0137      AK(I,9)=FERM5
0138      AK(I,9)=FERM3
0139      AK(I,13)=FERM1
0140      AK(I,13)=FERM4
0141      AK(I,10)=FERM8
0142      AK(I,10)=FERM4
0143      AK(I,13)=FERM5
0144      AK(I,10)=FERM3
0145      AK(I,10)=FERM2
0146      AK(I,10)=FERM4
0147      AK(I,10)=FERM7
0148      AK(I,10)=FERM8
0149      AK(I,15)=FERM5
0150

```

E









```

0001      FUNCTION SF(I,J)
0002      COMPAR=OMT(YE,YI)+M(XI),AM(XI),33(XI),8Y(XI),CJ(XI),C(XI),C(MC(XI),A),AREAD
0003      1/2*(AM(XI)+YI)+S(XI)/2
0004      CALL CUMUL(I,J,D)/SOLID COUPLING FUNCTION
0005      VERTICAL HILL
0006      FIND DIFFERENCE FUNCTIONS
0007      DIFFERENCE=SF(I,J)-SF(I,J-1)
0008      DIFFERENCE=DIFFERENCE/2
0009      DIFFERENCE=DIFFERENCE/2
0010      DIFFERENCE=DIFFERENCE/2
0011      DIFFERENCE=DIFFERENCE/2
0012      DIFFERENCE=DIFFERENCE/2
0013      DIFFERENCE=DIFFERENCE/2
0014      DIFFERENCE=DIFFERENCE/2
0015      DIFFERENCE=DIFFERENCE/2
0016      DIFFERENCE=DIFFERENCE/2
0017      DIFFERENCE=DIFFERENCE/2
0018      DIFFERENCE=DIFFERENCE/2
0019      DIFFERENCE=DIFFERENCE/2
0020      DIFFERENCE=DIFFERENCE/2
0021      DIFFERENCE=DIFFERENCE/2
0022      DIFFERENCE=DIFFERENCE/2
0023      DIFFERENCE=DIFFERENCE/2
0024      DIFFERENCE=DIFFERENCE/2
0025      DIFFERENCE=DIFFERENCE/2
0026      DIFFERENCE=DIFFERENCE/2
0027      DIFFERENCE=DIFFERENCE/2

```





```
FORTRAN IV LEVEL 21          FORCE          DATE = 78232          14/58/59          PAGE 0003

      ZUMBER IT=15/24 PRINTJ1 VARIABLE V=15/134 DJTOUT EVERY 15,24,5H
      PAGES/274 TIME AT FIRST ITERATION IS 512.5/12H DEBUG LEVEL 14)
      2000 FORMATTI(1,3)1,31
      3010 FORMATTI(1,3)1,517)
      3024 FORMATTI(1,3)1,3,3,3) IS PLACEMENT AND VELOCITY TIME= 151)
      3027 FORMATTI(1,3)1,3,3,3,3) FORCE DIAM 7)
      6000 FORMATTI(1,3)1,3,3,3,3,3,3) X-DIRECTION, Y-DIRECTION, 140, 84 PRESSURE
      150000 7-15-78 21:12:11 24,134 7-DIRECTION/14, 24, 84, 84, 84, 84, 84, 84)
      5001 FORMATTI(1,3)1,3,3,3,3,3,3,3)
      6012 FORMATTI(1,3)24,22HL IS GREATER THAN LMAX)
      END
```



```

0055 ECG=(RTRJ-RJNEI)
0056 D1A(0)J1=(EC+HEC1)/EC5+FDK
0057 D1A(1)J1=(CJ+VE+EC+R1)/EC51/EC5
0058 D1A(2)J1=(FJ+R2)EC4*(R1+R2)/EC5/EC6
0059 I(0)X(1) 31 33 13 234
0060 I(1)X(1) 31 33 13 234
0061 WRITE(5,2001) U,D1A(1)J1,D1A(1)J1,D1A(1)J1
0062 WRITE(5,2001) DELTY,VEGV,ZZZ,DVE5D,SINE,COSINE
0063 WRITE(5,2001) DELTY,VEGV,ZZZ,DVE5D,SINE,COSINE
0064 WRITE(5,2001) FDX,ECX,HEC2,EC3,EC4,EC5
0065 GO TO 214
0066 CONTINUE
0067 *
0068 *
0069 *
0070 *
0071 *
0072 *
0073 *
0074 *
0075 *
0076 *
0077 *
0078 *
0079 *
0080 *
0081 *
0082 *
0083 *
0084 *
0085 *
0086 *
0087 *
0088 *
0089 *
0090 *
0091 *
0092 *
0093 *
0094 *
0095 *
0096 *
0097 *
0098 *
0099 *
0100 *
0101 *
0102 *
0103 *
0104 *
0105 *
0106 *
0107 *
0108 *
0109 *
0110 *
0111 *
0112 *
0113 *
0114 *
0115 *
0116 *
0117 *
0118 *
0119 *
0120 *
0121 *
0122 *
0123 *
0124 *
0125 *
0126 *
0127 *
0128 *
0129 *
0130 *
0131 *
0132 *
0133 *
0134 *
0135 *
0136 *
0137 *
0138 *
0139 *
0140 *
0141 *
0142 *
0143 *
0144 *
0145 *
0146 *
0147 *
0148 *
0149 *
0150 *
0151 *
0152 *
0153 *
0154 *
0155 *
0156 *
0157 *
0158 *
0159 *
0160 *
0161 *
0162 *
0163 *
0164 *
0165 *
0166 *
0167 *
0168 *
0169 *
0170 *
0171 *
0172 *
0173 *
0174 *
0175 *
0176 *
0177 *
0178 *
0179 *
0180 *
0181 *
0182 *
0183 *
0184 *
0185 *
0186 *
0187 *
0188 *
0189 *
0190 *
0191 *
0192 *
0193 *
0194 *
0195 *
0196 *
0197 *
0198 *
0199 *
0200 *
0201 *
0202 *
0203 *
0204 *
0205 *
0206 *
0207 *
0208 *
0209 *
0210 *
0211 *
0212 *
0213 *
0214 *
0215 *
0216 *
0217 *
0218 *
0219 *
0220 *
0221 *
0222 *
0223 *
0224 *
0225 *
0226 *
0227 *
0228 *
0229 *
0230 *
0231 *
0232 *
0233 *
0234 *
0235 *
0236 *
0237 *
0238 *
0239 *
0240 *
0241 *
0242 *
0243 *
0244 *
0245 *
0246 *
0247 *
0248 *
0249 *
0250 *
0251 *
0252 *
0253 *
0254 *
0255 *
0256 *
0257 *
0258 *
0259 *
0260 *
0261 *
0262 *
0263 *
0264 *
0265 *
0266 *
0267 *
0268 *
0269 *
0270 *
0271 *
0272 *
0273 *
0274 *
0275 *
0276 *
0277 *
0278 *
0279 *
0280 *
0281 *
0282 *
0283 *
0284 *
0285 *
0286 *
0287 *
0288 *
0289 *
0290 *
0291 *
0292 *
0293 *
0294 *
0295 *
0296 *
0297 *
0298 *
0299 *
0300 *
0301 *
0302 *
0303 *
0304 *
0305 *
0306 *
0307 *
0308 *
0309 *
0310 *
0311 *
0312 *
0313 *
0314 *
0315 *
0316 *
0317 *
0318 *
0319 *
0320 *
0321 *
0322 *
0323 *
0324 *
0325 *
0326 *
0327 *
0328 *
0329 *
0330 *
0331 *
0332 *
0333 *
0334 *
0335 *
0336 *
0337 *
0338 *
0339 *
0340 *
0341 *
0342 *
0343 *
0344 *
0345 *
0346 *
0347 *
0348 *
0349 *
0350 *
0351 *
0352 *
0353 *
0354 *
0355 *
0356 *
0357 *
0358 *
0359 *
0360 *
0361 *
0362 *
0363 *
0364 *
0365 *
0366 *
0367 *
0368 *
0369 *
0370 *
0371 *
0372 *
0373 *
0374 *
0375 *
0376 *
0377 *
0378 *
0379 *
0380 *
0381 *
0382 *
0383 *
0384 *
0385 *
0386 *
0387 *
0388 *
0389 *
0390 *
0391 *
0392 *
0393 *
0394 *
0395 *
0396 *
0397 *
0398 *
0399 *
0400 *
0401 *
0402 *
0403 *
0404 *
0405 *
0406 *
0407 *
0408 *
0409 *
0410 *
0411 *
0412 *
0413 *
0414 *
0415 *
0416 *
0417 *
0418 *
0419 *
0420 *
0421 *
0422 *
0423 *
0424 *
0425 *
0426 *
0427 *
0428 *
0429 *
0430 *
0431 *
0432 *
0433 *
0434 *
0435 *
0436 *
0437 *
0438 *
0439 *
0440 *
0441 *
0442 *
0443 *
0444 *
0445 *
0446 *
0447 *
0448 *
0449 *
0450 *
0451 *
0452 *
0453 *
0454 *
0455 *
0456 *
0457 *
0458 *
0459 *
0460 *
0461 *
0462 *
0463 *
0464 *
0465 *
0466 *
0467 *
0468 *
0469 *
0470 *
0471 *
0472 *
0473 *
0474 *
0475 *
0476 *
0477 *
0478 *
0479 *
0480 *
0481 *
0482 *
0483 *
0484 *
0485 *
0486 *
0487 *
0488 *
0489 *
0490 *
0491 *
0492 *
0493 *
0494 *
0495 *
0496 *
0497 *
0498 *
0499 *
0500 *

```

```

0099 WRITE(S,5022) IJ,DIRADIS(IJ),DIIVEL(IJ),DIRACCC(IJ)
0100 WRITE(S,5000) DELT,ECJ,ECZ,EC3
0101 GO TO 204
0102 CONTINUE
0103
0104 FORMULATION 3 (C,VE-D,(K,VE-D))see
0105 FOC=TRAC(IJ)/DIRACK(IJ)
0106 TRAC=DIRACK(IJ)/DIRACK(IJ)
0107 TRAC=TRAC*(DIRADIS(IJ)-FOC)*EXP(DIRACK(IJ)*(-DELT)/DIRACK(IJ))
0108 IJ=DIRACK(IJ)+DIRACK(IJ)/DIRACK(IJ)+DIRACK(IJ)+FOC
0109 DIRACCC(IJ)=DIRACCC(IJ)+DIRACK(IJ)
0110 IF(DIRACCC(IJ) > 200) DIRACCC(IJ)
0111 WRITE(S,5021) IJ,DIRADIS(IJ),DIIVEL(IJ),DIRACCC(IJ)
0112 GO TO 204
0113 CONTINUE
0114 FORMULATION 4 (C,EG-D,(K,VE-D))see
0115 DIRADIS(IJ)=DIRACK(IJ)/DIRACK(IJ)
0116 DIRACCC(IJ)=0
0117 TRAC=DIRACK(IJ)
0118 TRAC=TRAC*(DIRADIS(IJ)-EG)*EXP(DIRACK(IJ)*(-DELT)/DIRACK(IJ))
0119 IJ=DIRACK(IJ)+DIRACK(IJ)/DIRACK(IJ)+DIRACK(IJ)+EG
0120 DIRACCC(IJ)=DIRACCC(IJ)+DIRACK(IJ)
0121 IF(DIRACCC(IJ) > 200) DIRACCC(IJ)
0122 WRITE(S,5022) IJ,DIRADIS(IJ),DIIVEL(IJ),DIRACCC(IJ)
0123 GO TO 204
0124 CONTINUE
0125 FORMULATION 5 (C,VE-D,(K,EG-D))see
0126 FOC=TRAC(IJ)/DIRACK(IJ)
0127 TRAC=DIRACK(IJ)/DIRACK(IJ)+FOC*DELT
0128 DIRACCC(IJ)=DELT
0129 DIRACCC(IJ)=FOC
0130 TRAC=TRAC*(DIRADIS(IJ)-FOC)*EXP(DIRACK(IJ)*(-DELT)/DIRACK(IJ))
0131 IJ=DIRACK(IJ)+DIRACK(IJ)/DIRACK(IJ)+DIRACK(IJ)+FOC
0132 DIRACCC(IJ)=DIRACCC(IJ)+DIRACK(IJ)
0133 CONTINUE
0134 FORMULATION 6 (K,VE-D,(C,EG-D)) see
0135 FOC=DIRACK(IJ)/DIRACK(IJ)
0136 DIRADIS(IJ)=DIRADIS(IJ)+DIRACK(IJ)+FOC*DELT+FOC*DELT*2)/2
0137 DIRACCC(IJ)=DIRACK(IJ)+FOC*DELT
0138 DIRACCC(IJ)=FOC
0139 TRAC=TRAC*(DIRADIS(IJ)-FOC)*EXP(DIRACK(IJ)*(-DELT)/DIRACK(IJ))
0140 IJ=DIRACK(IJ)+DIRACK(IJ)/DIRACK(IJ)+DIRACK(IJ)+FOC
0141 DIRACCC(IJ)=DIRACCC(IJ)+DIRACK(IJ)
0142 CONTINUE
0143 FORMULATION 7 (C,EG-D,(K,EG-D))see
0144 DIRADIS(IJ)=DIRADIS(IJ)+DIRACK(IJ)
0145 DIRACCC(IJ)=DIRADIS(IJ)
0146 TRAC=DIRACK(IJ)
0147 TRAC=TRAC*(DIRADIS(IJ)-EG)*EXP(DIRACK(IJ)*(-DELT)/DIRACK(IJ))
0148 IJ=DIRACK(IJ)+DIRACK(IJ)/DIRACK(IJ)+DIRACK(IJ)+EG
0149 DIRACCC(IJ)=DIRACCC(IJ)+DIRACK(IJ)
0150 CONTINUE
0151 WRITE(S,5022) IJ,DIRADIS(IJ),DIIVEL(IJ),DIRACCC(IJ)
0152 GO TO 204
0153 CONTINUE
0154 RETURN
0155 FORMATION 8 (H,DIRADIS,DIRACK(IJ))
0156 FORMATION 9 (H,DIRADIS,DIRACK(IJ))

```



PAGE 0034

14/58/39

DATE = 7820Z

UNITES

FORTRAN IV 6 LEVEL 21

```

0169      5202 FORMAT(1X,3H1J=,15,5(+,H)IS=,E12.5,3X,1HWEL=,E12.5,3X,+HACC=,E12.5
0170      1)
0171      5210 FORMATT(1,10X,25HFORMULATION 1--(UNDER DAMPED)
0172      1)
0173      5220 FORMATT(1,10X,13HFORMULATION 2)
0174      5230 FORMATT(1,10X,13HFORMULATION 3)
0175      5240 FORMATT(1,10X,13HFORMULATION 4)
0176      5250 FORMATT(1,10X,13HFORMULATION 5)
0177      5260 FORMATT(1,10X,13HFORMULATION 6)
0178      5270 FORMATT(1,10X,13HFORMULATION 7)
0179      5280 FORMATT(1,10X,13HFORMULATION 8)
0180      5290 FORMATT(1,10X,13HFORMULATION 9--(OVERDAMPED)
0181      1)
0182      5300 FORMATT(1,10X,13HFORMULATION 1--(CRITICALLY DAMPED)
0183      1)
0184
0185
0186
0187
0188
0189
0190
0191
0192
0193
0194
0195
0196
0197
0198
0199
0200
0201
0202
0203
0204
0205
0206
0207
0208
0209
0210
0211
0212
0213
0214
0215
0216
0217
0218
0219
0220
0221
0222
0223
0224
0225
0226
0227
0228
0229
0230
0231
0232
0233
0234
0235
0236
0237
0238
0239
0240
0241
0242
0243
0244
0245
0246
0247
0248
0249
0250
0251
0252
0253
0254
0255
0256
0257
0258
0259
0260
0261
0262
0263
0264
0265
0266
0267
0268
0269
0270
0271
0272
0273
0274
0275
0276
0277
0278
0279
0280
0281
0282
0283
0284
0285
0286
0287
0288
0289
0290
0291
0292
0293
0294
0295
0296
0297
0298
0299
0300
0301
0302
0303
0304
0305
0306
0307
0308
0309
0310
0311
0312
0313
0314
0315
0316
0317
0318
0319
0320
0321
0322
0323
0324
0325
0326
0327
0328
0329
0330
0331
0332
0333
0334
0335
0336
0337
0338
0339
0340
0341
0342
0343
0344
0345
0346
0347
0348
0349
0350
0351
0352
0353
0354
0355
0356
0357
0358
0359
0360
0361
0362
0363
0364
0365
0366
0367
0368
0369
0370
0371
0372
0373
0374
0375
0376
0377
0378
0379
0380
0381
0382
0383
0384
0385
0386
0387
0388
0389
0390
0391
0392
0393
0394
0395
0396
0397
0398
0399
0400
0401
0402
0403
0404
0405
0406
0407
0408
0409
0410
0411
0412
0413
0414
0415
0416
0417
0418
0419
0420
0421
0422
0423
0424
0425
0426
0427
0428
0429
0430
0431
0432
0433
0434
0435
0436
0437
0438
0439
0440
0441
0442
0443
0444
0445
0446
0447
0448
0449
0450
0451
0452
0453
0454
0455
0456
0457
0458
0459
0460
0461
0462
0463
0464
0465
0466
0467
0468
0469
0470
0471
0472
0473
0474
0475
0476
0477
0478
0479
0480
0481
0482
0483
0484
0485
0486
0487
0488
0489
0490
0491
0492
0493
0494
0495
0496
0497
0498
0499
0500
0501
0502
0503
0504
0505
0506
0507
0508
0509
0510
0511
0512
0513
0514
0515
0516
0517
0518
0519
0520
0521
0522
0523
0524
0525
0526
0527
0528
0529
0530
0531
0532
0533
0534
0535
0536
0537
0538
0539
0540
0541
0542
0543
0544
0545
0546
0547
0548
0549
0550
0551
0552
0553
0554
0555
0556
0557
0558
0559
0560
0561
0562
0563
0564
0565
0566
0567
0568
0569
0570
0571
0572
0573
0574
0575
0576
0577
0578
0579
0580
0581
0582
0583
0584
0585
0586
0587
0588
0589
0590
0591
0592
0593
0594
0595
0596
0597
0598
0599
0600
0601
0602
0603
0604
0605
0606
0607
0608
0609
0610
0611
0612
0613
0614
0615
0616
0617
0618
0619
0620
0621
0622
0623
0624
0625
0626
0627
0628
0629
0630
0631
0632
0633
0634
0635
0636
0637
0638
0639
0640
0641
0642
0643
0644
0645
0646
0647
0648
0649
0650
0651
0652
0653
0654
0655
0656
0657
0658
0659
0660
0661
0662
0663
0664
0665
0666
0667
0668
0669
0670
0671
0672
0673
0674
0675
0676
0677
0678
0679
0680
0681
0682
0683
0684
0685
0686
0687
0688
0689
0690
0691
0692
0693
0694
0695
0696
0697
0698
0699
0700
0701
0702
0703
0704
0705
0706
0707
0708
0709
0710
0711
0712
0713
0714
0715
0716
0717
0718
0719
0720
0721
0722
0723
0724
0725
0726
0727
0728
0729
0730
0731
0732
0733
0734
0735
0736
0737
0738
0739
0740
0741
0742
0743
0744
0745
0746
0747
0748
0749
0750
0751
0752
0753
0754
0755
0756
0757
0758
0759
0760
0761
0762
0763
0764
0765
0766
0767
0768
0769
0770
0771
0772
0773
0774
0775
0776
0777
0778
0779
0780
0781
0782
0783
0784
0785
0786
0787
0788
0789
0790
0791
0792
0793
0794
0795
0796
0797
0798
0799
0800
0801
0802
0803
0804
0805
0806
0807
0808
0809
0810
0811
0812
0813
0814
0815
0816
0817
0818
0819
0820
0821
0822
0823
0824
0825
0826
0827
0828
0829
0830
0831
0832
0833
0834
0835
0836
0837
0838
0839
0840
0841
0842
0843
0844
0845
0846
0847
0848
0849
0850
0851
0852
0853
0854
0855
0856
0857
0858
0859
0860
0861
0862
0863
0864
0865
0866
0867
0868
0869
0870
0871
0872
0873
0874
0875
0876
0877
0878
0879
0880
0881
0882
0883
0884
0885
0886
0887
0888
0889
0890
0891
0892
0893
0894
0895
0896
0897
0898
0899
0900
0901
0902
0903
0904
0905
0906
0907
0908
0909
0910
0911
0912
0913
0914
0915
0916
0917
0918
0919
0920
0921
0922
0923
0924
0925
0926
0927
0928
0929
0930
0931
0932
0933
0934
0935
0936
0937
0938
0939
0940
0941
0942
0943
0944
0945
0946
0947
0948
0949
0950
0951
0952
0953
0954
0955
0956
0957
0958
0959
0960
0961
0962
0963
0964
0965
0966
0967
0968
0969
0970
0971
0972
0973
0974
0975
0976
0977
0978
0979
0980
0981
0982
0983
0984
0985
0986
0987
0988
0989
0990
0991
0992
0993
0994
0995
0996
0997
0998
0999
1000

```

72 ELEMENT FLUID-3D,1D MODEL

ERRORS: 0.1000E-01  
 TITL: 3 LEVDE 1  
 REFIN: 2 LMAE 33  
 V2 78 1 3 KVF IC VPINT VO WOF WCIW  
 2 1 2 0 700 21 5 7  
 3 3 3 3 3 3 3 3  
 4 4 4 4 4 4 4 4  
 5 5 5 5 5 5 5 5  
 6 6 6 6 6 6 6 6  
 7 7 7 7 7 7 7 7  
 8 8 8 8 8 8 8 8  
 9 9 9 9 9 9 9 9  
 10 10 10 10 10 10 10 10  
 11 11 11 11 11 11 11 11  
 12 12 12 12 12 12 12 12  
 13 13 13 13 13 13 13 13  
 14 14 14 14 14 14 14 14  
 15 15 15 15 15 15 15 15  
 16 16 16 16 16 16 16 16  
 17 17 17 17 17 17 17 17  
 18 18 18 18 18 18 18 18  
 19 19 19 19 19 19 19 19  
 20 20 20 20 20 20 20 20  
 21 21 21 21 21 21 21 21  
 22 22 22 22 22 22 22 22  
 23 23 23 23 23 23 23 23  
 24 24 24 24 24 24 24 24  
 25 25 25 25 25 25 25 25  
 26 26 26 26 26 26 26 26  
 27 27 27 27 27 27 27 27  
 28 28 28 28 28 28 28 28  
 29 29 29 29 29 29 29 29  
 30 30 30 30 30 30 30 30  
 31 31 31 31 31 31 31 31  
 32 32 32 32 32 32 32 32  
 33 33 33 33 33 33 33 33  
 34 34 34 34 34 34 34 34  
 35 35 35 35 35 35 35 35  
 36 36 36 36 36 36 36 36  
 37 37 37 37 37 37 37 37  
 38 38 38 38 38 38 38 38  
 39 39 39 39 39 39 39 39  
 40 40 40 40 40 40 40 40  
 41 41 41 41 41 41 41 41  
 42 42 42 42 42 42 42 42  
 43 43 43 43 43 43 43 43  
 44 44 44 44 44 44 44 44  
 45 45 45 45 45 45 45 45

REFERENCE PROPERTIES  
 1 1.3300E+08 0.7400E-03 DENSITY  
 2 2.5000E+03 0.73552E-04  
 DAMPING FACTOR IS 0.0  
 MODULUS IS 0.0  
 SECT-I

NO.	YCOORD	ZCOORD	WCOORD	DENSITY
1	0.0	0.0	0.0	1.3300
2	1.000	1.000	1.000	1.3300
3	2.000	2.000	2.000	1.3300
4	3.000	3.000	3.000	1.3300
5	4.000	4.000	4.000	1.3300
6	5.000	5.000	5.000	1.3300
7	6.000	6.000	6.000	1.3300
8	7.000	7.000	7.000	1.3300
9	8.000	8.000	8.000	1.3300
10	9.000	9.000	9.000	1.3300
11	10.000	10.000	10.000	1.3300
12	11.000	11.000	11.000	1.3300
13	12.000	12.000	12.000	1.3300
14	13.000	13.000	13.000	1.3300
15	14.000	14.000	14.000	1.3300
16	15.000	15.000	15.000	1.3300
17	16.000	16.000	16.000	1.3300
18	17.000	17.000	17.000	1.3300
19	18.000	18.000	18.000	1.3300
20	19.000	19.000	19.000	1.3300
21	20.000	20.000	20.000	1.3300
22	21.000	21.000	21.000	1.3300
23	22.000	22.000	22.000	1.3300
24	23.000	23.000	23.000	1.3300
25	24.000	24.000	24.000	1.3300
26	25.000	25.000	25.000	1.3300
27	26.000	26.000	26.000	1.3300
28	27.000	27.000	27.000	1.3300
29	28.000	28.000	28.000	1.3300
30	29.000	29.000	29.000	1.3300
31	30.000	30.000	30.000	1.3300
32	31.000	31.000	31.000	1.3300
33	32.000	32.000	32.000	1.3300
34	33.000	33.000	33.000	1.3300
35	34.000	34.000	34.000	1.3300
36	35.000	35.000	35.000	1.3300
37	36.000	36.000	36.000	1.3300
38	37.000	37.000	37.000	1.3300
39	38.000	38.000	38.000	1.3300
40	39.000	39.000	39.000	1.3300
41	40.000	40.000	40.000	1.3300
42	41.000	41.000	41.000	1.3300
43	42.000	42.000	42.000	1.3300
44	43.000	43.000	43.000	1.3300
45	44.000	44.000	44.000	1.3300

LINE	MODE	TYPE	MODE	TYPE	MODE	TYPE	MODE	TYPE	MODE	TYPE	MODE	TYPE	MODE	TYPE	MODE	TYPE
46	27-930	12-000														
47	27-930	12-250														
48	27-930	12-500														
49	30-930	0-0														
50	30-930	4-000														
51	30-930	6-000														
52	30-930	12-000														
53	30-930	12-250														
54	30-930	12-500														
55	30-930	12-500														

LINE	MODE	TYPE	MODE	TYPE	MODE	TYPE	MODE	TYPE	MODE	TYPE	MODE	TYPE	MODE	TYPE	MODE	TYPE
1	1	1	1	1	1	1	1	1	1	1	1	1	1	1	1	1
2	1	1	1	1	1	1	1	1	1	1	1	1	1	1	1	1
3	1	1	1	1	1	1	1	1	1	1	1	1	1	1	1	1
4	1	1	1	1	1	1	1	1	1	1	1	1	1	1	1	1
5	1	1	1	1	1	1	1	1	1	1	1	1	1	1	1	1
6	1	1	1	1	1	1	1	1	1	1	1	1	1	1	1	1
7	1	1	1	1	1	1	1	1	1	1	1	1	1	1	1	1
8	1	1	1	1	1	1	1	1	1	1	1	1	1	1	1	1
9	1	1	1	1	1	1	1	1	1	1	1	1	1	1	1	1
10	1	1	1	1	1	1	1	1	1	1	1	1	1	1	1	1
11	1	1	1	1	1	1	1	1	1	1	1	1	1	1	1	1
12	1	1	1	1	1	1	1	1	1	1	1	1	1	1	1	1
13	1	1	1	1	1	1	1	1	1	1	1	1	1	1	1	1
14	1	1	1	1	1	1	1	1	1	1	1	1	1	1	1	1
15	1	1	1	1	1	1	1	1	1	1	1	1	1	1	1	1
16	1	1	1	1	1	1	1	1	1	1	1	1	1	1	1	1
17	1	1	1	1	1	1	1	1	1	1	1	1	1	1	1	1
18	1	1	1	1	1	1	1	1	1	1	1	1	1	1	1	1
19	1	1	1	1	1	1	1	1	1	1	1	1	1	1	1	1
20	1	1	1	1	1	1	1	1	1	1	1	1	1	1	1	1
21	1	1	1	1	1	1	1	1	1	1	1	1	1	1	1	1
22	1	1	1	1	1	1	1	1	1	1	1	1	1	1	1	1
23	1	1	1	1	1	1	1	1	1	1	1	1	1	1	1	1
24	1	1	1	1	1	1	1	1	1	1	1	1	1	1	1	1
25	1	1	1	1	1	1	1	1	1	1	1	1	1	1	1	1
26	1	1	1	1	1	1	1	1	1	1	1	1	1	1	1	1
27	1	1	1	1	1	1	1	1	1	1	1	1	1	1	1	1
28	1	1	1	1	1	1	1	1	1	1	1	1	1	1	1	1
29	1	1	1	1	1	1	1	1	1	1	1	1	1	1	1	1
30	1	1	1	1	1	1	1	1	1	1	1	1	1	1	1	1
31	1	1	1	1	1	1	1	1	1	1	1	1	1	1	1	1
32	1	1	1	1	1	1	1	1	1	1	1	1	1	1	1	1
33	1	1	1	1	1	1	1	1	1	1	1	1	1	1	1	1
34	1	1	1	1	1	1	1	1	1	1	1	1	1	1	1	1
35	1	1	1	1	1	1	1	1	1	1	1	1	1	1	1	1
36	1	1	1	1	1	1	1	1	1	1	1	1	1	1	1	1
37	1	1	1	1	1	1	1	1	1	1	1	1	1	1	1	1
38	1	1	1	1	1	1	1	1	1	1	1	1	1	1	1	1
39	1	1	1	1	1	1	1	1	1	1	1	1	1	1	1	1
40	1	1	1	1	1	1	1	1	1	1	1	1	1	1	1	1
41	1	1	1	1	1	1	1	1	1	1	1	1	1	1	1	1
42	1	1	1	1	1	1	1	1	1	1	1	1	1	1	1	1
43	1	1	1	1	1	1	1	1	1	1	1	1	1	1	1	1
44	1	1	1	1	1	1	1	1	1	1	1	1	1	1	1	1
45	1	1	1	1	1	1	1	1	1	1	1	1	1	1	1	1
46	1	1	1	1	1	1	1	1	1	1	1	1	1	1	1	1
47	1	1	1	1	1	1	1	1	1	1	1	1	1	1	1	1
48	1	1	1	1	1	1	1	1	1	1	1	1	1	1	1	1
49	1	1	1	1	1	1	1	1	1	1	1	1	1	1	1	1
50	1	1	1	1	1	1	1	1	1	1	1	1	1	1	1	1
51	1	1	1	1	1	1	1	1	1	1	1	1	1	1	1	1
52	1	1	1	1	1	1	1	1	1	1	1	1	1	1	1	1
53	1	1	1	1	1	1	1	1	1	1	1	1	1	1	1	1
54	1	1	1	1	1	1	1	1	1	1	1	1	1	1	1	1
55	1	1	1	1	1	1	1	1	1	1	1	1	1	1	1	1

MATH-13-



47	43	49	50	51	52	55	57	53	64	53	59	70	73	74	75	76	77
78	73	80	81	82	85	87	93	94	98	99	100	103	104	105	106	107	108
109	110	111	112	115	117	123	124	128	129	130	133	134	135	135	137	138	139
140	141	142	143	147	153	154	158	159	160	163	164	165	165	167	168	169	170
171	172	175	177	183	184	185	188	190	193	194	195	195	197	198	199	200	201
202	203	207	215	214	213	219	220	223	224	225	226	227	228	229	230	231	232
233	237	244	245	250	251	252	254	255	257	259	262	263	264				

THESE SPECIFIED FEEDINGS ARE  
 10.000

21521	1	11=	0.0
21521	2	11=	0.0
21521	3	11=	0.0
21521	4	11=	0.0
21521	5	11=	0.0
21521	6	11=	0.0
21521	7	11=	0.0
21521	8	11=	0.0
21521	9	11=	0.0
21521	10	11=	0.0
21521	11	11=	0.0
21521	12	11=	0.0
21521	13	11=	0.0
21521	14	11=	0.0
21521	15	11=	0.0
21521	16	11=	0.0
21521	17	11=	0.0
21521	18	11=	0.0
21521	19	11=	0.0
21521	20	11=	0.0
21521	21	11=	0.0
21521	22	11=	0.0
21521	23	11=	0.0
21521	24	11=	0.0
21521	25	11=	0.0
21521	26	11=	0.0
21521	27	11=	0.0
21521	28	11=	0.0
21521	29	11=	0.0
21521	30	11=	0.0
21521	31	11=	0.0
21521	32	11=	0.0
21521	33	11=	0.0
21521	34	11=	0.0
21521	35	11=	0.0
21521	36	11=	0.0
21521	37	11=	0.0
21521	38	11=	0.0
21521	39	11=	0.0
21521	40	11=	0.0
21521	41	11=	0.0
21521	42	11=	0.0
21521	43	11=	0.0
21521	44	11=	0.0
21521	45	11=	0.0
21521	46	11=	0.0
21521	47	11=	0.0
21521	48	11=	0.0
21521	49	11=	0.0
21521	50	11=	0.0
21521	51	11=	0.0
21521	52	11=	0.0
21521	53	11=	0.0
21521	54	11=	0.0
21521	55	11=	0.0
21521	56	11=	0.0
21521	57	11=	0.0
21521	58	11=	0.0
21521	59	11=	0.0
21521	60	11=	0.0
21521	61	11=	0.0
21521	62	11=	0.0
21521	63	11=	0.0
21521	64	11=	0.0
21521	65	11=	0.0
21521	66	11=	0.0
21521	67	11=	0.0
21521	68	11=	0.0
21521	69	11=	0.0
21521	70	11=	0.0
21521	71	11=	0.0
21521	72	11=	0.0
21521	73	11=	0.0
21521	74	11=	0.0
21521	75	11=	0.0
21521	76	11=	0.0
21521	77	11=	0.0
21521	78	11=	0.0
21521	79	11=	0.0
21521	80	11=	0.0
21521	81	11=	0.0
21521	82	11=	0.0
21521	83	11=	0.0
21521	84	11=	0.0
21521	85	11=	0.0
21521	86	11=	0.0
21521	87	11=	0.0
21521	88	11=	0.0
21521	89	11=	0.0
21521	90	11=	0.0
21521	91	11=	0.0
21521	92	11=	0.0
21521	93	11=	0.0
21521	94	11=	0.0
21521	95	11=	0.0
21521	96	11=	0.0
21521	97	11=	0.0
21521	98	11=	0.0
21521	99	11=	0.0
21521	100	11=	0.0









3	11	0-14090E-23	12	0-14090E-23	13	0-10000E 02	14	0-36358E-02	15	0-0
4	15	0-0	17	0-0	18	0-10000E 02	19	0-36358E-02	20	0-0
5	21	0-0	22	0-0	23	0-14090E-28	24	0-14090E-28	25	0-14090E-28
6	25	0-0	27	0-0	28	0-14090E-28	29	0-14090E-28	30	0-14090E-28
7	31	0-14090E-23	32	0-14090E-23	33	0-0	34	0-72715E-23	35	0-0
8	35	0-14090E-23	37	0-14090E-23	38	0-0	39	0-12119E-02	40	0-0
9	41	0-14090E-23	42	0-14090E-23	43	0-0	44	0-12119E-02	45	0-0
10	45	0-0	47	0-89917E-11	48	0-0	49	0-18179E-02	50	0-39139E-03
11	51	0-0	52	0-39950E-15	53	0-14090E-28	54	0-14090E-28	55	0-14090E-28
12	55	0-0	57	0-0	58	0-14090E-28	59	0-14090E-23	60	0-14090E-23
13	61	0-14090E-23	62	0-14090E-23	63	0-0	64	0-0	65	0-0
14	65	0-14090E-23	67	0-14090E-23	68	0-0	69	0-0	70	0-0
15	71	0-14090E-23	72	0-14090E-23	73	0-0	74	0-0	75	0-0
16	76	0-0	77	0-0	78	0-0	79	0-0	80	0-0
17	81	0-0	82	0-0	83	0-14090E-23	84	0-14090E-23	85	0-14090E-28
18	86	0-0	87	0-0	88	0-14090E-28	89	0-14090E-28	90	0-14090E-28
19	91	0-14090E-23	92	0-14090E-23	93	0-14090E-28	94	0-14090E-28	95	0-14090E-28
20	95	0-14090E-23	97	0-14090E-23	98	0-0	99	0-0	100	0-0
21	101	0-14090E-23	102	0-14090E-23	103	0-0	104	0-0	105	0-0
22	106	0-0	107	0-0	108	0-0	109	0-0	110	0-0
23	111	0-0	112	0-0	113	0-14090E-28	114	0-14090E-28	115	0-14090E-28
24	116	0-0	117	0-0	118	0-14090E-28	119	0-14090E-28	120	0-14090E-28
25	121	0-14090E-23	122	0-14090E-23	123	0-0	124	0-0	125	0-0
26	126	0-14090E-23	127	0-14090E-23	128	0-0	129	0-0	130	0-0
27	131	0-14090E-23	132	0-14090E-23	133	0-0	134	0-0	135	0-0
28	136	0-0	137	0-0	138	0-0	139	0-0	140	0-0
29	141	0-0	142	0-0	143	0-14090E-28	144	0-14090E-28	145	0-14090E-28
30	146	0-0	147	0-0	148	0-14090E-28	149	0-14090E-28	150	0-14090E-28
31	151	0-14090E-23	152	0-14090E-23	153	0-0	154	0-0	155	0-0
32	156	0-14090E-23	157	0-14090E-23	158	0-0	159	0-0	160	0-0
33	161	0-14090E-23	162	0-14090E-23	163	0-0	164	0-0	165	0-0
34	166	0-0	167	0-0	168	0-0	169	0-0	170	0-0
35	171	0-0	172	0-0	173	0-14090E-28	174	0-14090E-28	175	0-14090E-28
36	176	0-0	177	0-0	178	0-14090E-28	179	0-14090E-28	180	0-14090E-28
37	181	0-14090E-23	182	0-14090E-23	183	0-0	184	0-0	185	0-0
38	186	0-14090E-23	187	0-14090E-23	188	0-0	189	0-0	190	0-0
39	191	0-14090E-23	192	0-14090E-23	193	0-0	194	0-0	195	0-0
40	196	0-0	197	0-0	198	0-0	199	0-0	200	0-0
41	201	0-0	202	0-0	203	0-14090E-23	204	0-14090E-23	205	0-14090E-28
42	206	0-0	207	0-0	208	0-14090E-23	209	0-14090E-23	210	0-14090E-23
43	211	0-14090E-23	212	0-14090E-23	213	0-0	214	0-0	215	0-0
44	216	0-14090E-23	217	0-14090E-23	218	0-0	219	0-0	220	0-0
45	221	0-14090E-23	222	0-14090E-23	223	0-0	224	0-0	225	0-0
46	226	0-0	227	0-0	228	0-0	229	0-0	230	0-0
47	231	0-0	232	0-0	233	0-14090E-28	234	0-14090E-23	235	0-14090E-23
48	236	0-0	237	0-0	238	0-14090E-28	239	0-14090E-28	240	0-14090E-28
49	241	0-14090E-23	242	0-14090E-23	243	0-0	244	0-0	245	0-0
50	246	0-14090E-23	247	0-14090E-23	248	0-0	249	0-0	250	0-0
51	251	0-14090E-23	252	0-14090E-23	253	0-0	254	0-0	255	0-0
52	256	0-0	257	0-0	258	0-0	259	0-0	260	0-0
53	261	0-0	262	0-0	263	0-14090E-28	264	0-14090E-23	265	0-14090E-28
54	266	0-0	267	0-0	268	0-14090E-23	269	0-14090E-23	270	0-14090E-28

Finite Element Analysis, Integration Solution

SOLUTION FOR TIME T= 0.35899E-04
ELEMENTS: 258, TIME: 0.35899E-07
ITERATION NUMBER: 701
DIMENSIONAL VARIABLE N= 700
OUTPUT EVERY 700 TIMES
LARGEST ITERATION: 15 0.85714E-07
D.305 LEVEL

Table with columns: NODE, J, X-DIRECTION, J, Y-DIRECTION, J, X-DIRECTION, J, Y-DIRECTION, J, X-DIRECTION, J, Y-DIRECTION, J, X-DIRECTION, J, Y-DIRECTION, J, X-DIRECTION, J, Y-DIRECTION, J, X-DIRECTION, J, Y-DIRECTION, J, X-DIRECTION, J, Y-DIRECTION. Rows contain numerical data for nodes 1 through 54.

VITA

Rahim Falsafi-haghighi was born in                                  on                                  . In June, 1965, he was awarded a Bachelor of Science degree from The American University of Beirut, Beirut, Lebanon. He received a Master of Science degree from University of Maine, Orono, Maine in January 1968. He started working toward the Doctor of Engineering Science degree in Mechanical Engineering at New Jersey Institute of Technology, Newark College of Engineering, Newark, New Jersey, in September 1972.

The research upon which this dissertation is based was conducted at New Jersey Institute of Technology from November 1976 to August 1978.